DTIC FILE COPY

②

AFOSR-TR- 90 0763

AD-A224 596

THE DETERMINATION OF RATE-LIMITING STEPS DURING SOOT FORMATION

Annual Report

for

February 1989 to January 1990

Prepared by

M. B. Colket III
R. J. Hall
J. J. Sangiovanni
D. J. Seery

United Technologies Research Center

East Hartford, CT 06108

UTRC Report No. UTRC90-23

AIR FORCE OFFICE OF SCIENTIFIC RESEARCH (AFSC)
[illegible] Division

For

Air Force Office of Scientific Research
Bolling Air Force Base
Washington, D.C. 20332

Contract No. F49620-88-C-0051

Approved for public release; distribution unlimited.

J. M. Tishkoff

Program Manager

June 8, 1990

DTIC
ELECTE
JUL 13 1990
S E D

90 07 13 005

Unclassified
SECURITY CLASSIFICATION OF THIS PAGE

REPORT DOCUMENTATION PAGE

Form Approved OMB No. 0704-0188

1a. REPORT SECURITY CLASSIFICATION Unclassified	1b. RESTRICTIVE MARKINGS
2a. SECURITY CLASSIFICATION AUTHORITY	3. DISTRIBUTION/AVAILABILITY OF REPORT Approved for public release; distribution is unlimited.
2b. DECLASSIFICATION/DOWNGRADING SCHEDULE	
4. PERFORMING ORGANIZATION REPORT NUMBER(S) UTRC90-23	5. MONITORING ORGANIZATION REPORT NUMBER(S) AFOSR-TR- 90 0763
6a. NAME OF PERFORMING ORGANIZATION United Technologies Research Ctr	6b. OFFICE SYMBOL *(If applicable)*
7a. NAME OF MONITORING ORGANIZATION AFOSR/NA	
6c. ADDRESS *(City, State, and ZIP Code)* Hartford CT 06108	7b. ADDRESS *(City, State, and ZIP Code)* Building 410, Bolling AFB DC 20332-6448
8a. NAME OF FUNDING/SPONSORING ORGANIZATION AFOSR/NA	8b. OFFICE SYMBOL *(If applicable)* NA
9. PROCUREMENT INSTRUMENT IDENTIFICATION NUMBER F49620-88-C-0051	
8c. ADDRESS *(City, State, and ZIP Code)* Building 410, Bolling AFB DC 20332-6448	

10. SOURCE OF FUNDING NUMBERS

PROGRAM ELEMENT NO.	PROJECT NO.	TASK NO.	WORK UNIT ACCESSION NO.
61102F	2308	A2	

11. TITLE *(Include Security Classificati*
(U) The Determination of Rate-Limiting Steps During Soot Formation

12. PERSONAL AUTHOR(S)
Colket, M. B., Hall, R. J., Sangiovanni, J. J. and Seery, D. J.

13a. TYPE OF REPORT	13b. TIME COVERED	14. DATE OF REPORT *(Year, Month, Day)*	15. PAGE COUNT
Annual	FROM 2/1/89 TO 1/31/90	1990 - June - 8	121

16. SUPPLEMENTARY NOTATION

17. COSATI CODES

FIELD	GROUP	SUB-GROUP

18. SUBJECT TERMS ~~*(Continue on reverse if necessary and identify by block number)*~~
Pyrolysis , cyclopentadiene, benzene, hydrogen addition, ring formation, ring isomerization, soot formation, soot modeling, single-pulse shock tube

19. ABSTRACT *(Continue on reverse if necessary and identify by block number)*

A single-pulse shock tube has been used to examine the pyrolysis and rich oxidation of cyclopentadiene as well as its pyrolysis in the presence of acetylene, biacetyl, and benzene. In addition, mixtures of benzene and hydrogen have been copyrolyzed. These fuels have been diluted in argon and shock heated over the temperature range of 1200 to 2000K and at total pressures of ten to thirteen atmospheres. Dwell times were about 500-600 microseconds. Collected gas samples were analyzed using gas chromatography for hydrogen, carbon oxides and C_1- to C_{14}- hydrocarbons. Experimental results and preliminary chemical kinetic modeling lead to mechanistic proposals on the decomposition of C_5-rings as well as isomerization processes between C_5- and C_6-rings. In addition, data on cyclopentadiene indicates that this fuel has a sooting tendency comparable to that of benzene.

(continued on reverse side)

20. DISTRIBUTION/AVAILABILITY OF ABSTRACT ☒ UNCLASSIFIED/UNLIMITED ☒ SAME AS RPT. ☐ DTIC USERS	21. ABSTRACT SECURITY CLASSIFICATION Unclassified
22a. NAME OF RESPONSIBLE INDIVIDUAL Julian M Tishkoff	22b. TELEPHONE *(Include Area Code)* (202) 767-4935
22c. OFFICE SYMBOL AFOSR/NA	

DD Form 1473, JUN 86 *Previous editions are obsolete.* SECURITY CLASSIFICATION OF THIS PAGE

Unclassified

Abstract (Continued)

Simplified modeling techniques of soot formation based on the MAEROS code have been extended. Soot formation in a premixed propane/oxygen flame has been predicted assuming that naphthalene is the inceptor for soot. Parametric variations indicate that initial soot formation rates are strongly dependent on inception rates, but final soot fractions produced in flames are much less dependent on inception rates than had previously been assumed.

THE DETERMINATION OF RATE-LIMITING STEPS DURING SOOT FORMATION

Annual Report

for

February 1989 to January 1990

Prepared by

M. B. Colket III
R. J. Hall
J. J. Sangiovanni
D. J. Seery

United Technologies Research Center

East Hartford, CT 06108

UTRC Report No. UTRC90-23

For

Air Force Office of Scientific Research
Bolling Air Force Base
Washington, D.C. 20332

Contract No. F49620-88-C-0051

J. M. Tishkoff

Program Manager

June 8, 1990

UTRC90-23

THE DETERMINATION OF RATE – LIMITING STEPS DURING SOOT FORMATION

Annual Report

Table of Contents

List of Figures

UTRC90-23

THE DETERMINATION OF RATE-LIMITING STEPS DURING SOOT FORMATION

Annual Report

I. Summary

A single-pulse shock tube has been used to examine the pyrolysis and rich oxidation of cyclopentadiene as well as its pyrolysis in the presence of acetylene, biacetyl, and benzene. In addition, mixtures of benzene and hydrogen have been copyrolyzed at ratios of one-to-three. These fuels have been diluted in argon and shock heated over the temperature range of 1200 to 2000K and at total pressures of ten to thirteen atmospheres. Dwell times were about 500-600 microseconds. Collected gas samples were analyzed using gas chromatography for hydrogen, carbon oxides and C_1- to C_{14}-hydrocarbons. Experimental results and preliminary chemical kinetic modeling lead to mechanistic proposals on the decomposition of C_5-rings as well as isomerization processes between C_5- and C_6-rings. In addition, data on cyclopentadiene indicates that this fuel has a sooting tendency comparable to that of benzene. These results indicate that C_5-rings can play a very significant role in the formation of soot.

Simplified modeling techniques of soot formation based on the MAEROS code have been extended. Soot formation as measured by Bockhorn and coworkers in a premixed propane/oxygen flame has been predicted although better agreement with experimental data was obtained assuming that naphthalene is the inceptor for soot. Previous studies had indicated that benzene formation could be used as a surrogate for the inception rate of soot particles. In addition, some parametric studies on the effect of variation in temperature and inception rates have been performed. Calculations indicate that initial soot formation rates are strongly dependent on inception rates, but final soot fractions produced in flames are much less dependent on inception rates than had previously been assumed.

II. Introduction

There is increasing experimental evidence that important rate-limiting steps to soot formation are the production and growth of aromatic rings. Detailed modeling and comparison to experimental data has led to a good understanding of mechanisms and rates for the production of benzene (and phenyl radical). Existing mechanisms for the formation of naphthalene (plus related species) and higher order aromatics are principally thermochemical estimates and no experimental verification of these steps (mechanisms or rate constants) are available. A major unknown is the importance of C_5-species on ring growth. Flame studies indicate that cyclopentadiene has sooting characteristics similar to that of aromatics, but mechanisms are lacking to explain the rapid conversion to C_6-rings which are believed to dominate in ring growth processes. Another large uncertainty in soot formation mechanisms is the effect of oxidation. Under many conditions, growth of polyaromatic hydrocarbons (PAH's) may be quite fast but is counterbalanced by oxidation. Therefore, the net production rate of PAH's and therefore of soot is only a small fraction of the "gross" production rate of PAH's. Oxidation processes (mechanisms and rates) of aromatic hydrocarbons at elevated temperatures (> 1200K) are unfortunately very poorly known.

To investigate these important and competitive phenomena, an experimental and modeling program is being performed. The experimental phase of the program involves the use of a single-pulse shock tube to thermally stress mixtures of gases, which are then quenched, and the reaction products are analyzed. This program is focusing on detection of two- and three-ringed products in order to test mechanisms proposed for the formation of these species. In support of this work and under corporate sponsorship, the gas sampling system has been modified to collect and detect high molecular weight species. Results of these modifications were extremely successful and the modified facilities were described in last year's report. To examine the importance of C_5 rings, cyclopentadiene has been pyrolyzed, oxidized and copyrolyzed with acetylene, biacetyl, and benzene. Results on rich oxidation of benzene has been investigated and were reported in last years annual report. Furthermore, in order to help obtain additional information on species identification, a mass spectrometer will be added on to the gas chromatogragh. This added feature will insure greater confidence in the identification of high molecular weight intermediates.

Two types of modeling are being performed as part of this contract. Detailed chemical kinetic modeling is being used for comparison to experimental data and to test reaction mechanisms and rate constants for formation of multi-ringed species and for oxidation processes. Secondly, using concepts developed from this work and from the literature, simplified models are being examined which may be useful in describing the formation and growth of soot. Preliminary results of calculations described last year for an ethylene/air flame have been extended to include calculations of particulates produced in other laboratory flames.

III. Results

A. Experimental Results and Interpretations

Since the end of the previous AFOSR contract in November 1987, thirty-eight separate mixtures have been shock heated and products analyzed by gas chromatography. The mixtures are listed in Table I (for 1988) and Table II (for 1989). Six of the mixtures were examined as part of the first year of this AFOSR program and 10 mixtures were shock-heated in the second year of the program; the remainder were tested under corporate sponsorship. For these tests, dwell times were typically 500 microseconds and total pressures (balance argon) were 9 to 13 atmospheres. Typically each series of experiments consisted of 8 to 15 individual shocks.

For each of these series, gas chromatographic data for hydrogen, carbon oxides, and hydrocarbon species from methane up to C_{14}-species was obtained for product gases. Accuracy was decreased with increasing mass. Methane was measured to about three percent accuracy, benzene was measured to about seven percent accuracy and the heaviest hydrocarbons had about thirty percent uncertainty. The complexity of the gas chromatographic spectrum led to some uncertainty in product identification of the high molecular weight hydrocarbons. Consequently, the analytical system is being converted into a gc/ms system to enhance the qualitative analysis of this class of species. The mass spectrometer will be equipped with chemical ionization as well as electron ionization to assist in peak identification. It was originally desired to set up a capability to measure species concentrations in real time using a time-of-flight mass spectrometer coupled directly to the shock tube. Unfortunately, due to technical problems, this approach was terminated.

1. Cyclopentadiene decomposition and ring formation

Cyclopentadiene (CPD) is not sold commercially since it easily dimerizes into dicyclopentadiene (DCP). Initial shock tube experiments (corporate funded) using DCP had ambiguous interpretations, so a facility was set up to produce cyclopentadiene for subsequent shock tube experiments. DCP was decomposed to CPD at 170°C, the boiling point of DCP. Subsequently, CPD was separated from DCP in a distillation column and then condensed. Purity of the CPD was approximately 96% which could be further refined to 99.6% by bulb-to-bulb distillation when sufficient CPD was produced. The two principal impurities eluted just before CPD and are believed to be C_5-

Table I

Series of Experiments Completed During the First Year of AFOSR Program

Reactants	Initial Concentrations
Toluene	1%
Benzene	1.1%
Benzene/oxygen	1.1/0.22%
Benzene/oxygen	0.11/0.022%
Benzene/oxygen	1.1/1.1%
Dicyclopentadiene	0.125%
*Acetylene/ethene	1.1/2.2%
*Acetylene/ethene	0.125/0.25%
*Toluene/methanol	1.0/0.15%
*Toluene/hydrogen	1.0/3.1%
*Methylcyclohexane	1%
*Methanol	4%
*Natural Gas/oxygen	4/1%
*Methane/oxygen	4/1%
*Cyclopentadiene	1.4%
*Cyclopentadiene	0.1%

* Performed under corporate sponsorship

Table II

Series of Experiments Completed During the Second Year of AFOSR Program

Reactants	Initial Concentrations
CPD[+]/oxygen	1.4%/0.91%
CPD/oxygen	0.1%/0.065%
CPD/benzene	1.4%/0.4%
CPD/benzene	0.1%/0.03%
CPD/biacetyl	1.4%/0.35%
CPD/biacetyl	0.25%/0.062%
CPD/acetylene	1.4%/1.05%
CPD/acetylene	0.14%/0.105%
Benzene/hydrogen	1.1%/3.3%
Benzene/hydrogen	0.335%/1%
*Methane/oxygen	4%/0.5%
*Methane/oxygen	0.6%/0.075%
*Toluene/oxygen	1%/1%
*Toluene/oxygen	0.255%/1%
*Heptane	1%
*Heptane	0.1%
*Heptane/oxygen	1.0%/0.5%
*Heptane/oxygen	0.1%/0.05%

[+] cyclopentadiene

* performed under corporate sponsorship

compounds. Based on retention times, the impurities have been tentatively identified as 1-pentene and 1,3-pentadiene.

Including corporate-funded experiments, a total of eight series of experiments on CPD were completed. These included pyrolysis (although a small oxygen impurity was present), oxidative pyrolysis, and copyrolyses with biacetyl (a source of methyl radicals) and with acetylene.

Interpretation of these data has been complex due to a large number of high molecular weight species, the lack of any literature mechanisms for the decomposition pathways, and unknowns regarding the role of C_5-species in ring formation or growth. The overall decomposition of cyclopentadiene for 1.4% cyclopentadiene with various additives is shown in Figure 1. Pyrolysis exhibits the slowest rates of decomposition, while the copyrolysis with biacetyl exhibits the highest rates presumably because of the high rates of initiation from biacetyl[1]. Plots of the light hydrocarbon species as a function of initial post-shock temperatures are provided in Figures 2 and 3 for the pyrolysis and the oxidative pyrolysis. The distribution of products appears similar although the concentrations produced during the pyrolysis attain relatively lower levels (note the difference in scales). Of particular note is that the oxidation produces substantially greater relative concentrations of 1,3-butadiene (1,3-C_4H_6) and vinylacetylene (C_4H_4). It is believed that these products arise from an oxidation process of the cyclopentadienyl radical similar to that previously proposed[2]. This decomposition route which includes the formation of C_4-hydrocarbons differs from a proposed pyrolytic process presented in the next paragraph.

A preliminary mechanism for the pyrolysis is presented in Table III. This proposed mechanism does not include any growth reactions and features decomposition which is preceeded by H-atom addition to CPD. The proposed decomposition of the radical adduct to acetylene and the allyl radical is perhaps the lowest energy decomposition pathway for the C_5-ring. The overall endothermicity of Reaction 3 is only about 10 kilocalories per mole although the barrier to the reaction was assigned to that for H-atom abstraction from olefinic hydrocarbons. Other possible reactions involve H-atom shifts within the CPD molecule followed by isomerization to a linear aliphatic. Such steps are similar to those proposed for the decomposition of pyrrole[3]. Results of calculations using this scheme are shown in Figure 4 and compare qualitatively well with the experimental profiles of acetylene and methane in Figure 2. Other products not predicted by this mechanism but shown in Figures 2 and 3 may be from the direct decomposition/isomerization of CPD, from decomposition of the hydrocarbon impurities, or perhaps from a small fraction of oxidation due to an oxygen impurity. This preliminary mechanism underpredicts the amount of decomposition into products at elevated temperatures. Probably unimolecular decomposition or isomerization of CPD or the cyclopentadienyl radical occurs more rapidly at elevated temperatures. At 1400K, the model predicts that more than 10% of the CPD is converted to the cyclopentadienyl radical which is relatively unreactive according to the preliminary model. This prediction is probably not accurate. The fate of the cyclopentadienyl radical will have to be investigated further although it is reasonable to assume that it plays a significant role in ring growth reactions.

An important feature of the data from CPD pyrolysis is the large amount of mass that is converted to high molecular weight material. A plot of the carbon contained in all species with molecular weights of 128 gram/mole and less is shown Figure 5. This data is compared with that observed during the pyrolysis of other hydrocarbons. This figure demonstrates that cyclopentadiene produces large quantities of high molecular weight material (a qualitative measure of soot production) similar to that of aromatic hydrocarbons and much greater than observed for aliphatic species. This result is not surprising considering the aromatic character of CPD and the resonantly-enhanced stability of the cyclopentadienyl radical. This result however leads to some concerns about existing models for soot production since none of them include the potential role of C_5-species.

Figure 1

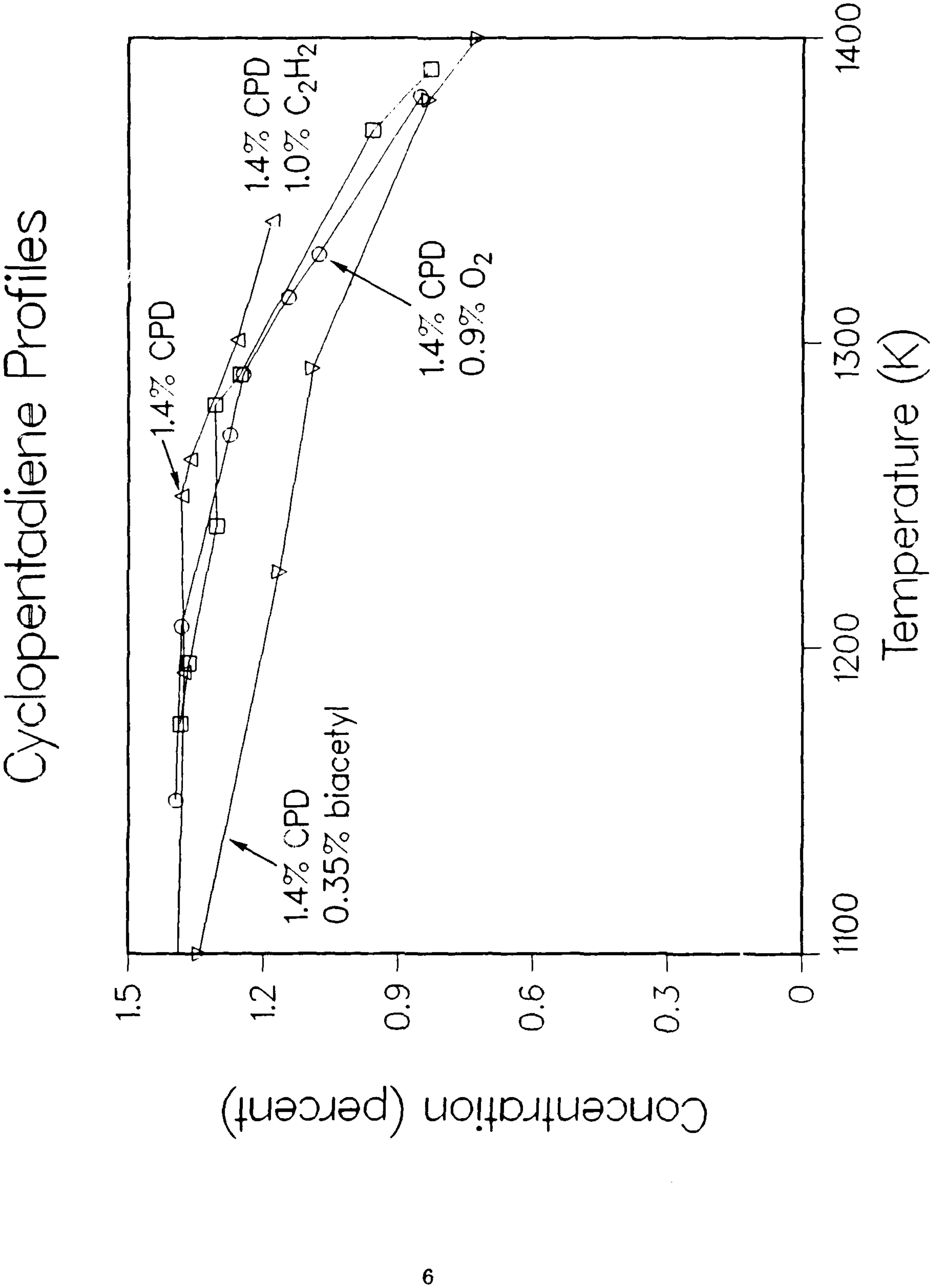
Cyclopentadiene Profiles
1.4% CPD
1.4% CPD
1.0% C_2H_2
1.4% CPD
0.9% O_2
1.4% CPD
0.35% biacetyl
Concentration (percent)
1.5
1.2
0.9
0.6
0.3
0
1100
1200
1300
1400
Temperature (K)

Figure 2

Light Products from Pyrolysis of 1.4% Cyclopentadiene

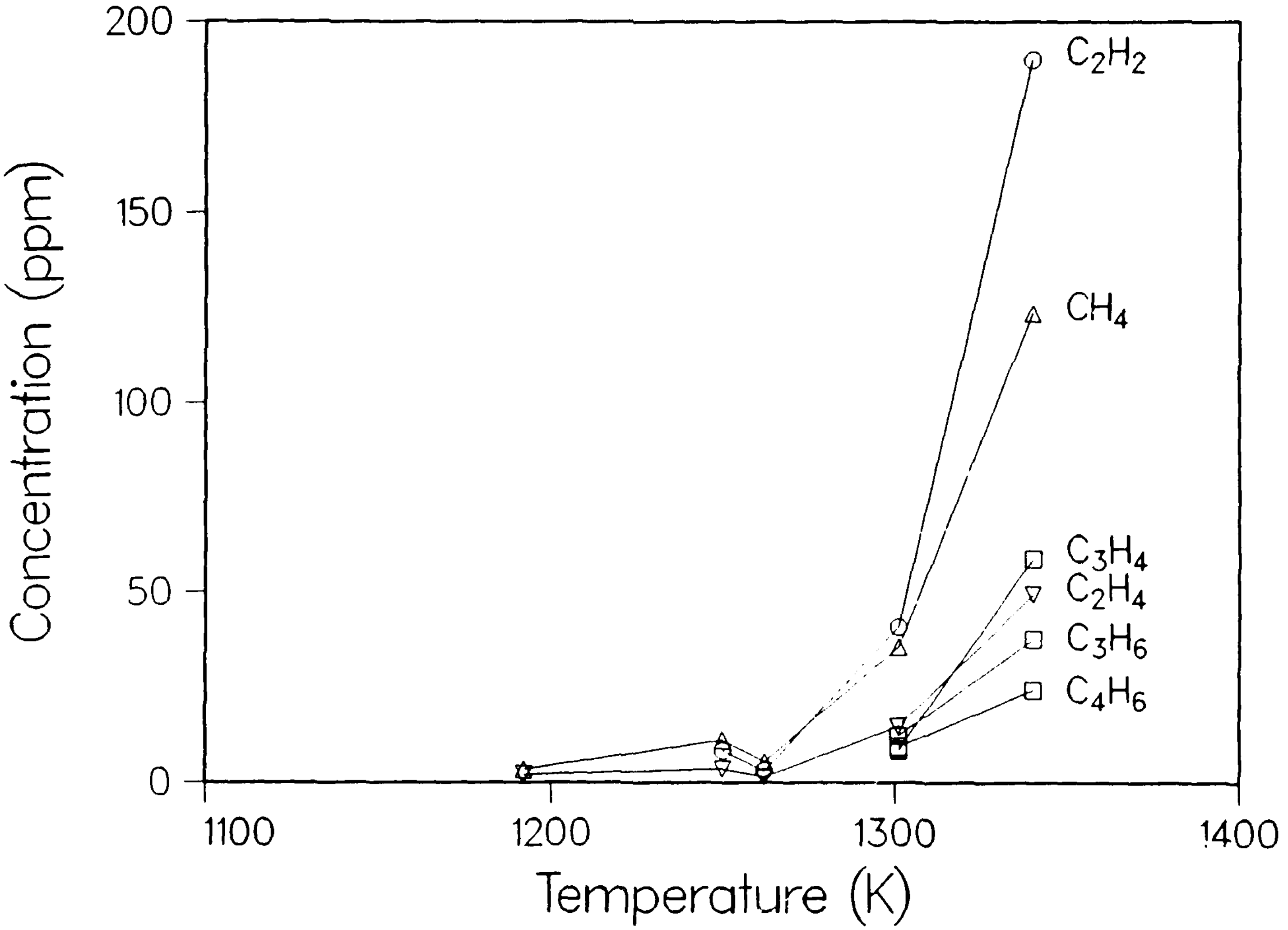

Figure 3

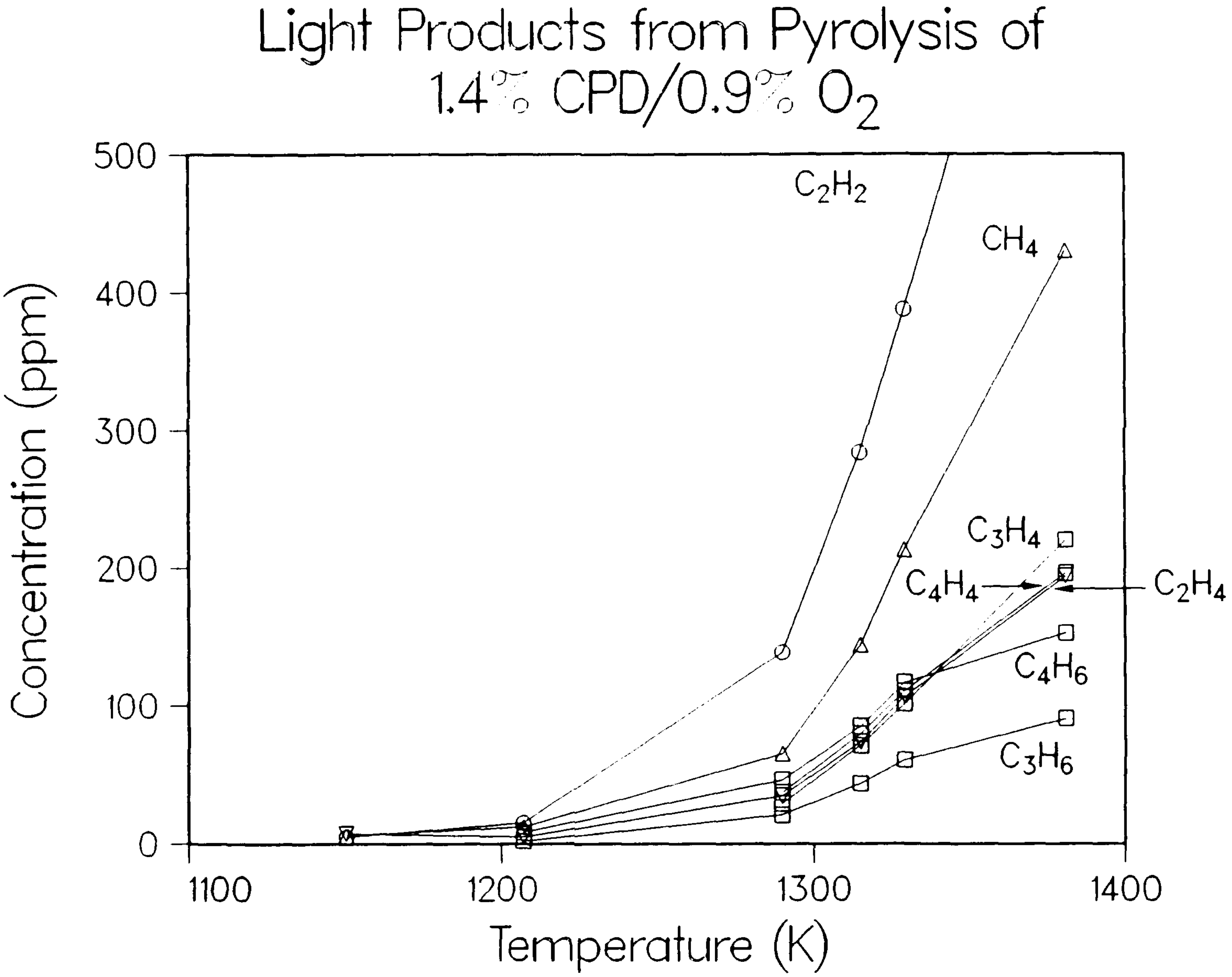

Light Products from Pyrolysis of 1.4% CPD/0.9% O_2

Table III

Preliminary Mechanism for the Pyrolysis of Cyclopentadiene

	Reactions Considered	Pre Exp	Act Eng
1.	$c\text{-}C_5H_6 \leftrightarrow H+c\text{-}C_5H_5$	0.600D+16	81000.
2.	$H+c\text{-}C_5H_6 \leftrightarrow H_2+c\text{-}C_5H_5$	0.100D+14	3000.
3.	$H+c\text{-}C_5H_6 \leftrightarrow C_2H_2+C_3H_5$	0.500D+14	14000.
4.	$H+c\text{-}C_5H_6 \leftrightarrow C_2H_2+C_3H_3+H_2$	0.300D+14	27000.
5.	$CH_2+C_2H_2 \leftrightarrow C_3H_3+H$	0.180D+13	0.
6.	$CH_3+C_2H_2 \leftrightarrow CH_3CHCH$	0.620D+12	7700.
7.	$H+C_3H_4 \leftrightarrow CH_3CHCH$	0.580D+13	3100.
8.	$CH_3CHCH \leftrightarrow C_3H_5$	0.140D+14	36000.
9.	$H+ALLENE \leftrightarrow C_3H_5$	0.400D+13	2700.
10.	$CH_3+c\text{-}C_5H_6 \leftrightarrow CH4+c\text{-}C_5H_5$	0.500D+13	5000.
11.	$CH_3+H \leftrightarrow CH_2+H_2$	0.724D+15	15100.
12.	$C_3H_3+H_2 \leftrightarrow C_3H4+H$	0.400D+13	18000.
13.	$C_3H_3+c\text{-}C_5H_6 \leftrightarrow C_3H4+c\text{-}C_5H_5$	0.100D+14	8000.
14.	$C_3H_3+c\text{-}C_5H_5 \leftrightarrow A1+C_2H_2$	0.400D+13	0.
15.	$H + C_2H_2 \leftrightarrow C_2H_3$	0.550D+13	2500.
16.	$C_2H4 + H \leftrightarrow C_2H_3 +H_2$	0.692D+15	14500.
17.	$C_3H_5+H \leftrightarrow CH_3+C_2H_3$	0.200D+14	12000.
18.	$H+C_3H_6 \leftrightarrow C_2H4+CH_3$	0.100D+13	5000.
19.	$C_3H_6+H \leftrightarrow C_3H_5+H_2$	0.501D+14	3500.
20.	$C_3H_5 \leftrightarrow C_3H4+H$	0.398D+14	70000.
21.	$C_3H_5+H \leftrightarrow C_3H_6$	0.400D+14	0.

Notes: Units in cc, moles, cal
$c\text{-}C_5H_5$ = cyclopentadienyl radical
$c\text{-}C_5H_6$ = cyclopentadiene
A1 = benzene

Figure 4

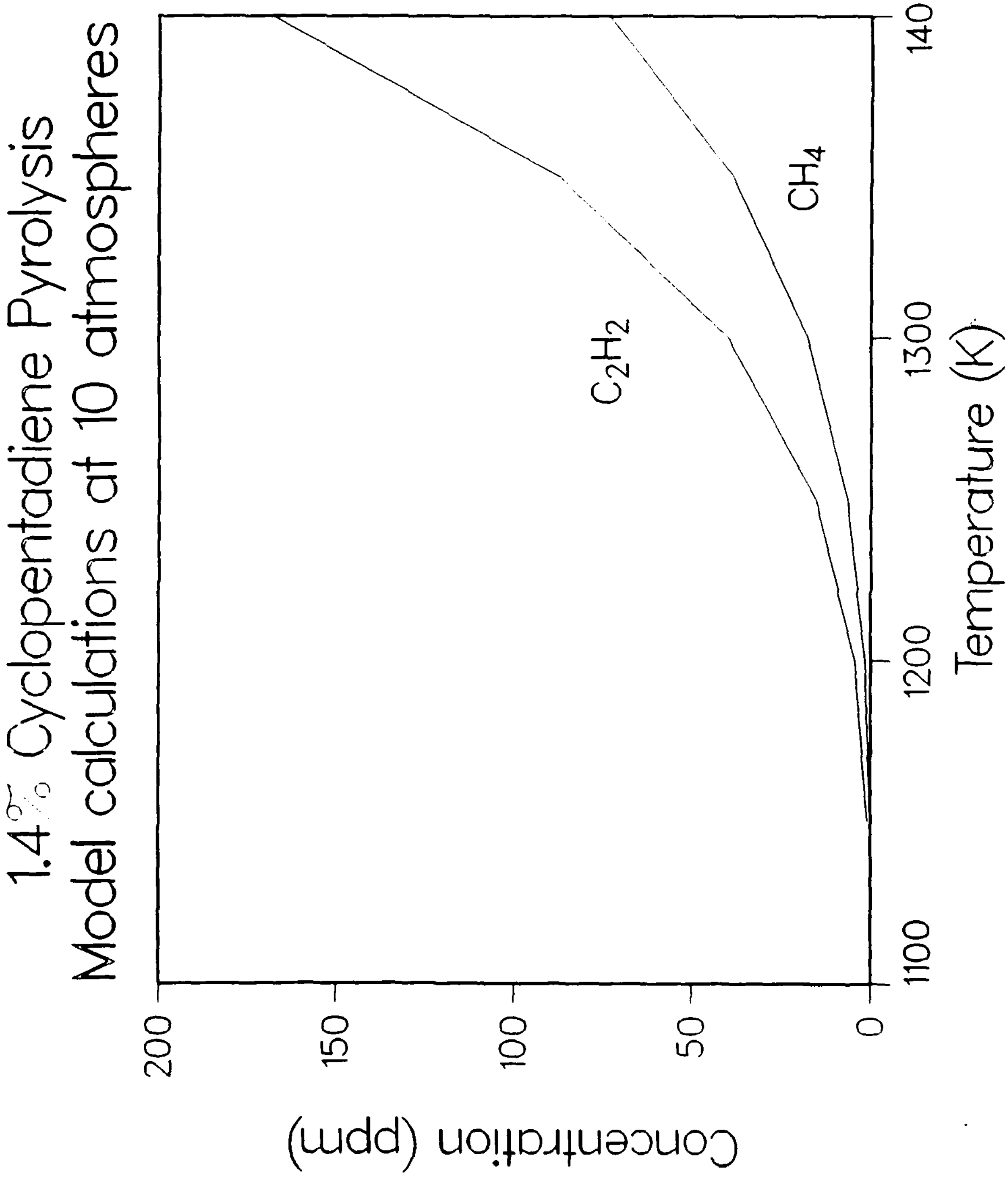

1.4% Cyclopentadiene Pyrolysis
Model calculations at 10 atmospheres

Figure 5

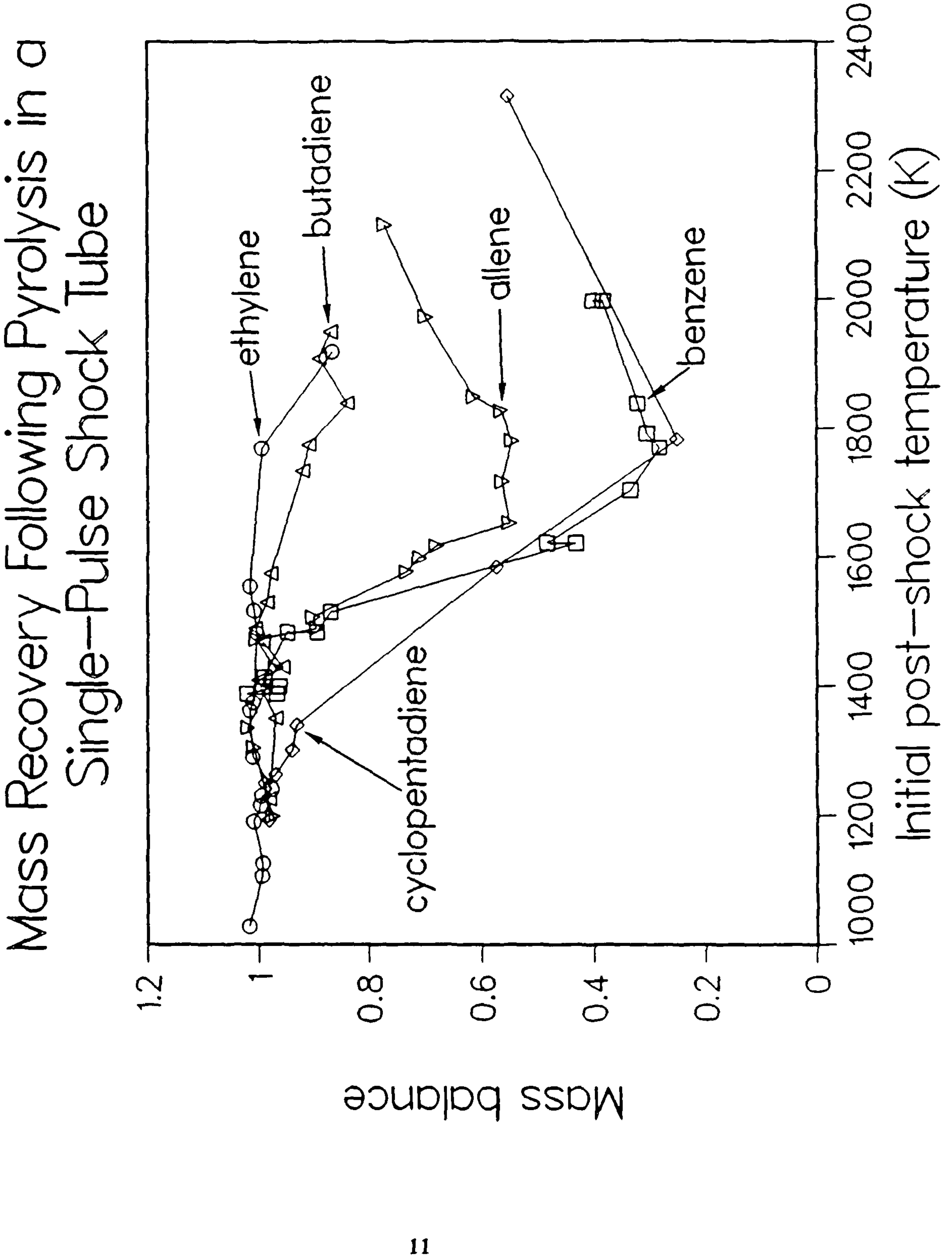

Mass Recovery Following Pyrolysis in a Single-Pulse Shock Tube

Since aromatic species have been linked to the growth to soot, it was of interest to compare benzene production from cyclopentadiene to that produced from other hydrocarbons. Benzene production has been previously shown to correlate well with soot production[4,5]. Shown in Figure 6 is the benzene production from cyclopentadiene as well as that from a few other fuels. As can be seen in this figure, the level of benzene production can be considered intermediate relative to that produced from other fuels, yet the mass deficit apparent from Figure 5 is much larger than the other fuels included in this figure. Thus, benzene production from cyclopentadiene does not correlate with soot production and suggests that benzene formation is skipped in the production of high molecular weight species. These results regarding ring growth from CPD are significant since they demonstrate that C_5-rings (as well as polyaromatic hydrocarbons containing C_5-rings) are much more important then present models describing soot formation assume.

Rapid interchange between C_5 and C_6-rings may also occur. To test this hypothesis, a series of pyrolysis experiments were performed with additives. One of the additives, biacetyl ($(CH_3)_2CO$) was selected since it provides a facile source of methyl radicals and easy modeling techniques are available for estimating the methyl radical concentrations[1]. Methyl radicals in turn may add to the cyclopentadienyl radical to form methylcyclopentadiene. After loss of an H-atom, the resulting radical may isomerize to cyclohexadienyl lose another H-atom and eventually form benzene. This process is similar to the reverse of the mechanism for benzene decomposition recently proposed by Ritter, et al.[6]. A second mechanism for ring interchange was investigated by adding acetylene to the pyrolysis of cyclopentadiene. We speculated that acetylene add to cyclopentadienyl radical and the resultant adduct undergoes a ring enlargement reaction to form the benzyl radical, which becomes toluene after H-atom addition. This process is the reverse of a proposed step for the decomposition of the benzyl radical[7], although many different proposals have been made (see for example Ref. 8).

Benzene production from pure cyclopentadiene is compared to benzene production during copyrolysis of cyclopentadiene and biacetyl in Figure 7. Also included on this plot is data on the two isomers of the speculated intermediate, methylcyclopentadiene. Biacetyl clearly and dramatically increases the concentration of the methylcyclopentadienes as well as significantly increase the concentration of benzene. In Figure 8, toluene produced from cyclopentadiene pyrolsis and from a mixture of CPD and acetylene is shown. Again large increases in the conversion to aromatics was observed by the presence of an additive. Together these results not only provide evidence supporting recent proposals for ring fracture, but also confirm speculation of rapid interchange mechanisms between C_5 and C_6-rings.

2. Explanation for Methane Formation During Benzene Pyrolysis

In many previous experiments on benzene pyrolysis, a significant amount of methane has been produced (on the order of 0.5% of the carbon)[9]. The magnitude of this methane production is large considering existing models for benzene production predict either no or negligible conversion to methane. The observed formation of methane has remained unexplained for several years. The work (experimental and modeling) described above on cyclopentadiene pyrolysis offers a very reasonable explanation for this methane formation. The general reaction scheme is as follows, although only a portion of the benzene ($\approx 5\%$) decomposes in this manner.

$$\begin{aligned} H + C_6H_6 &\leftrightarrow C_6H_7 \\ C_6H_7 &\leftrightarrow \mathrm{Me\dot{C}PD} \\ \mathrm{Me\dot{C}PD} + H &\leftrightarrow CH_3 + C_5H_5 \\ CH_3 + C_6H_6 &\leftrightarrow CH_4 + C_6H_5 \end{aligned}$$

Figure 6

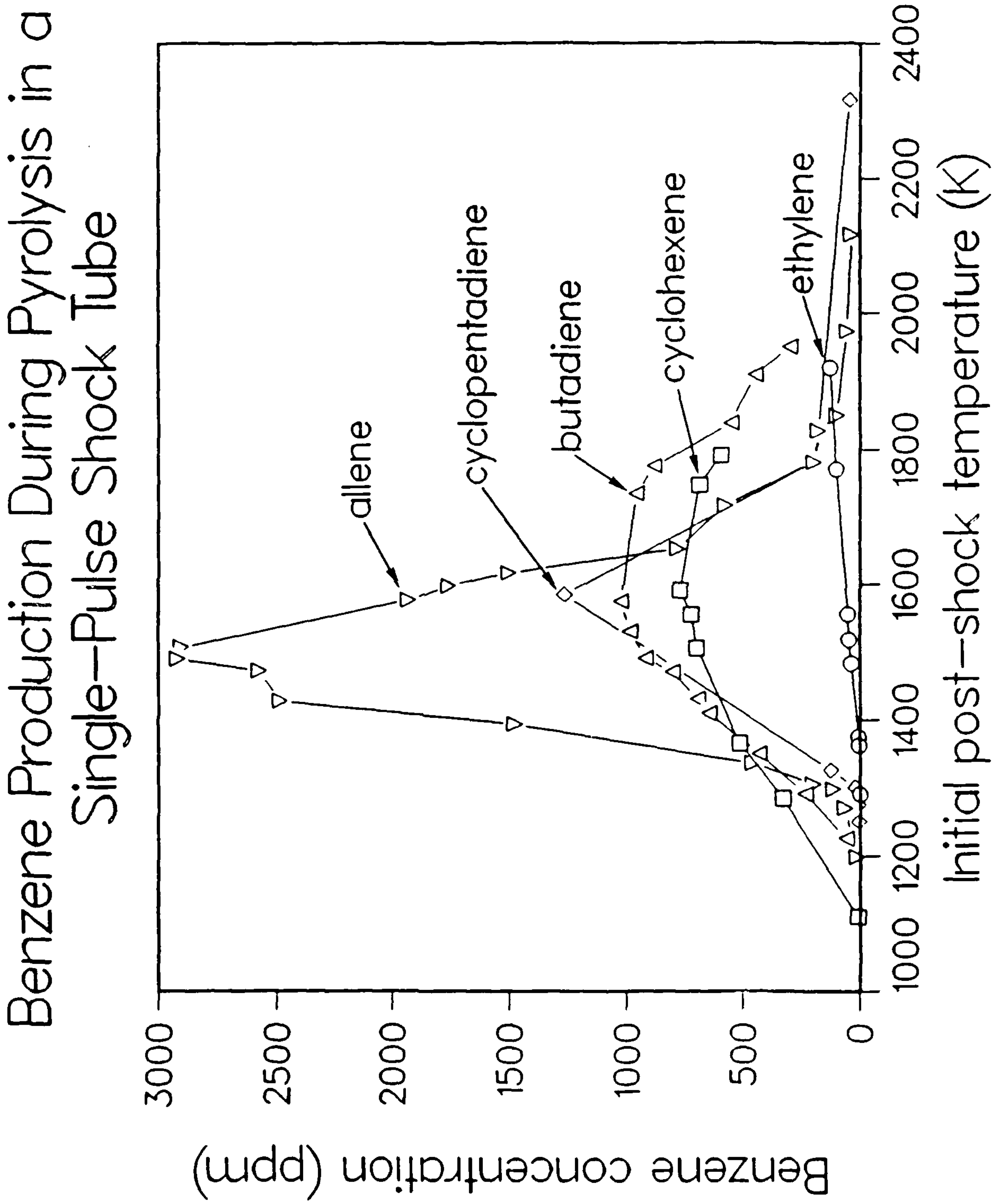
Benzene Production During Pyrolysis in a Single—Pulse Shock Tube
Benzene concentration (ppm)
3000
2500
2000
1500
1000
500
0
1000
1200
1400
1600
1800
2000
2200
2400
Initial post—shock temperature (K)
allene
cyclopentadiene
butadiene
cyclohexene
ethylene

Figure 7

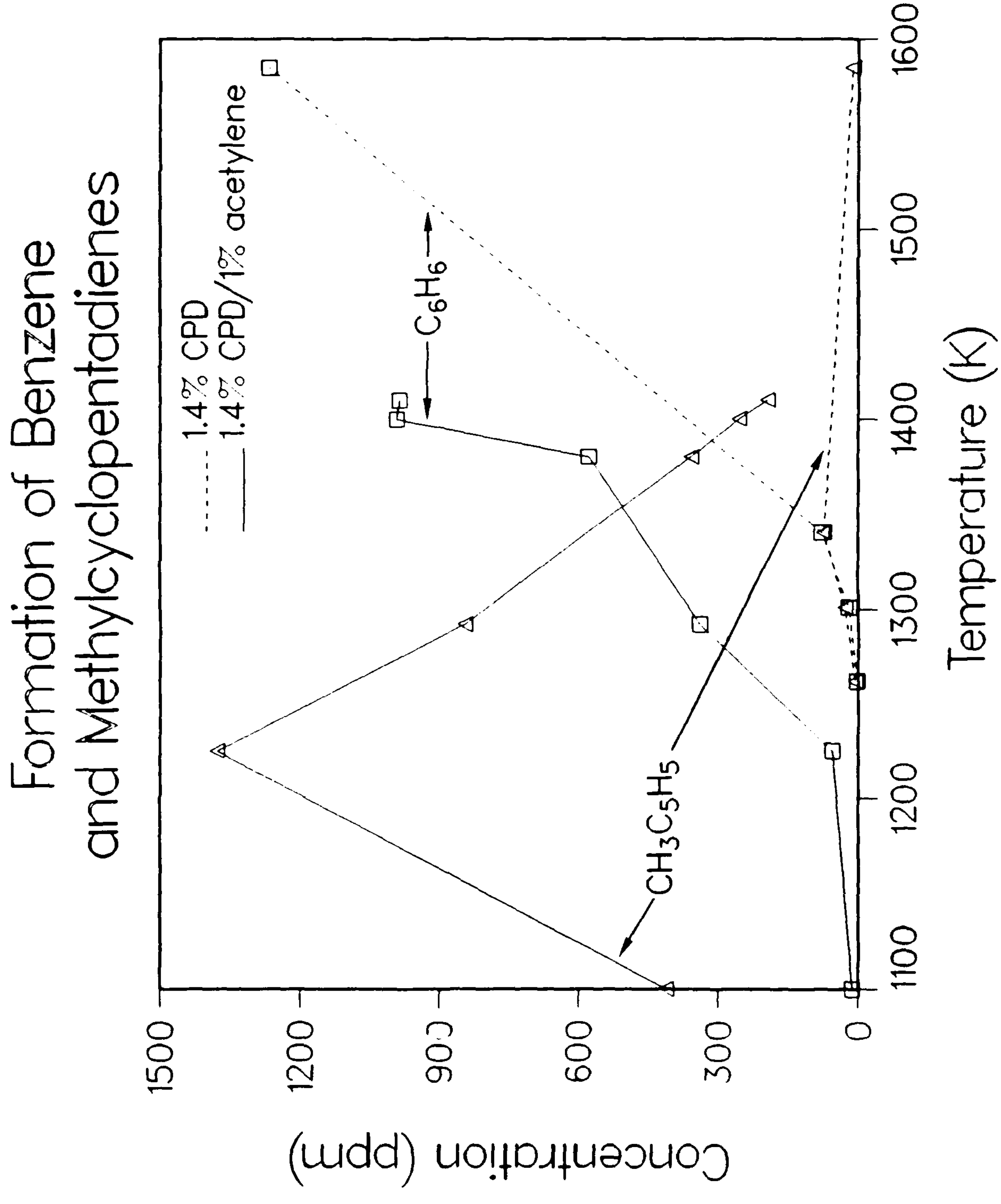
Formation of Benzene
and Methylcyclopentadienes
1.4% CPD
1.4% CPD/1% acetylene
C_6H_6
$CH_3C_5H_5$
Concentration (ppm)
0
300
600
900
1200
1500
Temperature (K)
1100
1200
1300
1400
1500
1600

Figure 8

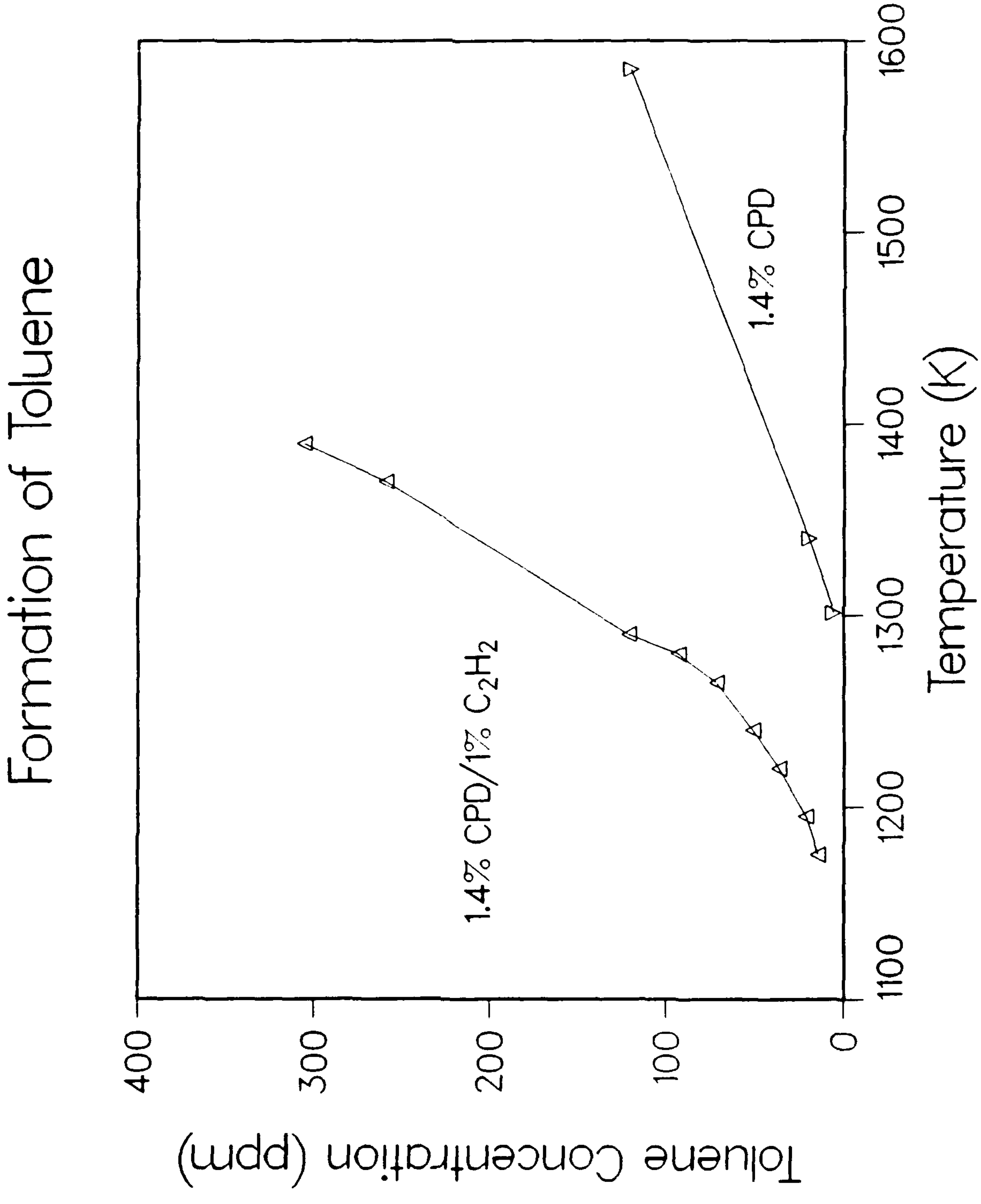
Formation of Toluene
Toluene Concentration (ppm)
400
300
200
100
0
Temperature (K)
1100
1200
1300
1400
1500
1600
1.4% CPD/1% C_2H_2
1.4% CPD

Subsequent decomposition of the cyclopentadienyl radical (C_5H_5) can be expected to form some additional methane. At the temperatures of benzene pyrolysis (1600-1700K), this decomposition should be fast.

3. Addition of Hydrogen to Benzene Pyrolysis

Profiles of end-product species produced from the copyrolysis of 1.1% benzene/3.3% hydrogen were compared with previously obtained data on the pyrolysis of 1.35% benzene. Of particular note was the fact that hydrogen addition suppressed both the decomposition of benzene at lower temperatures and the formation of high molecular weight species. Both of these effects can be traced to the reaction

$$C_6H_5 + H_2 \leftrightarrow C_6H_6 + H$$

which is pushed to the right with excess hydrogen and thus suppresses the phenyl radical concentration. Phenyl radical in turn is the controlling intermediate species which leads to ring decomposition as well as to ring growth. Plots of some polyaromatic hydrocarbons are shown in Figure 9 for the benzene/hydrogen mixture and can be compared to that produced from the pyrolysis in Figure 10. Hydrogen addition leads to approximately a 30% reduction in biphenyl and about a factor of two reduction in acenaphthylene. Phenanthrene production is essentially fully suppressed.

A simplified model was constructed for benzene pyrolysis based on reactions and rate constants previously published[10], although the rate constant by Fahr and Stein[11] for the reaction

$$C_6H_5 + C_6H_6 \leftrightarrow C_{12}H_{10} + H$$

was used. Predictions of the biphenyl production are shown in Figure 11. Calculations are shown for both the pyrolysis and the copyrolysis with hydrogen. Qualitatively, the predictions are very similar to the experimental data. Perhaps the most noticeable differences is the location of the peak which is predicted to be about 100K higher than the peak in experimental data. In addition the experiment indicates substantial quantities of biphenyl formation at low temperatures. Using a preliminary mechanism for the oxidative pyrolysis of benzene, both of these differences could be explained by small concentrations (a few hundred ppm) of oxygen. The absolute magnitude of biphenyl is, however, not dramatically effected.

In modeling work on toluene, it was found that substantial quantities of bibenzyl were formed in the rarefraction wave in the shock tube prior to collection and analysis of the gas sample. To test whether a similar phenomenon was occurring with biphenyl in the benzene system, calculated profiles of biphenyl as function of time were plotted. These curves are shown in Figure 12. At low temperatures, the production of biphenyl is dramatically reduced once the rarefraction wave arrives (at 600 microseconds). This occurs even at elevated temperatures when then the biphenyl concentration increases to a maximum and then falls before the arrival of the cooling wave. Thus the rarefraction wave appears to quench the production and decay of biphenyl so that the measured concentrations accurately reflect the actual concentrations at the end of the high temperature pyrolysis period.

B. Soot Aerosol Dynamics Simulations

In the last annual report, we presented the results of a simplified aerosol dynamics model for soot growth. With the aim of modelling the growth of soot spheroids, we adapted the most recent version of a well-known aerosol dynamics code, MAEROS, which is a fixed- grid, sectional

Figure 9

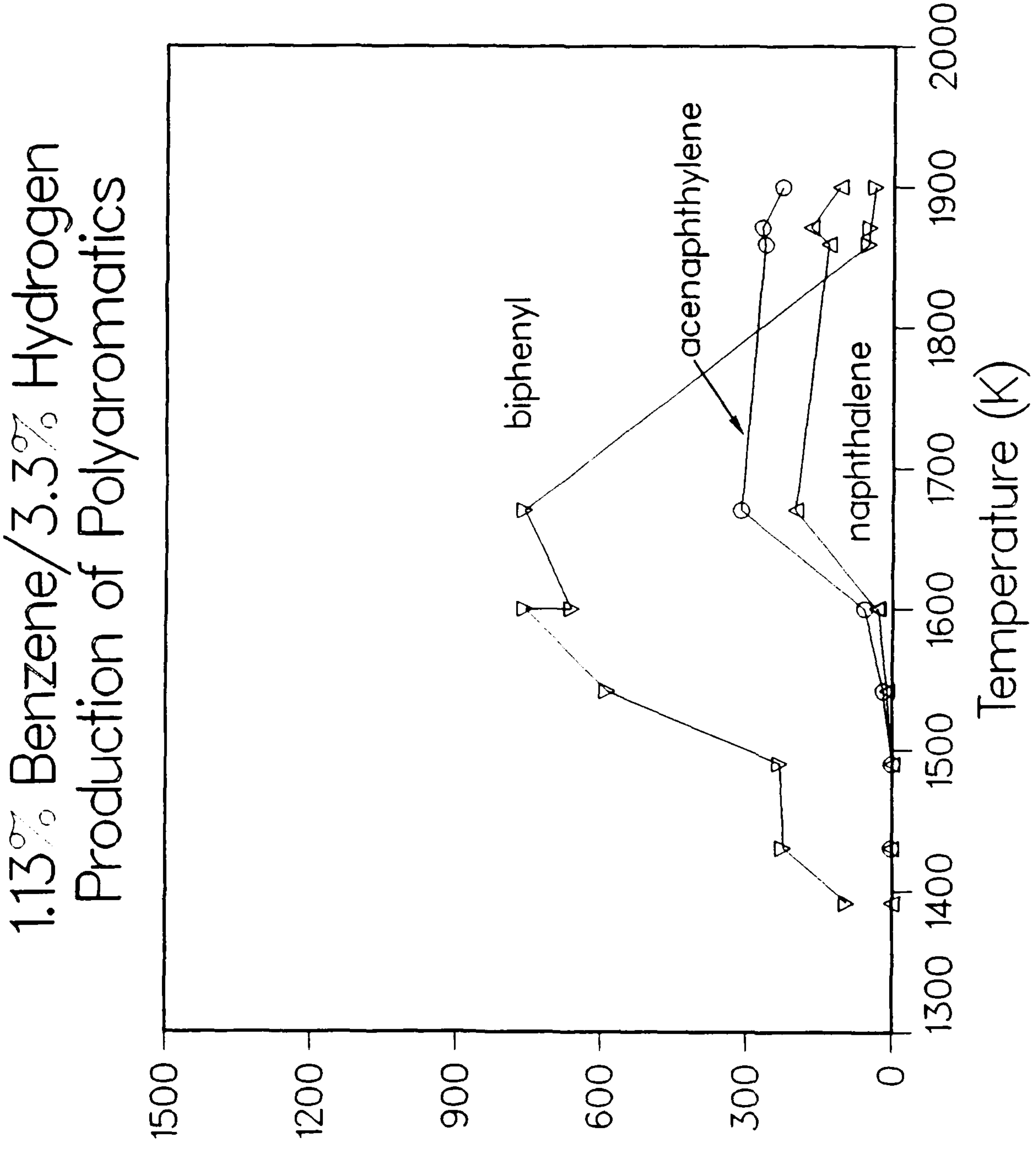
1.13% Benzene/3.3% Hydrogen
Production of Polyaromatics
Concentration
1500
1200
900
600
300
0
1300
1400
1500
1600
1700
1800
1900
2000
Temperature (K)
biphenyl
acenaphthylene
naphthalene

Figure 10

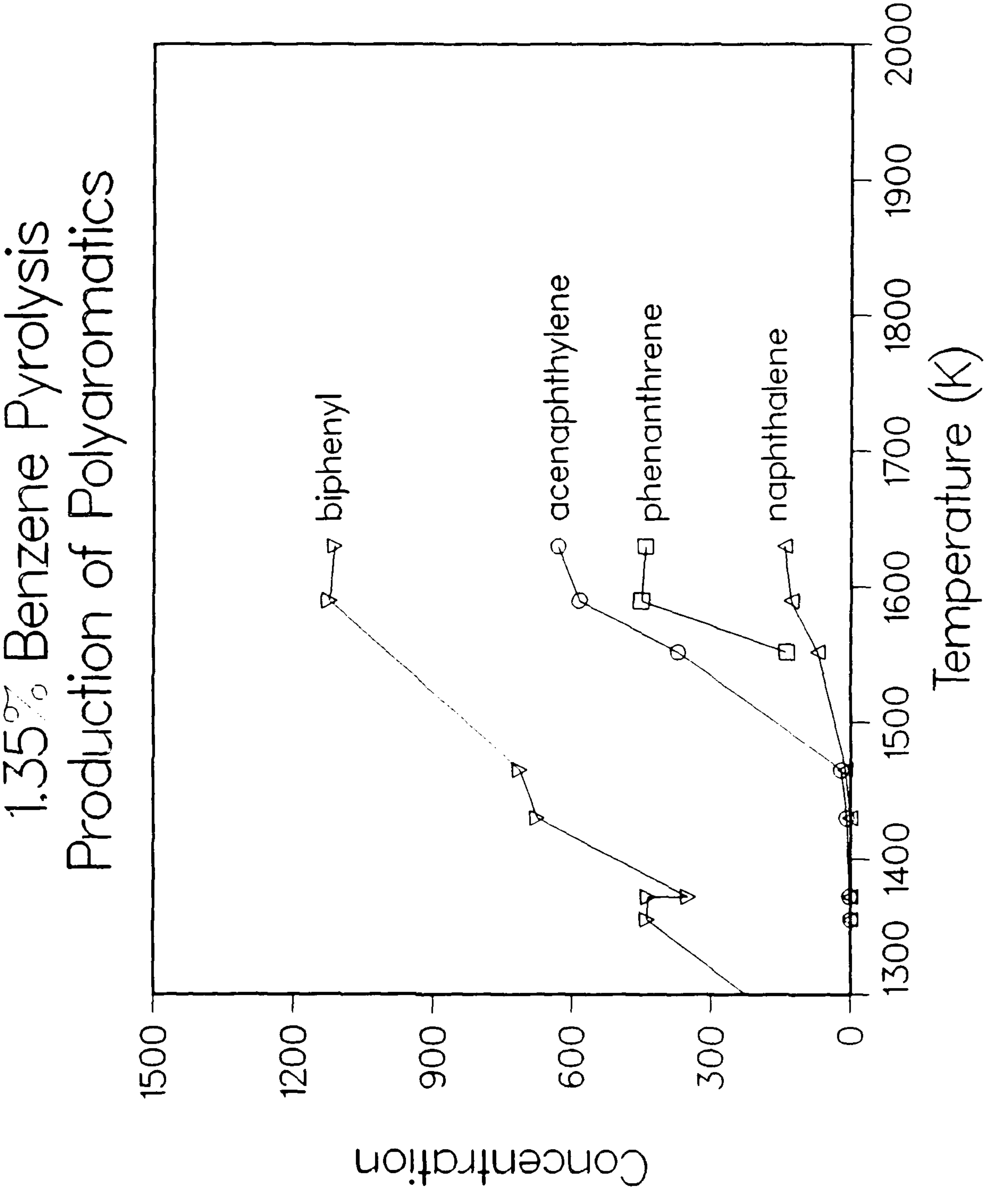

1.35% Benzene Pyrolysis
Production of Polyaromatics

Figure 11

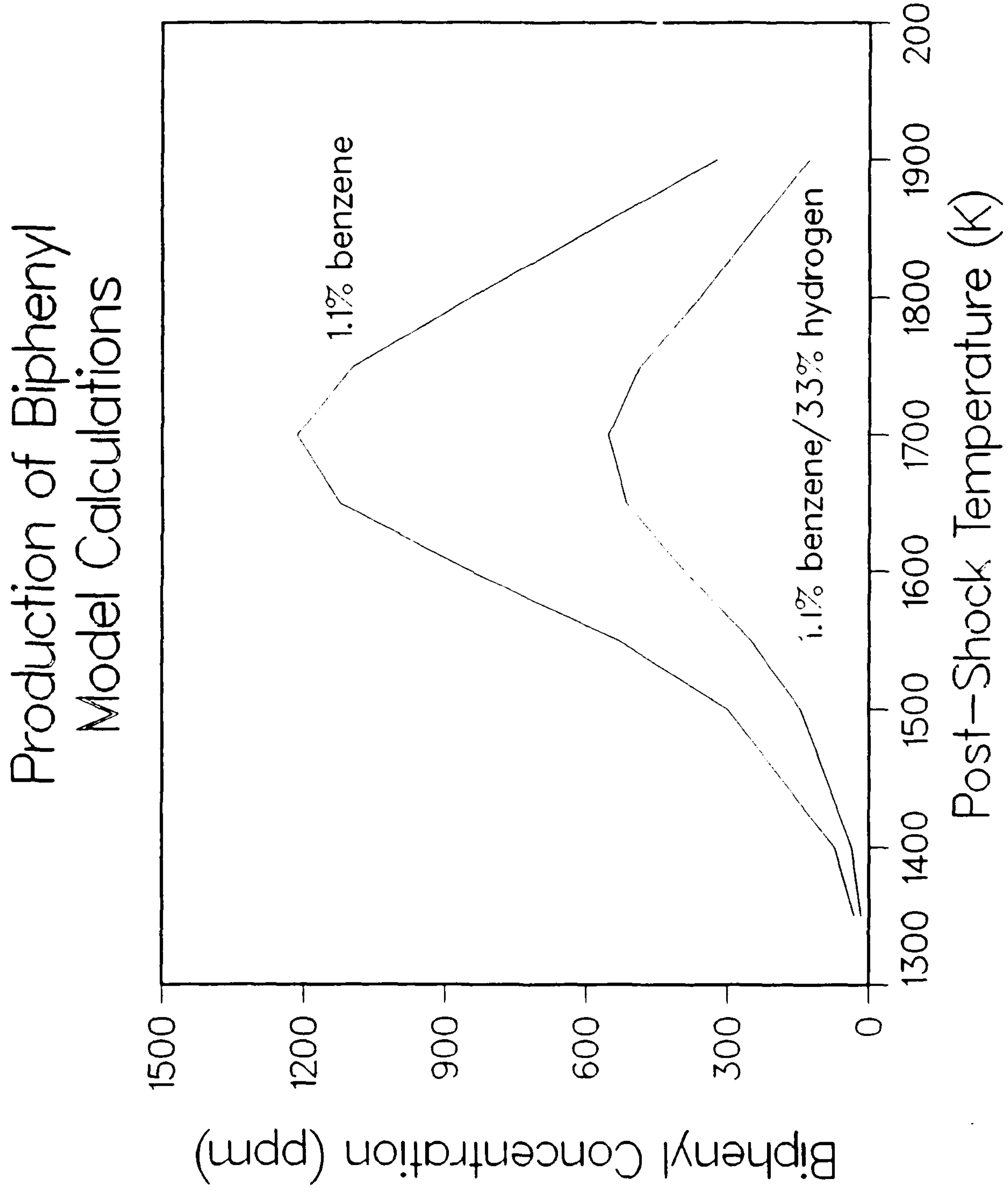
Production of Biphenyl
Model Calculations
1.1% benzene
1.1% benzene/33% hydrogen
Biphenyl Concentration (ppm)
0
300
600
900
1200
1500
Post-Shock Temperature (K)
1300
1400
1500
1600
1700
1800
1900
2000

Figure 12

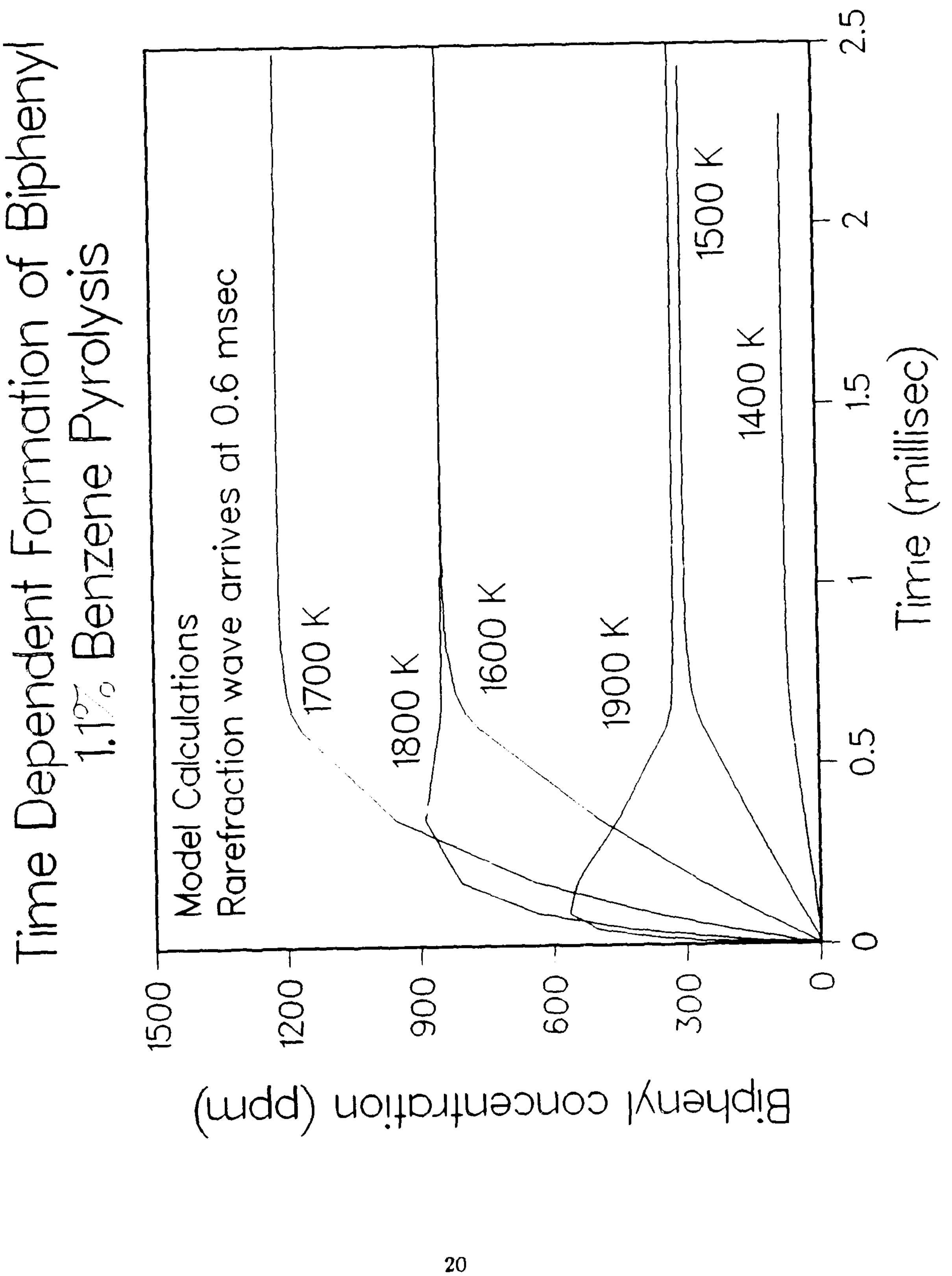
Time Dependent Formation of Biphenyl
1.1% Benzene Pyrolysis
Model Calculations
Rarefraction wave arrives at 0.6 msec
1700 K
1800 K
1600 K
1900 K
1500 K
1400 K
Biphenyl concentration (ppm)
0
300
600
900
1200
1500
Time (millisec)
0
0.5
1
1.5
2
2.5

model including nucleation, surface growth, and coagulation. The lowest size class was assumed to approximate that of a benzene molecule, with an effective nucleation/inception rate given by the production rate of the smallest aromatic molecules, typically taken to be benzene. Surface growth was assumed to be due to acetylene deposition alone, at a rate given by the Harris-Weiner growth rate expression[12]. Provision for oxidative mass removal at a rate given by the Nagle and Strickland-Constable expression[13] was also made in the model. The most important approximation inherent in this approach is the extrapolation of particle dynamic processes and rates into the pre-particle regime. This is a simplified picture of soot growth that glosses over many details of the inception process; the only medium parameters in addition to temperature that need to be specified are the inception (benzene formation) rate and the concentration of the condensible acetylene vapor. The first comparison of the model with the experimental volume fraction data of Harris and co-workers[12,14], taken in a premixed, atmospheric pressure, ethylene-oxygen flame, was very good. Both the magnitude and time dependence of the soot growth were modelled well, and there wa no need to allow for oxidation, a result that was consistent with the stoichiometry. Given the simplifications made, we recognized the possibility that the agreement obtained was fortuitous, and initiated efforts to model other well-characterized flames. One set of calculations in progress is to see if the model reproduces the stoichiometric variation of soot production in the Refs. 12,14 flames; this work involves using CHEMKIN to calculate the acetylene concentration and the benzene source rate, and is in progress at this time.

The only other well-characterized data suitable for modelling purposes have been reported by Bockhorn, et.al.[15] in low-pressure, premixed flames. Soot volume fraction profiles and all the other input data needed to perform the modelling calculations are available. The volume fraction data extend over a temperature range of about 450 K for the propane-oxygen flame we initially concentrated on. The Maeros2 program which we use employs a linear interpolation scheme to determine coagulation and condensation coefficients, these having been calculated exactly at four combinations involving two input temperatures and pressures. We found that the 450 K interval was too large for accurate linear interpolation, and thus had to confine attention to the first ten milliseconds. Work has begun on modifications to the program to permit interpolation between four input temperatures, which should suffice for the larger temperature variations. In any event, considerable growth of the soot volume fraction has occurred within the first ten milliseconds, and it is not felt that any incorrect conclusions will result from this restriction on the calculations. The Harris-Weiner surface growth rate was modified to include a 31.8 kcal activation energy[16], and the oxidation rate has the temperature dependences given in Ref. 13. Calculations performed so far have been limited to the 0.15 atmosphere propane-oxygen flame of Ref. 15. Figure 13 shows the comparison of the calculated and experimental soot volume fractions, assuming that the benzene source rate of Ref. 15 is the appropriate inception rate. With no oxidation, the calculated volume fractions are too large, but there is considerable sensitivity to the oxygen concentration, as seen. For an oxygen concentration of about 1%, the agreement is reasonable for longer times. This flame is somewhat leaner than the Harris flame discussed earlier, so the need to incorporate oxidation is at least qualitatively reasonable. Some indication of the predicted temperature sensitivity is shown in Figure 14. A reasonable temperature variation of ± 100 K does not appear to explain the theory-experiment discrepancy. The foregoing calculations assumed a coalescence sticking probability of unity. Choosing a value of 2.2, as recommended by Harris and Kennedy[17] improves the agreement somewhat, but does not change the basic conclusions. A slightly smaller oxygen concentration is required for agreement. naphthalene production rates are also available in Ref. 16, and we have found that taking naphthalene as the inception source results in much better agreement, as shown in Figure 15. The naphthalene source rate is about one-sixtieth that of benzene. A Van der Waals sticking probability of 2.2 has been employed in this calculation. Our sensitivity calculations show

Figure 13

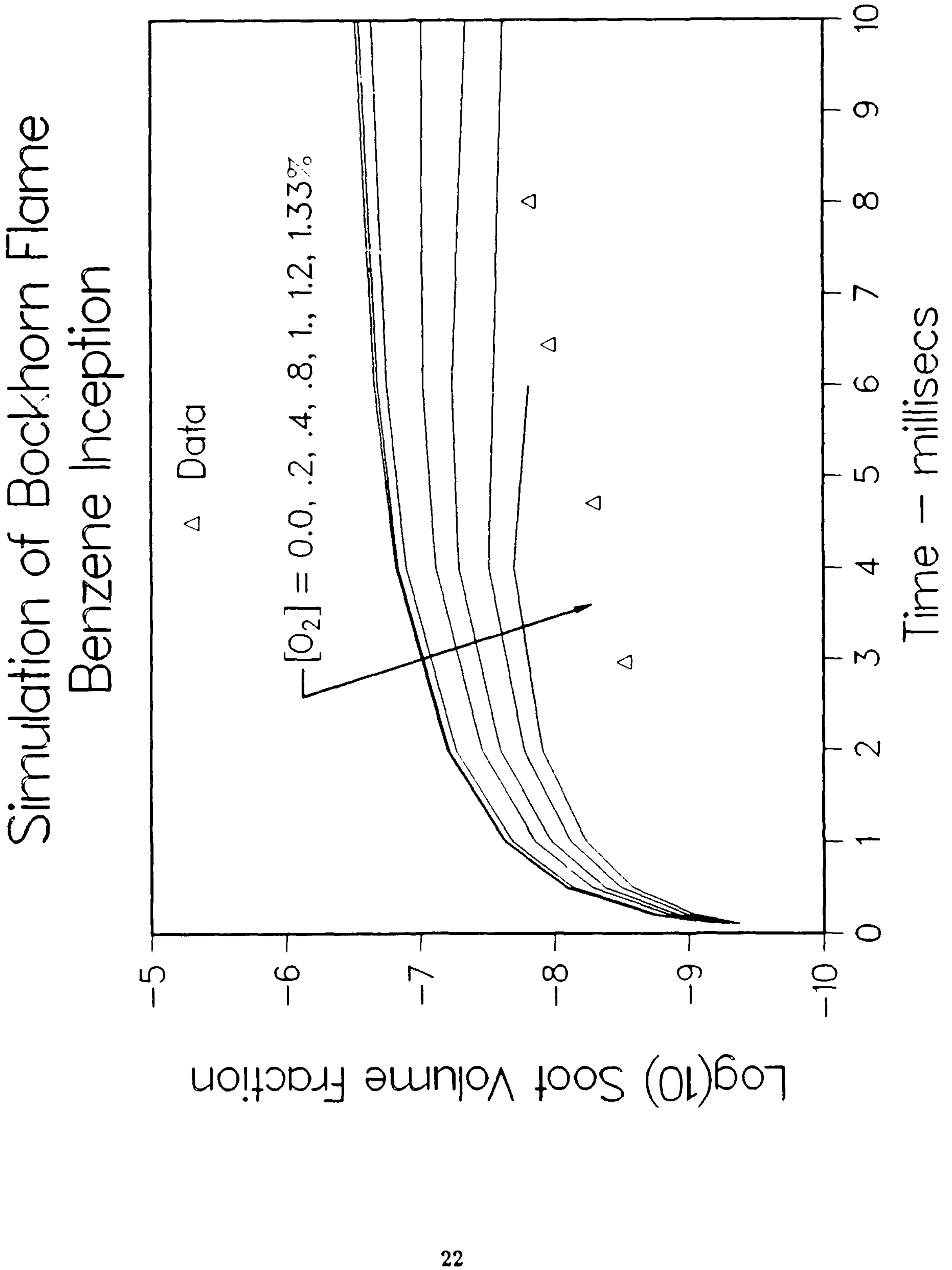

Simulation of Bockhorn Flame
Benzene Inception
△ Data
$[O_2]$ = 0.0, .2, .4, .8, 1., 1.2, 1.33%
Log(10) Soot Volume Fraction
−5
−6
−7
−8
−9
−10
Time — millisecs
0
1
2
3
4
5
6
7
8
9
10

Figure 14

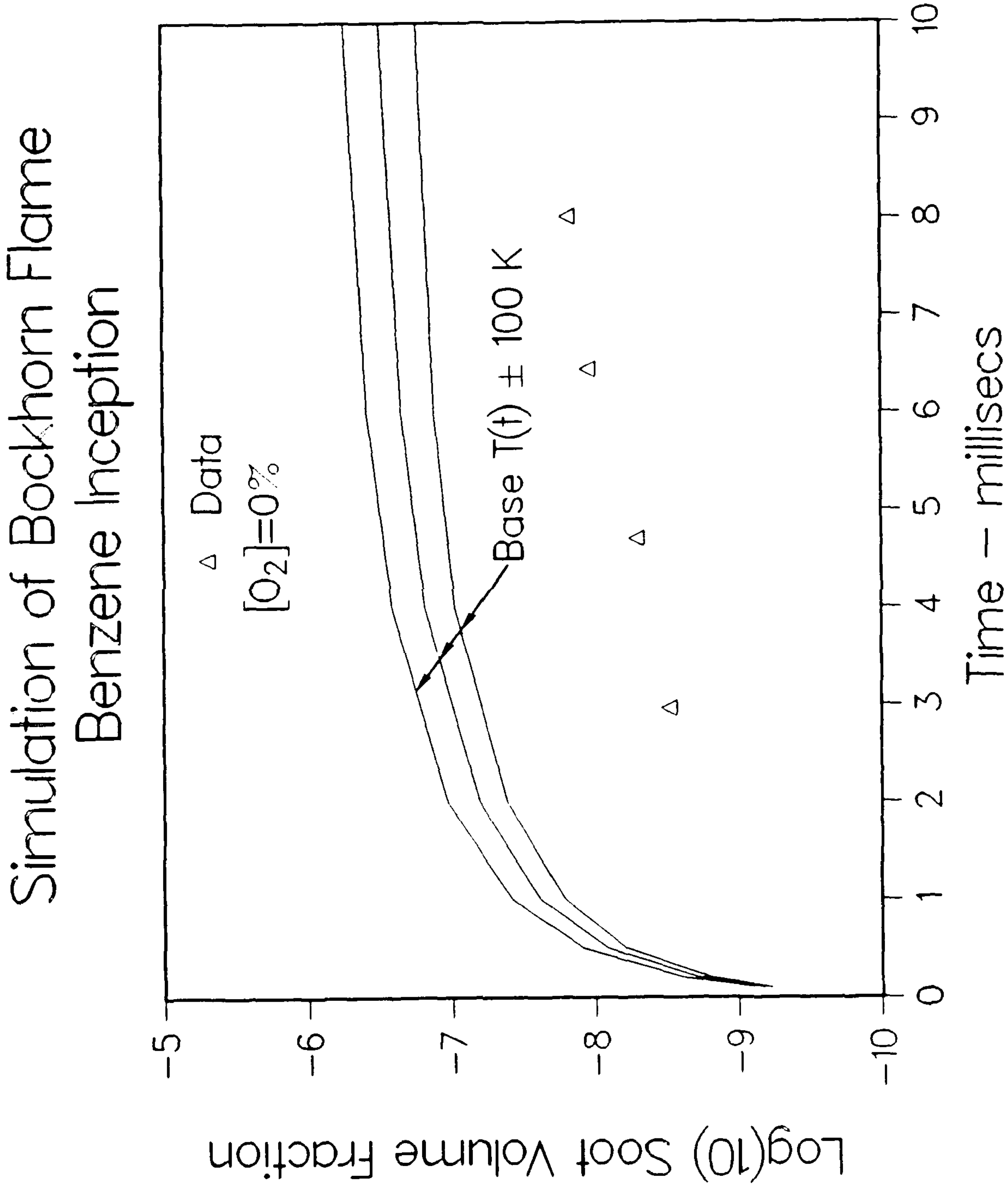
Simulation of Bockhorn Flame
Benzene Inception

Figure 15

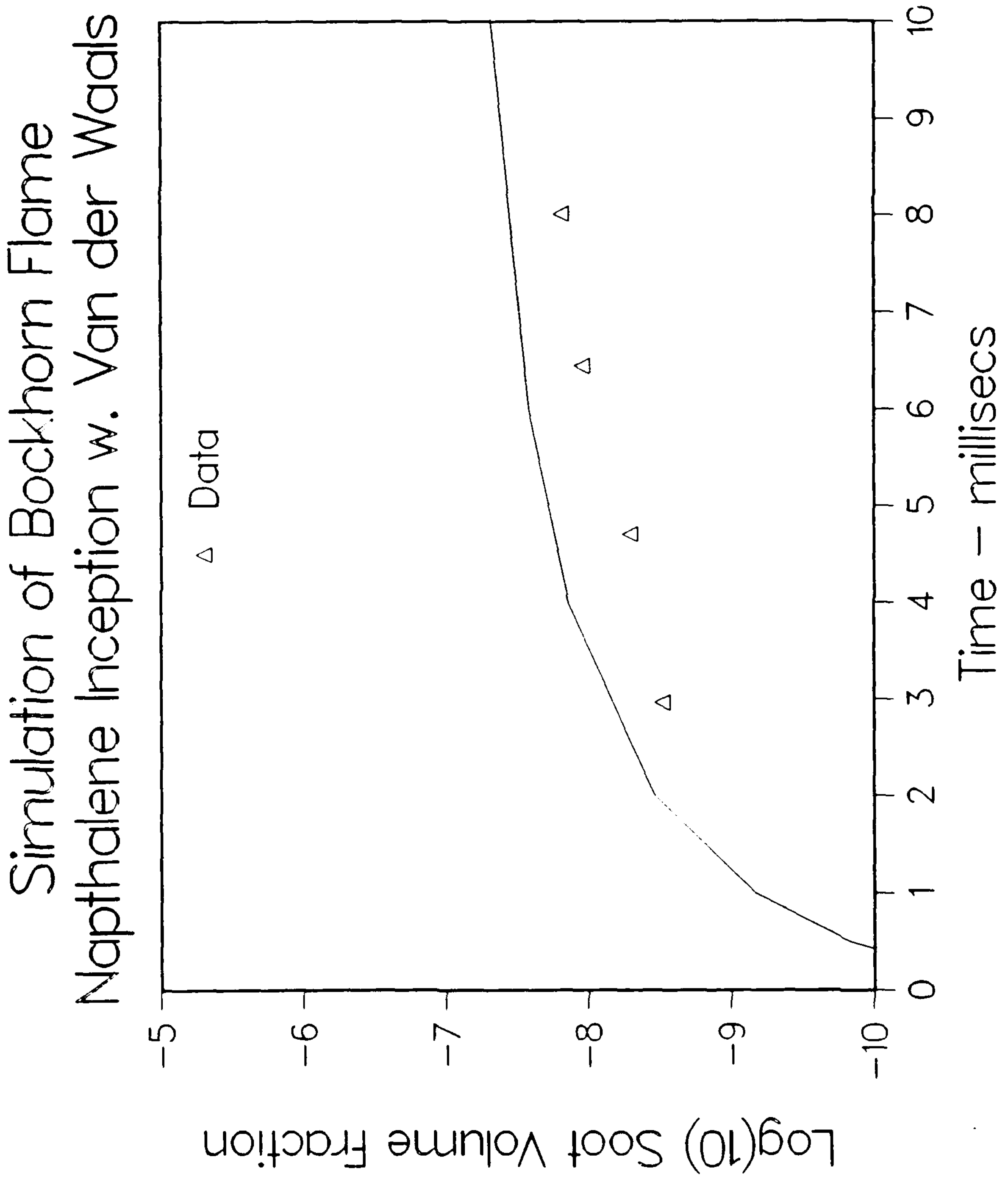
Simulation of Bockhorn Flame
Napthalene Inception w. Van der Waals
Log(10) Soot Volume Fraction
-5
-6
-7
-8
-9
-10
Time — millisecs
0
1
2
3
4
5
6
7
8
9
10
Data

that, compared to the benzene-based simulations, smaller temperature uncertainties and oxygen concentrations would need to be invoked to resolve the small remaining discrepancies. Picking naphthalene as the inception size class might seem to be a better choice than benzene, inasmuch as it is closer to the particle regime, but until more information is available about the oxygen concentrations in these flames, no quantitative conclusions can be drawn. The choice of benzene or naphthalene as the inception source mainly affects the calculated soot loadings at early times. Asymptotically, at long times, calculated differences are generally much less sensitive to inception rate. Because of the previously discussed temperature interpolation problem, however, we can't yet present the accurate long time behavior of the Ref. 15 simulations. Some indication of the sensitivity is presented, however, in Figure 16, where for a constant temperature of 1650 K the effect of reducing the nominal (benzene) inception rate by a factor of 100 is shown. At 100 milliseconds, there is only about a factor of two difference between the two predictions.

In addition to improving the temperature range capability of Maeros2, a need was also identified to improve the numerical integration scheme when there is net soot loss due to oxidation; the present scheme can become unstable when oxidation dominates acetylene deposition.

IV. List of Publications

A reply (to a comment) entitled "On Impurity Effects in Acetylene Pyrolysis" by M. B. Colket, H. B. Palmer and D. J. Seery has been accepted for publication in Combustion and Flame. A copy of this article is provided in Appendix B.

An article entitled "Shock Tube Pyrolysis of Pyridine" by J. C. Mackie, M. B. Colket, and P.F. Nelson has been accepted for publication by the Journal of Physical Chemistry. The final manuscript is included in Appendix C. The research was performed under corporate sponsorship.

A manuscript entitled "Shock Tube Pyrolysis of Pyrrole and Kinetic Modeling" by J. C. Mackie, M. B. Colket, P. F. Nelson and M. Esler has been submitted to the International Journal of Chemical Kinetics for review. A copy of the original manuscript is in Appendix D. The research was performed under joint sponsorship from UTRC and the University of Sydney.

An article entitled "The High Temperature Pyrolysis of Cyclopentadiene" by M. B. Colket will be written in 1990-91 and submitted to Combustion and Flame.

A manuscript entitled "A Simplified Model for the Production of Soot in Premixed Flames" by R. J. Hall and M. B. Colket will be written in 1990-91 and submitted to *Combustion Science and Technology*.

V. Meeting Interactions and Presentations

1. A round table discussion on "Current Problems in Soot Formation During Combustion, Especially the Mechanism of Soot Formation" was held in Göttingen, West Germany on March 29-30, 1989. The meeting was organized by Professor H. Gg. Wagner and was attended by about twenty engineers/scientists currently involved with understanding soot formation phenomena. Financial support was provided by the Commission for Condensation Phenomena of the Academy of Sciences in Göttingen, West Germany.
2. Department of Energy - Office of Basic Energy Sciences Combustion Research Meeting held at Hofstra University on Long Island. M. Colket was invited by W. H. Kirchhoff to be an observer and participant at this D.O.E. contractor's meeting. The meeting was attended under corporate sponsorship.
3. A paper entitled "Simplified Models for the Production of Soot in a Premixed Flame"

Figure 16

Inception Rate Sensitivity on Soot Growth
T = 1650 K; p = .15 atm

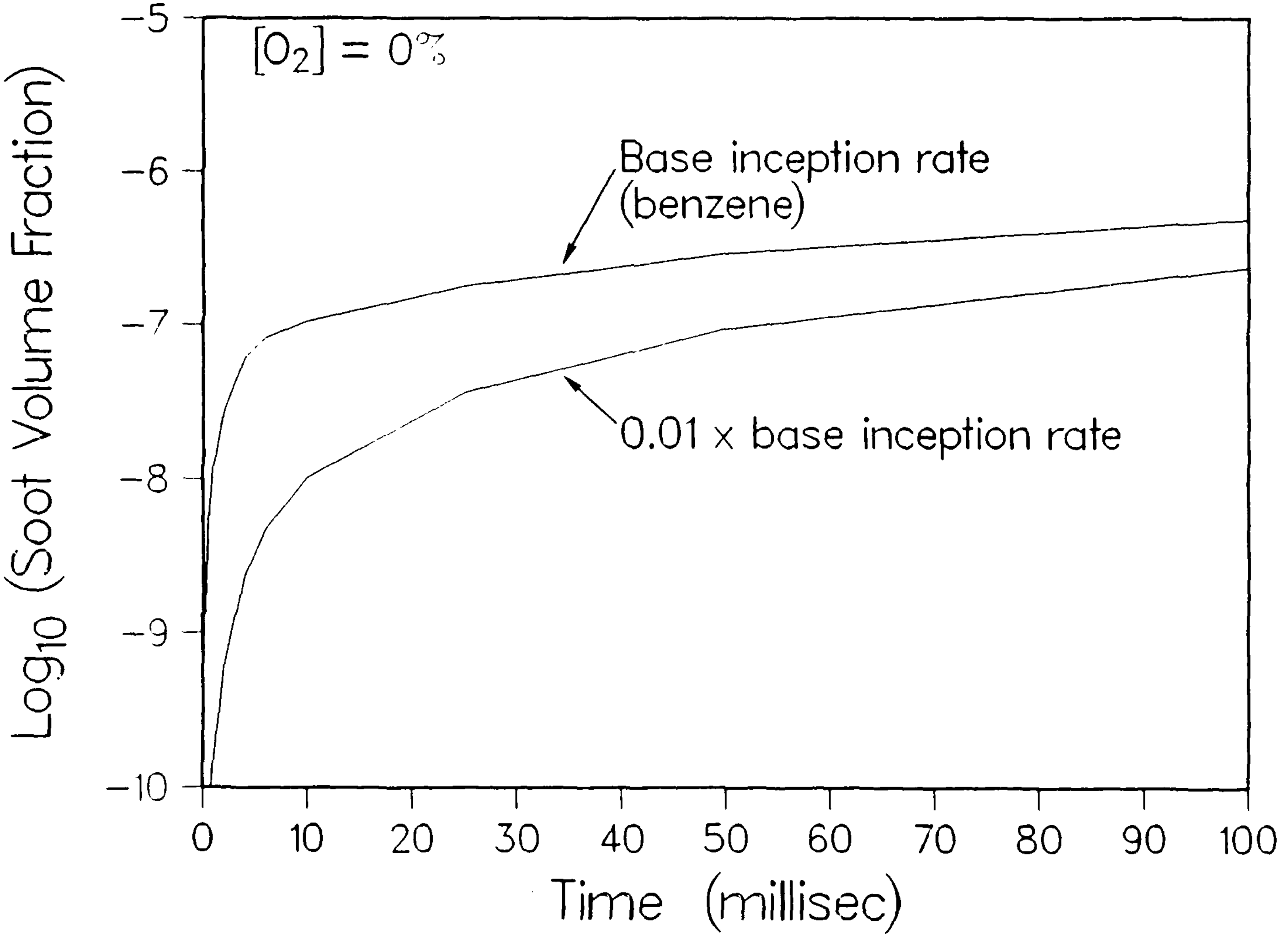

by R. J. Hall and M. B. Colket was presented at the Eastern Section of the Combustion Institute on October 30th - November 1st, 1989. The meeting was held in Albany, New York. A copy of this paper is provided in Appendix A.

4. M. B. Colket presented an invited lecture entitled "Progress Towards Understanding Soot Formation and Development of Global Models" to the Diesel Cooperative Meeting held at United Technologies Research Center on May 17-18, 1990.

References

1. M. B. Colket, "Formation of C_2-Hydrocarbons and Benzene from Pyrolysis of Biacetyl". Presented at the 1986 Spring Technical Meeting of the Central States Section of the Combustion Institute, May 5-6, 1986, Paper no. 1-C2.
2. A. B. Lovell, K. Brezinsky and I. Glassman, Twenty – Second Symposium (International) on Combustion, The Combustion Institute, pp.1063-1074, 1988.
3. J. C. Mackie, M. B. Colket, P. F. Nelson and M. Esler, "Shock Tube Pyrolysis of Pyrrole and Kinetic Modeling" submitted to the International Journal of Chemical Kinetics. 1990. See Appendix D.
4. R. D. Kern, C. H. Wu, J. N. Yong, K. M. Pamidimukkala, and H. J. Singh, "The Correlation of Benzene Production With Soot Yield Determined From Fuel Pyrolysis", presented at the 194th American Chemical Society, National Meeting, New Orleans, Aug. 31 - Sept. 4, (1987). Also see Division of Fuel Chemistry Preprints, Vol. 32(3) p. 456, 1987.
5. M. B. Colket, "Some Thoughts on Modeling Pre-Particle Chemistry", presented at the 1987 Technical Meeting of the Eastern Section of the Combustion Institute, Gaithersburg, MD, paper no. 1., Nov. 2-5, 1987.
6. E. R. Ritter, J. W. Bozzelli and A. M. Dean, "Kinetic Study on Thermal Decomposition of Chlorobenzene Diluted in H_2", to appear in J. Phys. Chem.
7. L. D. Brouwer, W. Müller-Markgraf and J. Troe, *Journal of Physical Chemistry* 92, 4905, 1988. Also see W. Müller-Markgraf and J. Troe, *Journal of Physical Chemistry* 92, 4899, 1988.
8. V. S. Rao and G. B. Skinner, Twenty – First Symposium (International) on Combustion, The Combustion Institute, pp.809-814, 1986.
9. M. B. Colket, Shock Waves and Shock Tubes, Proceedings of the Fifteenth International Symposium on Shock Waves and Shock Tubes, edited by D. Bershader and R. Hanson, Stanford University Press, p. 311, 1986.
10. M. B. Colket, Twenty – First Symposium (International) on Combustion, The Combustion Institute, pp.851-864, 1986.
11. A. Fahr and S. E. Stein, Twenty – Second Symposium (International) on Combustion, The Combustion Institute, pp. 1023-1029, 1988.
12. S.J. Harris and A.M. Weiner, *Combustion Science & Technology*, 131, 155 (1983).
13. J. Nagle and R.F. Strickland-Constable, *Proceedings of the Fifth Carbon Conference*, Vol. 1, Pergamon Press, 1963, p. 154.
14. S.J. Harris, A.M. Weiner and R.J. Blint, "Formation of Small Aromatic Molecules in a Sooting Ethylene Flame", from preprints of papers presented at 194th National Meeting of American

Chemical Society, Div. of Fuel Chemistry, New Orleans, LA, 31 August - 4 September 1987, Vol. 32, p. 488.

15. H. Bockhorn, F. Fetting, A. Heddrich and G. Wannemacher, Twentieth Symposium (International) on Combustion, The Combustion Institute, p. 979, 1984.

16. H. S. Hura and I. Glassman, Twenty – Second Symposium (International) on Combustion, The Combustion Institute, p. 371, 1988.

17. S.J. Harris and I.M. Kennedy, *Combustion Science & Technology,* 59, 443 (1988).

Appendix A

Simplified Models for the Production of Soot in a Premixed Flame

Simplified Models for the Production of Soot in a Premixed Flame

Robert J. Hall and Meredith B. Colket

United Technologies Research Center
East Hartford, CT 06108

Fall Technical Meeting of the
Eastern Section/Combustion Institute, Albany, NY
Oct. 30 to Nov. 1, 1989

Soot inception and growth kinetics have been studied using two types of modeling. In studies of inception, detailed kinetic modeling has been performed to test reaction mechanisms and calculate rate constants for formation of multiring aromatic species. One such process involves the stepwise acetylene addition mechanism

$$\dot{A}_i + H_2 \rightleftharpoons A_i + H \qquad (1)$$

$$\dot{A}_i + C_2H_2 \rightleftharpoons A_iC_2H + H \qquad (2)$$

$$A_iC_2H + H \rightleftharpoons \dot{A}_iC_2H + H_2 \qquad (3)$$

$$\dot{A}_iC_2H + C_2H_2 \rightarrow \dot{A}_{i+1} \qquad (4)$$

where A_i is a closed ring aromatic species A_1 = benzene, A_2 = naphthalene, $\dot{A}_1$ = phenyl, etc.)

This sequence reduces to the mechanism found by Frenklach, et al[1] to dominate for growth from one to two aromatic rings. A similar simplified growth process has also been suggested by Frenklach[2]. Rate constants used in the present study are listed in Table I. k_{-1}, k_2 were obtained from References 3 and 4 for the case of A_1=benzene. k_3 and k_4 were estimated by analogy to k_{-1} and k_2, respectively. The remaining rate constants were calculated from equilibrium. Using steady-state approximations for A_iC_2H and $\dot{A}_iC_2H$ analytical solutions for the concentration of A_{i+1} as a function of time can be obtained. Based on these results[5], characteristic times for the production of A_i can be determined. For the experimental conditions of Harris and co-workers[6,7], the production of a 1000 amu particle (~20 aromatic rings) would take 10 to 20 milliseconds, a time considered long for production of an incipient particle. We come to the conclusion that either (1) rate constants selected in Table 1 are significantly in error, (2) the mechanism is not the dominant reaction path, or (3) the simplified reaction sequence does not describe adequately a more complex path for PAH growth. The steady- state approximation has been compared to standard integration techniques and shown to be a reasonably simple assumption. We have also considered variation of rate constants due to size (collision cross-section, number of active sites, etc.) and although some acceleration in rate is observed, the rate enhancement appears insufficient to describe soot production within a few milliseconds as experimentally observed.

The possible role of agglomerative reactions of the form

$$A_i + A_j \longrightarrow (A_i)(A_j) \equiv A_{ij} \qquad \text{(large i, j)}$$

and of the reaction sequence

$$\dot{A}_1 + A_1 \rightleftharpoons A_1A_1 + H$$

$$A_1A_1 + H \rightleftharpoons A_1\dot{A}_1 + H_2$$

$$A_1\dot{A}_1 + C_2H_2 \rightleftharpoons A_3H + H$$

has also been considered. This series of reactions is similar to the sequence found by Frenklach et al[8], to accelerate soot formation during benzene pyrolysis.

Soot primary spheroid growth has also been modeled as an aerosol dynamics problem using the MAEROS code[9]. The size range of spherical particles is divided into discrete classes, and an equation of motion for each size class is solved with terms for nucleation (inception), surface growth, oxidation, and coalescence. Using an experimentally determined value for the benzene formation rate[6], calculations for hydrogen atom concentrations[7], choosing the smallest size class to be that of the benzene molecule, and extrapolating the Harris-Wiener rate expression[10] for surface growth by acetylene deposition to this size range, we obtained very good theoretical agreement with soot volume fractions measured in a pre-mixed flame[11]. The uncertainties in the calculation will be discussed, and the sensitivity to such quantities as the coalescence sticking probabilities, the number of size intervals, and rate constant for surface growth will be discussed.

Figure 1 shows the calculated evolution of the normalized soot spheroid size distributions with time for the premixed flame conditions of Ref. 6 and 7. With simultaneous nucleation, surface growth, and coalescence (assumed to occur here with unit sticking probability), a "self-preserving" form is attained after about four milliseconds in this atmospheric pressure simulation. Figure 2 shows the calculated evolution of the soot volume fraction, using the coalescence sticking probability as a parameter. For slow coagulation, the surface area of the spheroids remains high, surface growth is correspondingly rapid, and the computed volume fraction large. For sticking probabilities in the range one to 2.2, the agreement of theory with the experimental measurements of Ref. 11 (interpolated estimate for c/o=0.92) is very good.

Table I

Rate Constants for Growth Reactions

Reaction	log (A^*_{for})	E_{for}/R	log (A_{rev})	E_{rev}/R
1	12.7	5400	14.4	8052
2	13.6	5083	15.4	5885
3	14.4	8052	12.7	5400
4	13.6	5083		

* cm^3/mole/sec

ACKNOWLEDGEMENTS

This work has been supported in part by the Air Force Office of Scientific Research (AFSC).

REFERENCES

1. M. Frenklach, D.W. Clary, W.C. Gardiner, Jr., and S.E. Stein Twentieth Symposium (International) on Combustion, The Combustion Institute, p. 887, 1984.
2. M. Frenklach, Twenty – Second Symposium International on Combustion, The Combustion Institute, p. 1075, 1988.
3. J.H. Kiefer, L.J. Mizerka, M.R. Patel, H.C. Wei, J. Phys. Chem. 89, 2013 (1985).
4. A. Fahr and S.E. Stein, Twenty – Second Symposium International) on Combustion, The Combustion Institute, p. 1023, 1988.
5. M.B. Colket, R.J. Hall, J.J. Sangiovanni, and D.J. Seery, "The Determination of Rate-Limiting Steps During Soot Formation", AFOSR annual report, F49620-88-C-0051, United Technologies Research Center Report No. UTRC89-13, April, 1989.
6. S.J. Harris, A.M. Weiner, and R.J. Blint, Comb. Flame, 72, 91 (1988).
7. S.J. Harris, A.M. Weiner, R.J. Blint, and J.E.M. Goldsmith, Twenty – First Symposium (International) on Combustion, The Combustion Institute, p. 1033, 1986.
8. M. Frenklach, D.W. Clary, W.C. Gardiner, Jr., and S.E. Stein, Twenty – First Symposium (International) on Combustion, The Combustion Institute, p. 1067, 1986.
9. F. Gelbard, MAEROS User Manual, NUREG/CR-1391 (SAND80-0822) 1982. The version of the code which we use is "MAEROS2".
10. S.J. Harris and A.M. Weiner, Combustion Science & Technology, 131, 155 (1983).
11. S.J. Harris and A.M. Weiner, Combustion Science & Technology, 32, 267 (1983).

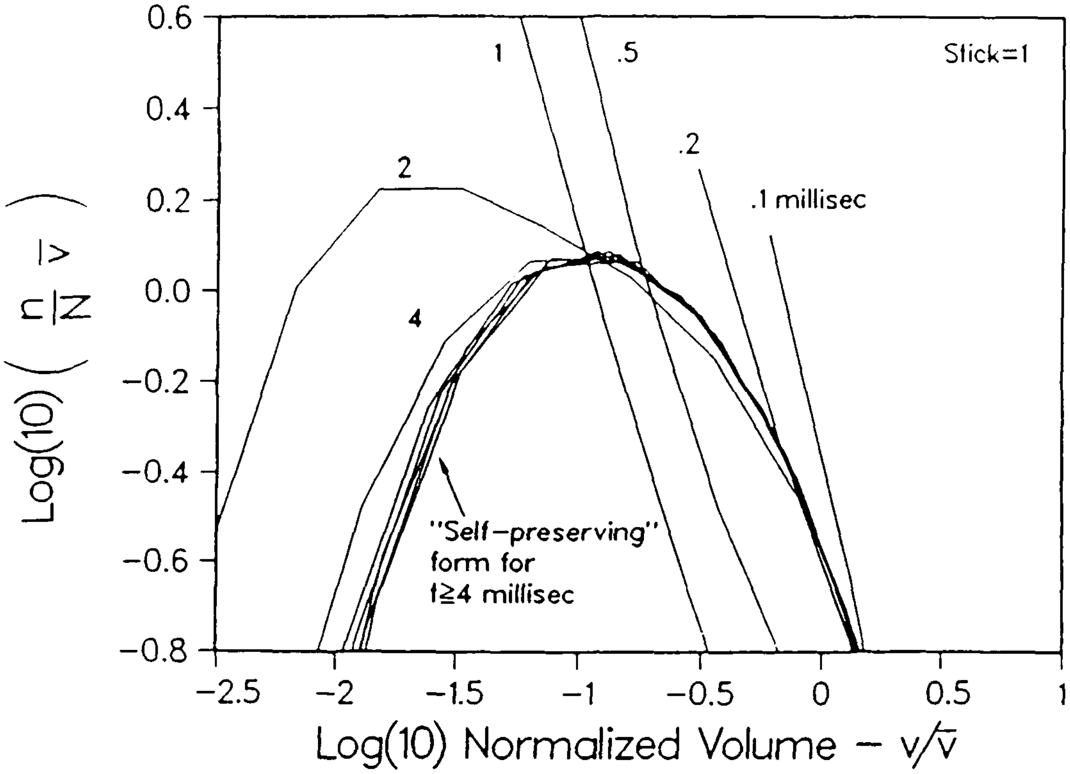

1. Calculated evolution of soot spheroid size distribution in simulation of Ref. 6 flame.

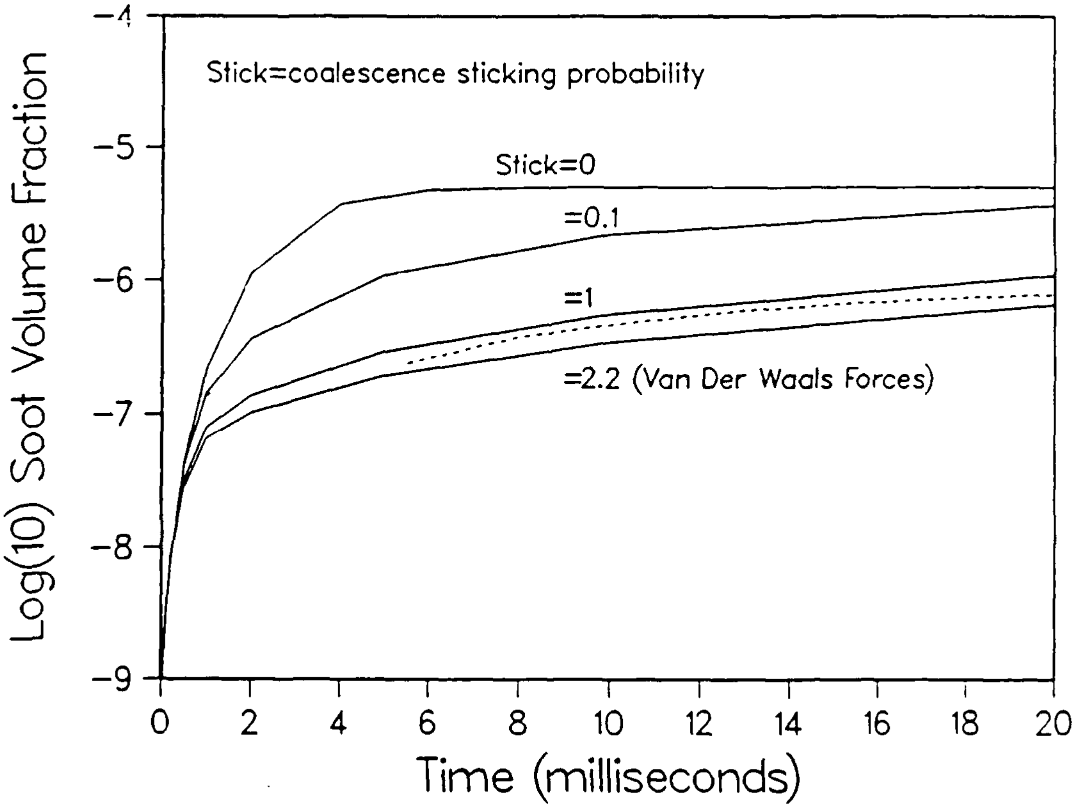

2. Comparison of calculated (————) and measured (- - - - - -) soot volume fraction profiles for premixed flame conditions of Ref. 11.

Appendix B

On Impurity Effects in Acetylene Pyrolysis

ON IMPURITY EFFECTS IN ACETYLENE PYROLYSIS

by

M. B. Colket, III., H. B. Palmer* and D. J. Seery
United Technologies Research Center
East Hartford, CT 06108

* Pennsylvania State University
University Park, PA 16802

In our recent paper[1] (CSP), we concluded that a radical-chain mechanism of acetylene pyrolysis must be appreciable and possibly dominant and argued that impurities, for example acetone, may contribute significantly to chain initiation. To support our conclusions, a model including acetone chemistry was developed but it did not invoke vinylidene reactions or other non-chain processes despite reasonable arguments[2] in support of such steps. Nevertheless, we also recognized, and stated in the paper, that the vinylidene mechanism could not be disproven and may in fact play a role.

This analysis apparently prompted Duran, Amorebieta, and Colussi[3] (DAC1) to perform additive experiments. They pyrolyzed acetone/acetylene mixtures at ratios of about 0.2 to 2, selected a decomposition rate expression and determined associated rate constants. Colussi[4] extrapolated this rate expression down to concentration ratios of 0.001 and concluded that the impurity effect can be neglected since it can account for only 2 to 14% of the decomposed acetylene at 910K. In contrast to the suggestion of Colussi, we do not consider these results to be in conflict with our conclusions.

First of all, the uncertainty in extrapolating a rate expression derived from experiments with acetone/acetylene ratios of 0.2 down to ratios of only 0.001 may be significant. Our calculations suggest that at high acetone/acetylene ratios, acetone is rapidly depleted by radical (H-atom, methyl, or vinyl) attack and therefore is no longer available to initiate the reaction. Although absolute rate constants for R + acetylene may in fact be higher than R + acetone, the former is a reversible process and the latter is not, because of the rapid decomposition of the product acetonyl radical from the latter reaction. As radical concentrations increase (i.e., as the initial acetone concentration increases), the rate of R + acetone relative to the net rate of R + acetylene increases dramatically. This result differs from the conclusion reached in Appendix I of DAC1. If acetone is rapidly depleted by radical attack, then radical initiation rates will be lower and overall decomposition rates will be lower than if acetone were not removed by radicals. Rate expressions derived from high concentration experiments may then underestimate decomposition when extrapolated to very low acetone levels. Therefore, we believe that the experiments of DAC1 (which suggest acetone could contribute about 10% to the overall decomposition of acetylene) underestimate the role of low concentrations of acetone.

A second reason for our view of the experimental results of DAC1 is that the analysis described in our paper suggests that acetone could play a relatively more important role in radical initiation at higher temperatures. As stated in the conclusions of our paper, 900K is approximately the lower limit for which acetone was predicted to play a significant role. Our lower limit is very close to the temperature of the DAC1 study, 910K.

The comment by Colussi implies that trace acetone concentration levels cannot appreciably accelerate overall rates of acetylene pyrolysis. This statement is not apparent from the pre-publication manuscript (DAC1), since acetone and acetylene were copyrolyzed at comparable concentrations. Typical concentrations were 51.4 torr acetylene and 100 torr acetone. Low-level impurity experiments apparently were not performed.

We have performed some calculations based on the conditions cited by Duran, Amorebieta, and Colussi[5] (DAC2) for pyrolysis of neat acetylene. We have slightly modified our published mechanism to account for the pressure dependence. The modifications include selection of $k/k_\infty = 0.5$ for the following reactions.

$$H + C_2H_2 \leftrightarrow C_2H_3 \qquad (2)$$

$$CH_3COCH_3 \leftrightarrow CH_3 + CH_3CO \qquad (5)$$

In addition, the high pressure rate constant recommended by Benson and O'Neal[6] is used for Reaction 5. At 910K and 100 torr acetylene, we calculate a steady-state decomposition rate (after a transient less than two seconds) to be 2.2×10^{-8} moles/cm^3/sec (2.2×10^{-5} M s^{-1}) and a rate constant of 7.1×10^3 cm^3/moles/sec (7.1 M^{-1} s^{-1}). These values are very close to the values cited by DAC1 and DAC2. The excellent agreement is probably fortuitous, but these calculations were performed using a chain mechanism, an impurity of 0.1 torr of acetone, and did not include contributions of vinylidene. Detailed product information is not available from these publications for comparison.

It should be emphasized that the thermochemistry for several radical intermediates potentially important to acetylene decomposition cannot be considered to be well known. Consequently it is difficult to draw definitive conclusions based on such arguments. The uncertainty in the heat of formation of C_4H_3 isomers was cited as an example in CSP, but uncertainties in the entropy also exist. Values vary depending on the estimation (calculation) technique as well as the individual performing the evaluation. Most evaluations are unpublished, but examples of some reported values of $\Delta H^0_{f,298}$, S^0_{298}, and $C_p(T)$ for the i-C_4H_3 radical are reproduced in Table I. Also included are calculations of the rate constant for the suggested reaction

$$C_2H_2 + C_2H_2 \leftrightarrow i - C_4H_3 + H \qquad (1a)$$

After DAC1, k_{1a}'s were calculated assuming the reverse, recombination rate constant is 5×10^{13} cm^3/mole/sec. DAC1 estimated that Reaction 1a had to have rate of at least 85 cm^3/mole/sec at 910K in order for it to contribute to acetylene pyrolysis. As can be seen from the different values listed in Table I, any conclusion can be drawn, although most recent estimates using group additivity techniques support the conclusion of DAC1 regarding the importance of Reaction 1a.

Lacking sufficiently accurate thermochemical data, one must consider experimental evidence. It is our own interpretation[1] that available data supports contribution from a chain mechanism. Radical initiation, if not from Reaction 1a or similar step, could arise from impurities or walls. Although we have argued that acetone plays an important role, acetone is not always present. Acetylene made from water and calcium carbide, for example, will not contain acetone, although other impurities (possibly inorganic) could be present. If the impurity has a relatively weak bond, large concentrations are not required.

The difficulty of accurately making measurements of acetylene pyrolysis near 1000K should not be underestimated. In addition to being susceptible to radical sources from impurities (see CSP), the pyrolysis is extremely exothermic. Formation of vinylacetylene, benzene, or solid carbon plus hydrogen is 19, 48, and 54 kilocalories exothermic per mole of acetylene decomposed, respectively. Thus, nearly ninety percent of the potential energy release arises just by forming benzene and helps to explain the explosive behavior of neat acetylene. Assuming that only 2% of the acetylene forms benzene (an important low temperature product) and taking $c_p(C_2H_2)$ =16 cal/mole/K, the temperature rise is 60K for undiluted samples of acetylene. For a reaction with E=40 kcal/mole, the rate constant would rise by a factor of 2.5. For larger extents of reaction, this problem will be more severe. Formation of vinylacetylene, benzene and other higher molecular weight species will lead to a reduction in the number of moles and to a pressure reduction (for constant volume reactors) as the reaction progresses. The pressure cannot be directly related to the rate of reaction unless detailed information on product distribution is also known. An additional complication in interpreting pressure traces arises from the temperature rise due to the heat of reaction. The temperature rise would lead to a pressure increase (ideal gas law) which partially offsets the pressure decay due to reaction. For flow reactors in which constant pressure can be maintained, the above effects lead to changes in velocity which complicate determination of reaction time. On-line diagnostics such as mass spectrometers may be pressure sensitive and so calibrations and experiments must be carefully interpreted. In some reactor designs, energy release from the reaction may be absorbed by the walls, but in such situations, the rate of wall collisions must be high and there may be surface contributions to the chemistry. Pretreatment of vessels at elevated temperatures may simply 'stabilize' the source of radical production/termination at the walls. The difficulty in accurately measuring the rate of pyrolysis of neat acetylene is dramatically illustrated by the scatter (factor of two to three) obtained in the work of DAC2 (Fig. 1) but is significantly less ($\approx$ 20%) when a stable source of radicals (acetone or neopentane) is added (see Figs. 1-3 in DAC1). The scatter in the 'neat' acetylene experiments may be due to run-to-run variations in impurities or wall effects.

As we consider the varying evidence and conclusions from previous work, the need for careful documentation in future experiments becomes very evident. Levels of impurities must be measured and specified. Equipment sensitive to concentrations lower than 1000 ppm acetylene must be used. Based on the confused situation identified in Table 3 of CSP, the reaction order should be redetermined and demonstrated to readers. (Towell and Martin[7], for example, claimed second order dependence, but their data indicated an order much closer to 1.5.) Based on the literature cited in CSP, the last time experimental data was presented showing second order behavior was 1964; since then there have been many dissimilar results. Considering the relative sophistication of present-day experimental techniques, it should be straightforward to establish the kinetic order of acetylene pyrolysis.

In conclusion, we are convinced that there are uncertainties still to be resolved in the acetylene system. The trace impurity experiment has not yet been performed. An extrapolation of a rate expression to low acetone concentrations suggests a contribution of 10% to the overall rate at about 900K. We feel that the results of DAC1 do not disprove our suggestion that even small concentrations of impurities can have a significant impact on acetylene pyrolysis.

REFERENCES

1. Colket, M.B., Seery, D.J., and Palmer, H.B., *Combust. Flame* 75: 343-366 (1989). (CSP).
2. Kiefer, J.H. and Von Drasek, W.A., "The Mechanism of the Homogeneous Pyrolysis of Acetylene", to be published in *Int. J. Chem. Kin.* .
3. Duran, R.P., Amorebieta, V.T. and Colussi, A.J., "Radical Sensitization of Acetylene Pyrolysis", to be published in *Int. J. Chem. Kin.* (DAC1).
4. Colussi, A.J., *Combust. Flame*, this issue.
5. Duran, R. P., Amorebieta, V. T. and Colussi, A. J., *J. Am. Chem. Soc.* 109: 3154 (1987). (DAC2).
6. Benson, S.W. and O'Neal, "Kinetic Data on Gas-Phase Unimolecular Reactions", NSRDS-NBS 21, U.S. Govt. Printing Office, Washington, D.C. (1970).
7. Towell, G. D. and Martin, J. J., *A. I. Ch. E. Journal* 7: 693 (1961).
8. Bittner, J., "A Molecular Beam Mass Spectrometer Study of Fuel-Rich and Sooting Benzene-Oxygen Flames", Ph.D. Dissertation, Appendix P, Massachussetts Institute of Technology, 1981.
9. Ghibaudi, E. and Colussi, A.J., *J. Phys. Chem.* 92: 5839 (1988).
10. Westmoreland, P. R., "Prediction of Kinetics for C_4 *Species which form Benzene*", *American Chemical Society, Fuel Chemistry Preprints* 32: 480 (1987). NOTE: The original reference incorrectly lists the heat of formation of i-C_4H_3 (personal comminication from P. R. Westmoreland).
11. Stein, S. E., National Bureau of Standards, Gaithersburg, MD, Personal Communication, 1987.
12. Cowperthwaite, M. and Bauer, S. H., *J. Chem. Phys.* 36: 1743 (1962).
13. Melius, C., Sandia National Laboratories, Personal Communication, 1988.
14. Montgomery, J.A., and Michels, H.H. United Technologies Research Center, Personal Communication, 1989.

Table I

Reported Thermodynamics for 1-Buten-3-yn-2-yl (i-C_4H_3)

$\Delta H^\circ_{f,298}$ kcal/mole	S°_{298} cal/mole/K	C°_p – cal/mole/K					k^*_{1a} cm^3/mole/sec	Ref.
		300	500	800	1000	1500		
110.8	63.7	16.3	21.9	27.8	29.8	33.1	0.37	8
115.2	66.1	16.9	22.1	27.0	29.3	33.0	0.11	9
114.5	68.3	17.5	22.5	27.4	29.6	33.2	0.56	10
116.1	68.1	16.8	22.2	27.1	29.3	32.8	0.19	11
102.0	65.4	17.4	22.4	27.1	29.2	32.5	126	12
110.0	71.6	17.4	22.4	27.1	29.2	32.5	33.8	13

* assuming a $k_{-1a} = 5x10^{13}$ cm^3/mole sec

Note: The low heat of formation calculated by Ref. 11 is probably in error, but is the value included in many thermodynamic compilations. The relatively high value of entropy determined by Melius[13] has recently been supported by additional calculations[14].

Appendix C

Shock Tube Pyrolysis of Pyridine

MRB928

Shock Tube Pyrolysis of Pyridine+

John C. Mackie*, Department of Physical Chemistry,
University of Sydney, NSW 2006, Australia

Meredith B. Colket III, United Technologies Research Center,
Silver Lane, East Hartford CT 06108

Peter F. Nelson, CSIRO Division of Coal Technology,
North Ryde, NSW 2113, Australia

+ Presented in part as a Poster Paper at 21st Symposium (International) on Combustion, Seattle, August 1988

Abstract

The kinetics of pyrolysis of pyridine dilute in argon have been studied in a single-pulse shock tube, using capillary column GC together with GC/MS and FTIR spectroscopy for product determination, over the temperature range of 1300-1800K and total pressures of 7-11 atm. At the lower end of the studied temperatures, cyanoacetylene was found to be the principal nitrogen-containing product. At elevated temperatures hydrogen cyanide predominated. Other major products were acetylene and hydrogen.

Thermochemical estimates of the isomeric cyclic pyridyls produced in the pyrolysis indicate that the ortho-isomer is unique in being able to undergo facile cleavage to an open-chain cyano-radical from which cyanoacetylene is produced. Several sources of HCN were identified in the system. The m- and p-pyridyls may eliminate HCN in a molecular process. An important source of HCN at high temperatures is the addition of H atoms to cyano-compounds, especially cyanoacetylene, but also acetonitrile and acrylonitrile which are produced in the pyrolysis.

The pyrolysis is a chain process initiated principally by C-H bond fission to form o-pyridyl. A 58-step reaction model is presented and shown to substantially fit the observed profiles of the major product species. From this model we derive a value for the rate constant of the principal initiation reaction

$$C_5H_5N \rightarrow o\text{-}C_5H_4N + H \qquad (1)$$

of $k_1 = 10^{15.9\pm0.4} \exp(-98\pm3\,\mathrm{kcal\ mol^{-1}}/RT)\,s^{-1}$ between 1300-1800K and at a total pressure of about 10 atm.

Introduction

Heavy fuels such as coal and coal-derived liquids contain considerable amounts of chemically bound nitrogen and the combustion of these fuels can lead to significant amounts of fuel-derived NO_x[1-3]. Much of the nitrogen originally bound in the fuel is in the form of aromatic heterocyclic structures containing pyridine and pyrrole ring systems[4,5]. Under pyrolytic conditions these heterocycles may form nitrogen precursors of NO_x so that the rates of pyrolysis and product formation from representative nitrogen heterocycles will determine NO_x formation in the combustion of heavy fuels.

The thermal decomposition of pyridine has been studied previously[6-8] in flow systems between 1100-1400K. Acetylene and hydrogen cyanide have been found to be major products. Other nitrogen-containing products have been identified as acrylonitrile, benzonitrile, quinoline and acetonitrile, although dispute exists[7,8] over the observation of acetonitrile.

Axworthy et al.[7] found that the decomposition of pyridine followed first order kinetics with an overall rate constant of $3.8 \times 10^{12} \exp(-70 \text{ kcal mol}^{-1}/RT) s^{-1}$ between 1100-1200K. Houser et al.[8] found that the decomposition kinetics were complex and did not follow first order kinetics exactly. However, they derived an approximate first order rate constant of $1 \times 10^{12} \exp(-75 \text{ kcal mol}^{-1}/RT) s^{-1}$, about an order of magnitude lower than that of Axworthy et al.

Recently, Kern et al[9] carried out a shock tube study of the pyrolysis of pyridine over the temperature range of 1700-2400 K and at pressures between 0.2-0.5 atm using both laser schlieren densitometry and time-of-flight mass spectrometry as diagnostic tools. They proposed a chain mechanism with first-order initiation involving a ring hydrogen fission

$$C_5H_5N \rightarrow C_5H_4N + H \qquad (1a)$$

with a specific pressure-dependent rate constant of $1.08 \times 10^{12} \exp(-74.5$ kcal $\text{mol}^{-1}/RT)$ s^{-1}. In their analysis the C_5H_4N represented a weighted average of the isomeric pyridyl radicals. From a RRKM extrapolation of their rate data, Kern et al derived an average value of 76±10kcal mol^{-1} for the heat of formation of the pyridyl radicals, a value higher than that implied by the earlier flow studies[6-8].

In a recent shock tube study Leidreiter and Wagner[10] measured the rate of decomposition of pyridine at temperatures between 1700-2000K and at total densities of 2×10^{-6} - 3×10^{-5} mol cm^{-3}, using time resolved absorption measurements at 279 nm. They did not determine products but from fall-off curves they were able to extrapolate their rate data to obtain the limiting high pressure rate constant for disappearance of pyridine of $k_\infty = 10^{16.2} \exp(-100 \text{ kcal mol}^{-1}/RT)$ s^{-1}.

The lower reported values of the activation energy of the initiation step (70-75 kcal mol^{-1}) imply that the C-H bond energy in pyridine is considerably lower than that in benzene (assuming that the initiation step is C-H fission). Also, Kern et al.[9] detected only one nitrogen-containing product - hydrogen cyanide - although in flow studies several other nitrogen products were observed. Thus, the present shock tube kinetic study of pyridine pyrolysis, using capillary column gas chromatography and gas chromatography/mass spectrometry for detection, is oriented towards detailed product identification and elucidation of the pyrolysis mechanism.

Experimental

Pyrolyses were carried out on two single-pulse shock tubes, one of diameter 3.8 cm at UTRC which was primarily used for kinetic studies, the other, at the University of Sydney (diameter 7.6 cm), was used principally for product identification in conjunction with FTIR and a GC/MS at CSIRO. Both shock tubes are basically similar; the UTRC tube and on-line capillary GC analytical system have been described previously[11].

Pyridine samples were purchased from Aldrich (HPLC grade) and from Merck (A.R. grade). Further purification by several bulb-to-bulb distillations produced pyridine samples of purity exceeding 99.9% (by GC with CH_3CN as the only detectable impurity). No difference between the two sources of pyridine was observed.

For the kinetic studies, mixtures of 0.7 and 0.15% pyridine in argon were prepared and stored in glass bulbs. Pressures and temperatures behind the reflected shock were computed from the measured incident shock velocity. Residence times and quenching rates by the rarefaction wave were measured from pressure profiles recorded by Kistler gauges. Reflected shocked gas temperatures ranged from 1200-1800K and total pressures from 7-11 atm. Residence times at uniform temperatures behind the reflected shock front ranged from 450-600 μs. For the product analyses, three separate capillary GC columns were used. The UTRC shock tube was equipped with a Chrompack CP Sil 5 capillary column. The Sydney shock tube employed a SGE BP-1 (5μm bonded phase dimethysiloxane) widebore column whereas the CSIRO GC/MS was equipped with an SGE BP-1 0.5 μm bonded phase.

Where commercial samples were available, product identification and calibration were made from capillary GC retention times and areas by direct comparison with standards. HCN was purchased as a standard mixture in N_2 from Scott Specialty Gases. Acetonitrile, acrylonitrile and benzonitrile (all > 99% purity) were obtained from Aldrich. C_1-C_6 hydrocarbons were calibrated gas standards prepared and analyzed by Scott Environmental Laboratories.

Cyanoacetylene (HCCCN) was identified in the product gases by FTIR absorption spectroscopy in a 7m cell (via its strong CCH bend at 663.4 cm and the CN stretch at 2272 cm^{-1}). Product samples from the Sydney shock tube were collected in gas burettes and transported to CSIRO for GC/MS analysis. The GC peak assigned to cyanoacetylene was confirmed not only by the observation of the parent peak at 51 a.m.u., but also through the observation of its fragmentation pattern whose intensities were in excellent agreement with those reported by Dibeler et al[12].

Other products confirmed both by FTIR and GC/MS were hydrogen cyanide, vinylacetylene and diacetylene. In addition, triacetylene (C_6H_2) and cyanodiacetylene (HC_5N) were positively identified by GC/MS.

Both hydrocarbons and nitrogen-containing compounds were detected by FID; the sensitivity of detection of HCN, however, was only about one tenth that of C_2H_2, permitting measurements of HCN to be made with adequate precision above about 30 ppm. Hydrogen was detected by TCD.

The capillary column/sampling system exhibited a "memory effect" for the nitrogen-containing compounds, especially pyridine, benzonitrile, acetonitrile and acrylonitrile. Repeatability of injections of these compounds was only ± 10%. Pyridine mixtures in argon slowly decreased in concentration with storage, requiring frequent recalibrations.

Adsorption and/or polymerization of the product cyano-compounds on to the walls of the gas burettes was a problem leading to significant losses in sensitivity of these products in transportation of samples for GC/MS analyses.

Results

Yields of all products of significance (scaled by the initial concentration of pyridine) are shown in Figure 1 as a function of temperature for the 0.7% mixture of pyridine in argon. The variation of pyridine concentration with temperature is also given in Figure 1.

The principal hydrocarbon product at all temperatures and for both series of mixtures was acetylene. Hydrogen was an important product at all temperatures. The C_2H_2/H_2 ratio varied from about 1/3 at 1300K to about 1.5/1 at 1800K. At the lower end of the studied temperature range cyanoacetylene was the principal nitrogen-containing product being higher in yield than HCN by about a factor of 2. From FTIR difference spectra of the products from successive runs in the lower range of temperatures it was shown that the rates of increase with temperature of both acetylene and cyanoacetylene were approximately equal. With increasing temperature HCN yields overtook those of HCCCN such that the yield of HCN is about 4 times that of HCCCN at 1800K. Much smaller yields of acetonitrile and acrylonitrile were recorded at all temperatures. An additional product was detected and was assumed to be a cyano-containing species due both to the characteristic tailing of the GC peak that this class of compounds exhibits on the capillary column and also to the lack of appearance of this peak during pyrolysis of pure hydrocarbons. This product peaked in yield at about 1500K and was present even at the lowest temperatures at which decomposition could be detected. From its retention time, eluting just after C_6H_2, which, in turn, eluted soon after HC_5N, it has been tentatively assigned as cyanovinylacetylene (β-ethynylacrylonitrile:- (HC≡C-CH=CHCN). Attempts to confirm this assignment by GC/MS were unsuccessful, however, as the level of this peak after transportation of the product gases for analysis had dropped below sensitivity limits. Cyanovinylacetylene is known to polymerize rapidly[13] above -30°C.

Other products included vinylacetylene (C_4H_4) - important at the lower temperatures, diacetylene and triacetylene - important over the entire temperature range, methane, ethylene and benzene. There were also significiant yields of benzonitrile, allene and/or propyne (unresolved by the capillary columns) together with traces of propene, butadiene, styrene and phenylacetylene. Cyanodiacetylene (HC_5N) yields only became significant at the higher temperatures of this study.

When results from the two series of initial pyridine concentrations (0.7 and 0.15%) were compared, it was found that the overall decomposition of pyridine and formation of major products HCN, C_2H_2, HCCCN and H_2 were essentially independent of initial pyridine concentration. This independence upon initial pyridine concentration was also observed for products C_4H_4, CH_4 and acrylonitrile. Thus, overall first order kinetics are observed for pyridine decomposition, and for the formation of the major as well as many of the minor species. The first order behavior is consistent with that previously observed.[7] Because of the first order behaviour it is therefore convenient in reporting species data to present normalized concentrations of reactant and products in Figures 1 and 3-6.

DISCUSSION

Thermochemistry of the Pyridine System

The reaction mechanism developed to interpret the above results involves a chain reaction initiated by C-H bond scission, as suggested previously. Subsequent reactions are dependent on the thermochemistry of the cyclic pyridyl radicals produced by the scission. The enthalpies of formation of the pyridyls were estimated under the assumption that the C-H bond energy in pyridine was equal to that in benzene together with a stabilization energy[14] of 1.5 kcal mol^{-1} for the o- and p-pyridyls. Using the assumption of equality of C-H bond energies of pyridine and benzene, Dewar and co-workers[15a,b] have calculated enthalpies of atomization of pyridine and other molecules containing the pyridine ring, in very good agreement with experiment by SCF MO techniques. Heat capacities and entropies of the pyridyls have been estimated by group additivity methods[14] by assuming that the contribution of the C_B group to the pyridyl thermochemistry was equal to that in phenyl.

All pyridyl radicals may undergo thermal ring fissure. However, the o-pyridyl is unique in its ability to produce directly an open-chain cyano-radical (I). Figure 2 shows all possible open-chain "linear" radicals $1\text{-}C_5H_4N$ arising from simple ring cleavage. As the values in

Table I indicate, the cyano-radical (I) should be overwhelmingly more stable that any other open-chain radical produced by ring fissure of pyridyls.

Because of the lack of thermochemical data for the pyridyls we have had to resort to approximate group additivity methods to arrive at the estimates of the thermochemical parameters given in Table I. To estimate thermochemical parameters for radical (I), thermochemical data for group C_d-(H)(CN) were obtained by additivity methods[14] from the acrylonitrile thermochemistry together with data for $n\text{-}C_4H_5^{\cdot}$ (Ref. 16). Estimates for radical (II) were calculated from the thermochemistry of CH=NH, 1-C_6H_5 and C_2H_3 (Ref. 16). Thermochemical data for CH=NH were calculated by Melius using the BAC-MP4 technique[17]. The enthalpy of formation of 1-C_6H_5 was estimated by additivity methods[18] and the value of $\Delta H^0_{f,300} = 139$ kcal mol^{-1} used in the present work compares well with a recent determination by Braun-Unkhoff et al[19] of 144±3kcal mol^{-1}. $\dot{N}_I$ group data (required for radical (III)) were estimated by comparing group differences between $>C=\dot{C}H$ and $>C=CH_2$ with $>C=\dot{N}$ and $>C=NH$ where N_I-(H) data are available from $CH_2=NH$. The enthalpy of formation of $CH_2=NH$ has been measured experimentally[20]. Heat capacities and entropies are obtained from spectroscopy[21].

Thermochemical data for HCCCN, HC_5N and $H_2C=CHCN$ were computed by statistical methods using molecular constants from Refs. 22-24. Other relevant group data are available in the thermochemistry literature.[14,25].

Reaction Mechanism

Based on the assumption of the stability of the open-chain cyanoradical (I), the dominant mechanism in the pyrolysis of pyridine in the lower end of the studied temperature range of 1300-1800K is postulated to be (Reaction numbering as in Table II):

	ΔH^{0}_{300}/kcal mol^{-1}	
$C_5H_5N \rightarrow o\text{-}C_5H_4N + H$	109 ± 3	(1)
$o - C_5H_4N \rightarrow HC{=}CH{-}CH{=}CHCN$ (I)	22 ± 6	(3)
$HC{=}CH{-}CH{=}CHCN \rightarrow C_2H_2 + HC{=}CHCN$	37 ± 6	(4)
$HC = CHCN\ (+M) \rightarrow HCCCN + H\ (+M)$	40 ± 3	(5)
$H + C_5H_5N \rightarrow o\text{-},\ p\text{-},\ m\text{-}C_5H_4N + H_2$		(6,7)

This is the major low temperature chain mechanism although a minor chain process may arise via fission of a secondary H from (I), producing cyanovinylacetylene (CVA).

$$HC{=}CH{-}CH{=}CHCN \rightarrow HC{\equiv}C{-}CH{=}CHCN + H \quad \Delta H^{o}_{300} = 38 \pm 3 \text{ kcal mol}^{-1} \qquad (8)$$

The HCCHCN radical was found to decompose principally via Reaction (5). Other possibilities include

$$HCCHCN \rightarrow C_2H_2 + CN \qquad \Delta H^{o}_{300} = 61 \text{ kcal mol}^{-1}$$

$$HCCHCN \rightarrow C_2H + HCN \quad \Delta H^o_{300} = 63 \text{ kcal mol}^{-1}$$

but the larger endothermicities of these reactions make them less likely at least at the lower temperatures of this study.

The above short chain mechanism is in accord with the experimental observations that HCCCN is the principal nitrogen-containing product at low temperatures, and of the equivalence in production rates of C_2H_2 and HCCCN. It also gives an explanation for the product peak (assigned as CVA) which appears at low temperatures.

The thermochemistry of the m- and p-pyridyls suggests that these radicals will be stable with respect to simple ring cleavage, hence the reverse of Reaction (2)

$$p\text{-},m\text{-}C_5H_4N + H \rightarrow C_5H_5N \qquad (-2)$$

terminates radicals. However, both of these isomers may also undergo elimination of HCN to produce the n-C_4H_3 radical (Reaction (9)). There are other possible sources of HCN. Open-chain radical (I) could eliminate HCN in a molecular process involving a cyclic transition state (Reaction (10)). Although we are unaware of any previous studies of HCN elimination from cyclic radicals, Braun-Unkhoff et al[19] have analysed the decomposition of benzyl radicals by invoking a rearrangement to a bicyclic $C_7H_7^{\cdot}$ radical which can molecularly eliminate C_2H_2 in an analogous process to our HCN elimination.

At elevated temperatures where high concentrations of H atoms exists, an important source of HCN arises from the addition of H atoms to cyano-compounds. The most important of these is reaction (-27) which leads to the decay of HCCCN at high temperatures. The abstraction reaction of CN with H_2 also plays a significant role at elevated temperatures.

The detailed reaction mechanism postulated to simulate the yields of the major products is presented in Table II. In addition to the nitrogen chemistry, the mechanism includes acetylene and benzene formation reactions as subsets. For many of the reactions involving nitrogen - containing species, few or no rate constant evaluations are available in the literature. For these reactions estimates were made using rate constants from analogous reactions or thermochemistry. Based on reaction path analyses and sensitivity analyses, selected rate constants were adjusted to fit the experimental data. These latter rate constants are denoted "PW" in Table II.

For simplification, only one C_4H_3 radical is considered and this is taken to be the n- radical whose $\Delta H^{0}_{f,300}$ is assumed to be 125 kcal mol^{-1}. Allene/propyne is considered to be propyne, the more thermodynamically favoured form of C_3H_4 at high temperatures. The reaction model includes, in addition to the short chain mechanism referred to previously, secondary reactions of the product species and radical-radical reactions. There appear to be strong parallels between the addition reactions of acetylene and those of cyanoacetylene. Thus rate constants for radical additions to HCCCN have been chosen by analogy with literature constants for additions to C_2H_2. Also, acrylonitrile should be able to undergo 2,2 and 3,3 eliminations of HCN and H_2 respectively, analogous to the 1,1 elimination of H_2 and vinylidene formation reactions of ethylene and vinylacetylene[26]. Integration of the kinetic equations was made using the CHEMKIN package[27a], LSODE[27b] and the SANDIA shock tube code[27c] which was modified to account for the effects of quenching. Rate of production and sensitivity analyses were carried out by the SENKIN code[28].

Comparison of the kinetic model with experiment is given in Figures 3-6 for the major products (i.e., species whose yields are >0.1 over the studied temperature range). The model adequately describes the temperature dependence of the major products and minor products also from both series of runs. The model also reproduces the experimental pyridine profiles up to about 80% decomposition. Although about 5% of the initial pyridine remains unreacted due to boundary layer effects at 1800K, this has little effect on the profiles of the major species. For example, a decrease of about 5% in the HCN concentration at 1800K is well within our experimental error.

It should be noted that the mechanism of Table II contains certain reactions postulated to simulate minor products' formation. Rate constants were determined based on best fits to experimental data and/or estimates as necessary. In particular, CH_4, allene/propyne and acetonitrile were observed experimentally in appreciable yields at quite low temperatures, implying their formation through reactions of low activation energy. To simulate the formation of these minor products, a route of low activation energy via H addition to pyridine has been postulated. Reactions (30) and (31) are actually a simplification for a complex addition and ring contraction mechanism:-

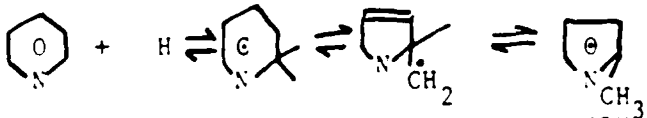

(IV)

The methylpyrrolyl radical (IV) produced in the above scheme, should possess considerable resonance stability as it is analogous to the methylcyclopentadienyl radical. The group additivity estimate for $\Delta H°_f$ (IV) = 46 kcal mol^{-1} (Table I). The methylpyrrolyl may thus be formed in a chemically activated state. It is further suggested that (IV) may undergo rapid unimolecular reaction to CH_3CN and propargyl radical (C_3H_3). Methane can then arise from methyl radicals produced by reaction of CH_3CN with H (Reaction 29). Propargyl radicals are an important source of the C_3H_4. The proposed reaction scheme to (IV) is analogous to an addition and ring contraction mechanism postulated by Ritter, Bozzelli and Dean[29] for H addition to benzene andmight be regarded as controversial. Nevertheless, these and other reactions of the mechanism postulated to simulate formation of the minor species have only a slight effect on the major products' profiles, and have been included solely for completeness.

A brief selection of results of sensitivity analyses of the reaction mechanism is given in Table III. This Table contains normalized sensitivity coefficients evaluated at 1600K and at 100 μs for the mixture of 0.7% pyridine in argon. The accuracy and usefulness of a sensitivity analysis is dependent strongly on the validity of the selected mechanism as well as the specific rate constants. Considering that this detailed chemical kinetic model of pyridine decomposition is the first to describe the formation of cyanoacetylene and several other important nitrogen-containing products and intermediates, the results in Table III should be considered qualitative rather than quantitative. This fact is particularly true for portions of the model that are speculative. For the main reaction sequence which is considered less speculative, the sensitivity analysis indicates that the reactions most important to the decay of the reactant and formation of major products are Reactions 1,4,5,6 and 7. The low sensitivity to k_3 (the sensitivity coefficient for all the species listed in Table III to this rate constant was less than 10^{-4}) indicates that, at least for the value of k_3 estimated in this work, Reaction 3 is not a rate limiting step to thermal decomposition of pyridine; rather, it is the production of the o-pyridyl radical via Reaction 6 (at 1600K) which is rate limiting. At lower temperatures (1300-1400K), the value of the sensitivity coefficient for the pyridine concentration with respect to k_1 (at 100 microseconds) is a factor of four greater than for that with respect to any other rate constant. Under these conditions, Reaction 1 is a rate-limiting step for the formation of o-pyridyl as well as for the overall decomposition of pyridine.

Our optimized value of the rate constant, $k_1 = 10^{15.9 \pm 0.4}$ exp $(-98\pm3\text{kcal mol}^{-1}/RT)s^{-1}$, is in excellent agreement at 1700K with the limiting high pressure rate constant obtained by Leidreiter and Wagner[10] for disappearance of pyridine. Our value differs from theirs by less than 5% at this temperature, and both sets of Arrhenius parameters agree well within experimental error. Thus, based on Leidreiter and Wagner's[10] fall-off calculations we may assume that under our experimental conditions (≈10 atm pressure) the unimolecular decomposition of pyridine was taking place at or very close to the high pressure limit and that Leidreiter and Wagner's[10] rate constant for disappearance of pyridine may be equated with our value of k_1, rate constant for the fission of the ortho-hydrogen of pyridine.

The reaction mechanism of Table II contains several other pressure-dependent rate constants. Some of these reactions may be in the fall-off region and the rate constants for these reactions may therefore be specific for the present conditions.

Our values of k_1 and k_2 (Table II) imply experimental heats of formation for o-pyridyl radical of ΔH°_f = 82±6 kcal mol^{-1} and for m- and p-pyridyls of 86 ± 6 kcal mol^{-1}. The latter value just encompasses the thermochemical estimate (Table I) within its error limits, however, the difference in heats of formation of o- and the m-, p-pyridyls is larger than the thermochemical estimate[10]. An ortho-stabilization energy as large as 4 kcal is, however, predicted by ab initio molecular orbital calculations on o-pyridyl[30] in which there is appreciable stabilizing interaction between the nitrogen non-bonding orbital and the singly occupied molecular orbital on the ortho-carbon. This interaction is not possible for the m- and p-radicals.

Our values of ΔH°_f for the pyridyls are also larger but within uncertainties of 76±10 kcal mol^{-1} obtained as an average value for the pyridyls by Kern et al[9] using an RRKM extrapolation of their rate data. However, in view of the possible effects of trace impurities, uncertainties in single pulse shock tube measurements at large extent of conversion and the additional possibility that the reaction might still be in the fall-off region, we cannot yet positively reject the thermochemical estimates of $\Delta H_{f,300}$ for the pyridyls in favor of our experimental values.

Our kinetic model when applied directly to simulate the TOF profiles of Kern et al.[9] overpredicts the rates of decomposition of pyridine and formation of C_2H_2 although its prediction of HCN rates is in agreement. Since our model was developed for a higher range of pressures and in view of the likelihood that the unimolecular initiation reactions (1) and (2) are likely to be well into the fall-off region at their pressures, the disagreement is not surprising. The failure of Kern, et al[9] to observe cyanoacetylene amongst their products is probably not inconsistent with our results - we estimate that at their highest temperature (2092K) HCCCN should be only one fifth of the concentration of HCN. At the lowest temperature of their studies (1703K) HCCCN and HCN should be of comparable concentration. However, sensitivity problems might then obscure mass spectral detection of HCCCN, especially as pyridine itself has a strong fragment peak at 51 A.M.U. (Ref. 31).

Sooting Tendency of Pyridine

In many previous studies (see references in Leidreiter and Wagner[10]) the sooting tendencies of pyridine in flames or shock tubes have been found to be substantially less than that of other aromatics (e.g. benzene). The results of this investigation are consistent with the previous studies since (except for benzonitrile) very few species with molecular weights higher than pyridine were observed. Negligible quinoline and naphthalene were detected. Furthermore, the carbon balance was reasonable (±15%) considering the difficulty in measuring accurately the concentrations of pyridine and other nitrogenous species. This situation differs dramatically from the pyrolyses of toluene[32] and benzene[18] which exhibited carbon losses of 70% or more (presumably to polyaromatic species and/or soot). In addition several multi-ringed species were observed, e.g., indene and naphthalene.

Explanations for the different sooting characteristic of pyridine usually include the fact that with an N-atom in the ring large pericondensed polyaromatic compounds cannot be formed. Based on the present experimental results, it appears that it is also difficult (although not impossible) to grow a second ring. We offer two possible explanations for this phenomenon. The most likely explanation is the short lifetime of the pyridyl radical which is less than a nanosecond at temperatures of this study. Our rate constant used in this half-life calculation, is based on the endothermicity of Reaction 3 and a selection of 10^{14} for the A-factor. Although the model calculations were insensitive to this rate constant, we estimate a potential uncertainty of up to one and one-half orders of magnitude. In comparison, the half-life of the phenyl radical is about 50 microseconds (or 500 microseconds using the recent rate data of Braun-Unkhoff et al[19] at 1500K. Phenyl radical, in turn, is believed to be a critical intermediate leading to the growth of polyaromatic hydrocarbons. The calculated life-time of o-pyridyl is unlikely to be in error by as much as four orders of magnitude and so we conclude that its relatively short lifetime prevents it from playing a critical role in the growth of two-ringed species. (The other pyridyls will attain larger concentrations but due to rapid interchange with o-pyridyl, their concentrations will also be low.) A second more speculative explanation relates to the relative reactivity of the carbon atoms on pyridine. We speculate that the carbon atom with the lowest reactivity is located at the meta position. Analogous to the growth mechanism for polyaromatic hydrocarbons, acetylene will add to pyridyl but specifically to o-pyridyl or p-pyridyl. An addition of a second acetylene and subsequent ring closure will be inhibited since external bonding to the N-atom will result in the loss of aromaticity and since the meta carbon is relatively unreactive. Growth to form a two-ringed compound will therefore be suppressed relative to that for a pure hydrocarbon.

Acknowledgement

The authors wish to thank Drs D. Seery and J.D. Freihaut for helpful discussions. Mr D. Kocum, (UTRC) and Mr M. Esler (University of Sydney) are also thanked for their technical and research assistance with experiments. J.C.M. gratefully acknowledges the assistance and encouragement of United Technologies Research Center through the agency of Drs J.D. Freihaut and D. Seery whilst on leave from University of Sydney on a Special Studies program.

References

1. Pershing, D.W.; Wendt, J.O.L. Sixteenth Symposium (International) on Combustion, p. 389, the Combustion Institute, 1977.
2. Painter, P.C.; Coleman, M.M. Fuel 1979 58, 301.
3. Turner, D.W.; Andrews, R.L.; Siegmund, C.W. AIChE Symposium Series No. 126, 1972, 68, 55.
4. Snyder, L.R. Anal. Chem. 1969, 41, 314.
5. Brandenburg, C.F.; Latham, D.R. J. Chem. Eng. Data 1968 13, 391.
6. Hurd, C.D.; Simon, J.I. J. Am. Chem. Soc. 1962 84, 4519.
7. Axworthy, A.E.; Dayan, V.H.; Martin, G.B. Fuel 1978 57, 29.
8. Houser, T.J.; McCarville, M.E.; Biftu, T. Int. J. Chem. Kinet. 1980, 12, 555.
9. Kern, R.D.; Yong, J.N.; Kiefer, J.H.; Shah, J.N. Shock Tube Studies of Pyridine Pyrolysis and their Relation to Soot Formation. Paper presented at 16th International Symposium on Shock Tubes and Waves, 1987.
10. Leidreiter, H.I.; Wagner, H.Gg. Z. Phys. Chem. Neve Folge 1987, 153, 99.
11. Colket, M.B.; Shock Tubes and Waves, Proceedings of the 15th International Symposium, Stanford University Press, Stanford, CA, 1986; 311.
12. Dibeler, V.H.; Reese, R.M.; Franklin, J.L. J. Amer. Chem. Soc. 1961, 83, 1813.
13. August, J.; Kroto, H.W.; McNaughton, D.; Phillips, K.; Walton, D.R.M. J. Mol. Spectrosc. 1988, 130, 424.
14. Benson, S.W.; Cruikshank, F.R.; Golden, D.M.; Haugen, G.R.; O'Neal, H.E.; Rodgers, A.S.; Shaw, R.; Walsh, R. Chem. Rev. 1969 69, 279.

15(a) Dewar, M.J.S.: Morita, T. J. Am. Chem. Soc. 1969, 91, 796.

(b) Dewar, M.J.S.: Harget, A.J.: Trinajstic, N. J. Am. Chem. Soc. 1969, 91, 6321.

16. Weissmann, M.A.; Benson, S.W. J. Phys. Chem. 1988, 92, 4080. Revised vinyl radical thermochemistry presented in this reference is used in the present work.

17. Melius, C.F. "BAC-MP$_4$ Heats of Formation and Free Energies", Sancha National Laboratories, Livermore July, 1986.

18. Colket, M.B. Twenty-First Symposium (International) on Combustion, p.851, the Combustion Institute, 1986.

19. Braun-Unkoff, M.; Frank, P.; Just, T. Twenty-Second Symposium (International) on Combustion, p.1053, the Combustion Institute, 1988.

20(a) De Frees, D.J.; Hehre, W.J. J. Phys. Chem. 1978, 82, 391.

(b) Grela, M.A.; Colussi, A.J. Int. J. Chem. Kinet. 1988, 20, 713.

21. Jacox, M.E.; Milligan, D.E. J. Mol. Spectros. 1975, 56, 333.

22. Job, V.A.; King, G.W. J. Mol. Spectrosc. 1966, 19, 155.

23. Alexander, A.J.; Kroto, H.W.; Walton, D.R.M. J. Mol. Spectros. 1976, 62, 175.

24(a) Costain, C.C.; Stoicheff, B.P. J. Chem. Phys. 1959, 30, 777.

(b) Kamesaka, I.; Miyawaki, K.; Kawai, K. Spectrochem. Acta 1976 32A, 195.

25. Kee, R.J.; Ruley, F.M.; Miller, J.A. The Chemkin Thermodynamic Data Base, Sandia Report SAND87-8215, April, 1987.

26. Kiefer, J.H.; Mitchell, K.I.; Kern, R.D.; Yong, J.N. J. Phys. Chem. 1988, 92; 677.

27(a) Kee, R.J.; Miller, J.A.; Jefferson, T.H. *Chemkin: A General-Purpose, Problem-Independent Transportable Fortran Chemical Kinetus Code Package,* Sandia Report SAND80-8003, March, 1980.

(b) Hindmarsh, A.C. *LSODE and LSODI: Two New Initial Value Differential Equation Solvers, ACM Signum Newsletter* 15 *[4], (1980)*

(c) Mitchell, R.E. and Kee, R.J. *A General-Purpose Computer Code for Predicting Chemical Kinetic Behavior Behind Incident and Reflected Shocks*, Sandia National Laboraotries SAND 82-8205, March 1982.

28\. Lutz, A.E.; Kee, R.J.; Miller, J.A. *Senkin: A Fortran Program Predicting Homogeneous Gas Phase Chemical Kinetics with Sensitivity Analysis*, Sandia Report SAND87-8248, February, 1988.

29\. Ritter, E.R.; Bozzelli, J.W.; Dean, A.M. *Mechanisms of CH_4, Cyclopentadiene, Biphenyl, Chlorobiphenyl, Toluene and Naphthalene Formation from Pyrolysis of Chlorobenzene in H_2*. Paper presented at Eastern States Meeting of the Combustion Institute, Washington, D.C., November, 1987.

30\. Kikuchi, O.; Hondo, Y.; Morihashi, K.; Nakayama, M. *Bull. Chem. Soc. Japan* 1988, *61*, 291.

31\. A.S.T.M. Index of Mass Spectral Data, A.S.T.M., 1969, p.7.

32\. Colket, M.B., Seery, D.J. *Mechanisms and Kinetics of Toluene Pyrolysis*, poster presentation at 20th Symposium (International) on Combustion, Ann Arbor, MI, 1984.

33\. McCullough, J.P.; Douslin, D.R.; Messerly, J.F.; Hossenlopp, I.A.; Kincheloe, T.C.; Waddington, G. *J. Am. Chem. Soc.* 1957, *79*, 4289.

34\. Harland, P.W. *Int. J. Mass Spectrometry and Ion Processes*, 1986. *70*, 231.

35\. Hall, H.K. and Baldt, J.H.: *J. Am. Chem. Soc.* 1971 *93*, 140.

36. Szekely, A.; Hanson, R.K.; Bowman, C.T. *Int. J. Chem. Kinet.* 1983, **15**, 915.

37. Kiefer, J.H.; Kapsalis, S.A.; Al-Alami, M.Z.; Budach, K.A. *Combust. Flame* 1983, **51**, 79.

38. Westmoreland, P.R. Preprints A.C.S. Division of Fuel Chem. 1987, **32** (3), 480.

39. Payne, W.A.; Stief, L.J. *J. Chem. Phys.* 1976, **64**, 1150.

40. Warnatz, J. In *Combustion Chemistry*; Gardiner, W.C., Jr., Ed.; Springer: New York, 1984; p.197.

41. Hsu, D.S.Y.; Lin, C.Y.; Lin, M.C. Symp. (Int.) on Combust. (Proc.) 1984, **20th**, 623.

42. Tsang, W. In *Shock Waves in Chemistry*; Lifshiz, A., Ed.; Marcel Dekker. New York, 1981, p.60.

43. Kiefer, J.H.; Mizerka, L.J.; Patel, M.R.; Wei, H.-C. *J. Phys. Chem.* 1985, **89**, 2013.

44. Organ, P.; Mackie, J.C. 1989 to be published.

TABLE I: Thermochemical Parameters for the Pyridine System

Species	$\Delta H^0_{f,300}$ (kcal mol^{-1})	S°_{300} (cal mol^{-1} K^{-1})	C_p (cal mol^{-1} K^{-1}) 300	500	1000	1500	2000
C_5H_5N	33.48[a]	69.99	18.70	30.85	46.56	53.14	56.27
C_5H_4N	91.7[b]	72.6	18.0	28.9	42.8	48.5	51.1
I[c]	114±3	79	23.6	32.6	43.1	48.2	50.8
II[c]	142±6						
III[c]	152±6						
HCCCN	84.6[d]	56.54	15.48	18.66	22.38	24.24	25.19
HC=CHCN	97±3	64.7	15.9	19.8	25.3	27.8	29.3
H_2CCHCN	43.9[e]	65.32	15.26	20.93	28.90	32.66	34.53
CVA[f]	99.5	76.92	22.53	30.17	39.55	43.82	45.99
HC_5N	142	73.91	22.45	27.03	32.54	35.21	36.52
$c\text{-}C_4H_3NCH_3$[g]	46.4	77.5	20.3	32.3	48.6	58.2	62.7
Groups							
$C_d\text{-}(H)(CN)$	37.6	37.7	10.12	13.47	17.67	19.48	20.38
$C_t\text{-}(CN)$	57.7	31.8	10.20	12.11	14.31	15.28	15.71
$\dot{N}_I$	76 ± 5						

---

a. Ref. 33

b. For o- and p-pyridyls, add -1.5 kcal mol^{-1}. (See Ref. 10)

c. For structures of these open-chain radicals from pyridyls, see Fig. 2. $\Delta^\circ H_{f,300}$ values have been estimated for all other possible open-chain radicals from pyridyls and are all >150±6 kcal mol^{-1}.

d. Ref. 34

e. Ref. 35

f. CVA = cyanovinylacetylene, HC ≡ C - CH = CH - CN

g. $C\text{-}C_4H_3NCH_3$ ≡ 

Table II: Reaction Model for Pyridine Pyrolysis

		FORWARD REACTION			REVERSE REACTION			
	REACTIONS	log A	n	E	log A	n	E	REF
1	C5H5N=o-C5H4N+H	15.90	0.0	98.0	14.10	0.0	-9.8	PW
2	C5H5N=C5H4N+H	15.48	0.0	102.0	13.67	0.0	-7.3	PW
3	o-C5H4N=C4H4CN	14.00	0.0	25.0	11.74	0.0	-0.3	est
4	C4H4CN=C2H2+HCCHCN	13.18	0.0	37.0	11.49	0.0	3.7	PW
5	HCCHCN=HCCCN+H	15.90	0.0	40.0	16.14	0.0	0.2	PW
6	C5H5N+H=o-C5H4N+H2	13.48	0.0	5.0	12.29	0.0	1.6	PW
7	C5H5N+H=C5H4N+H2	13.70	0.0	9.0	12.51	0.0	4.1	PW
8	C4H4CN=CVA+H	12.00	0.0	40.0	11.30	0.0	3.2	est
9	C5H4N=HCN+C4H3	14.48	0.0	57.0	9.65	0.0	-4.8	PW
10	C4H4CN=HCN+C4H3	13.70	0.0	45.0	11.13	0.0	7.1	PW
11	C4H4CN=C2H3+HCCCN	12.70	0.0	37.0	10.98	0.0	4.3	PW
12	H+HCCHCN=H2CCHCN	13.30	0.0	0.0	14.60	0.0	104.6	est
13	C2H2+HCN=H2CCHCN	13.48	0.0	40.0	15.08	0.0	80.0	est
14	H+H2CCHCN=HCCHCN+H2	13.70	0.0	8.0	13.02	0.0	7.8	est
15	HCCHCN=C2H2+CN	17.90	0.0	58.0	16.50	0.0	0.4	PW
16	C4H4CN=VA+CN	14.70	0.0	59.0	13.01	0.0	4.6	PW
17	CN+H2=HCN+H	13.88	0.0	0.0	14.35	0.0	17.9	36
18	CN+C2H2=C2H+HCN	12.70	0.0	3.0	12.45	0.0	0.6	est
19	H+H2CCHCN=HCN+C2H3	13.00	0.0	4.0	11.12	0.0	4.4	est
20	H2CCHCN=HCCCN+H2	14.00	0.0	80.0	13.56	0.0	40.0	est
21	CVA+H=C2H2+HCCHCN	13.00	0.0	4.0	12.02	0.0	7.6	est
22	C4H3+C5H5N=o-C5H4N+VA	12.30	0.0	8.0	12.47	0.0	6.0	est
23	C4H3+C5H5N=C5H4N+VA	12.30	0.0	10.0	12.47	0.0	6.5	est
24	CH3+C5H5N=o-C5H4N+CH4	11.70	0.0	10.0	11.98	0.0	7.2	est
25	CH3+C5H5N=C5H4N+CH4	11.70	0.0	11.5	11.98	0.0	7.2	est
26	CVA+H=HCN+C4H3	13.00	0.0	4.0	11.13	0.0	2.9	est
27	C2H+HCN=HCCCN+H	12.30	0.0	0.0	14.19	0.0	20.2	est
28	C2H+HCCCN=C4H2+CN	12.85	0.0	3.0	12.34	0.0	0.3	PW
29	CH3CN+H=HCN+CH3	13.70	0.0	2.0	12.22	0.0	10.2	PW
30	H+C5H5N=C-C4H3NME	12.30	0.0	2.0	12.12	0.0	41.1	PW
31	C-C4H3NME=CH3CN+C3H3	14.70	0.0	60.0	11.02	0.0	7.4	PW
32	C3H3+H=C3H4P	12.70	0.0	0.0	15.24	0.0	89.1	44
33	2C3H3=C2H2+VA	12.70	0.0	0.0	13.68	0.0	38.2	est
34	CH3+C2H=C3H4P	12.70	0.0	0.0	16.28	0.0	115.6	est
35	C4H3=C2H2+C2H	14.48	0.0	57.0	13.71	0.0	1.7	18

Table II(cont.)

		FORWARD REACTION			REVERSE REACTION			
	REACTIONS	log A	n	E	log A	n	E	REF
36	C4H3=C4H2+H	12.00	0.0	46.0	12.37	0.0	5.8	PW
37	C2H+H2=H+C2H2	12.85	0.0	0.0	13.57	0.0	20.2	37
38	C2H+C2H2=C4H2+H	12.00	0.0	0.0	13.14	0.0	15.1	38[a]
39	C2H+C4H2=C6H2+H	12.70	0.0	0.0	14.03	0.0	14.8	PW
40	H+C2H2=C2H3	12.64	0.0	2.4	12.37	0.0	42.8	39[b]
41	H+C2H4=C2H3+H2	13.70	0.0	8.0	11.87	0.0	6.9	16[c]
42	CH3+H2=CH4+H	2.81	3.0	7.7	15.14	0.0	17.3	40
43	C2H+C2H3=VA	13.00	0.0	0.0	16.01	0.0	120.8	est
44	C2H4=C2H2+H2	17.41	0.0	79.3	15.86	0.0	37.8	40
45	C4H3+C2H2=L-C6H5	12.00	0.0	3.0	14.15	0.0	36.9	18
46	L-C6H5=C6H5	10.30	0.0	1.4	13.65	0.0	65.2	18
47	C6H6=H+C6H5	15.70	0.0	107.9	13.10	0.0	-2.8	41
48	C2H3+C4H2=L-C6H5	12.00	0.0	3.0	14.06	0.0	36.7	18
49	2C6H5=C12H10	12.48	0.0	0.0	16.47	0.0	107.5	42
50	C6H6+H=C6H5+H2	14.40	0.0	16.0	12.42	0.0	9.8	43
51	2C3H3=L-C6H6	12.70	0.0	0.0	14.95	0.0	57.8	44
52	L-C6H6=C6H6	12.00	0.0	33.0	16.87	0.0	116.0	44
53	C4H4CN+C2H2=C6H6CN	12.70	0.0	1.2	14.57	0.0	37.2	est
54	C6H6CN=C-C6H6CN	11.30	0.0	0.0	14.22	0.0	49.7	est
55	BZN+H=C-C6H6CN	13.60	0.0	2.4	13.56	0.0	26.0	est
56	2C2H2=VA	13.77	0.0	44.6	15.17	0.0	81.1	26
57	VA=H2+C4H2	14.32	0.0	87.0	13.34	0.0	45.4	26
58	C2H+HCCCN=HC5N+H	12.00	0.0	0.0	11.98	0.0	15.3	est

Notes: Units for A : cm^3, mol, s.
Units for E : kcal mol^{-1}
PW indicates rate constant evaluated in present work.
est indicates rate constant was estimated in present work.

[a] Reverse rate constant agrees with value given in Reference at 1600K.

[b] Fall-off value. Pressure dependence as given in Reference.

[c] Revised vinyl thermochemistry presented in Reference has been used in the present work.

Species Identification

o-C5H4N: o-pyridyl, C5H4N: m- and p-pyridyls, VA: vinylacetylene, CVA: cyanovinylacetylene, BZN: benzonitrile, C3H4: allene and propyne, C4H4CN: HC=CH-CH=CHCN.
"L-" denotes open-chain radical.
C-C4H3NME:

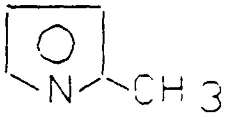

Table III. Sensitivity Coefficients in the Pyridine System for Selected Major Products Evaluated at 1600K and at 100 μs.

Reaction	Normalized Sensitivity Coefficients							
No.	C_5H_5N	C_2H_2	H_2	HCN	HC_3N	C_4H_2	C_4H_4	CH_4	C_6H_6
1	-0.054	0.166	0.165	0.165	0.173	0.160	0.156	0.393	0.274
4	-0.040	0.164	0.125	0.067	0.213			0.290	0.180
5			0.108	-0.111	0.160				
6	-0.067	0.254	0.345		0.491			-0.555	-0.313
7	-0.044	0.117	0.109	0.350	-0.104	0.432	0.229	-0.277	
9	-0.015	0.044		0.060		0.063			
10	-0.010			0.150	-0.113	0.191	0.113		
11	-0.014		0.087		0.140			0.115	
15		0.048	-0.090	0.111	-0.133				
16							0.225		
22							0.324		
23							0.179		
24								0.175	
28				0.047	-0.055	0.104			
29								0.734	
30	0.011	-0.051	-0.081	-0.050				0.326	0.351
31	0.012	-0.055	-0.088	-0.054	-0.058			0.344	0.378
33							0.116		-0.358
35						-0.066			
36		-0.081	0.084			0.354	-0.185		
37		0.084				-0.161	-0.088		
38						0.090			
39						-0.137			
42								0.260	
45	0.003							0.151	
47									0.078
51									0.392
52									0.132
56							-0.367		

List of Figures

Fig. 1: Distribution of all products of significance behind reflected shocks in the 0.7% pyridine in argon mixture over the temperature range studied.

Fig. 2: Possible open-chain radicals arising from simple ring cleavage of pyridyls.

Figs. 3-6: Comparison between the simulated yield of the designated product (lines) and experimental yields (symbols).

____ and o : .7% mixture
--- and [] : .15% mixture of pyridine in argon.

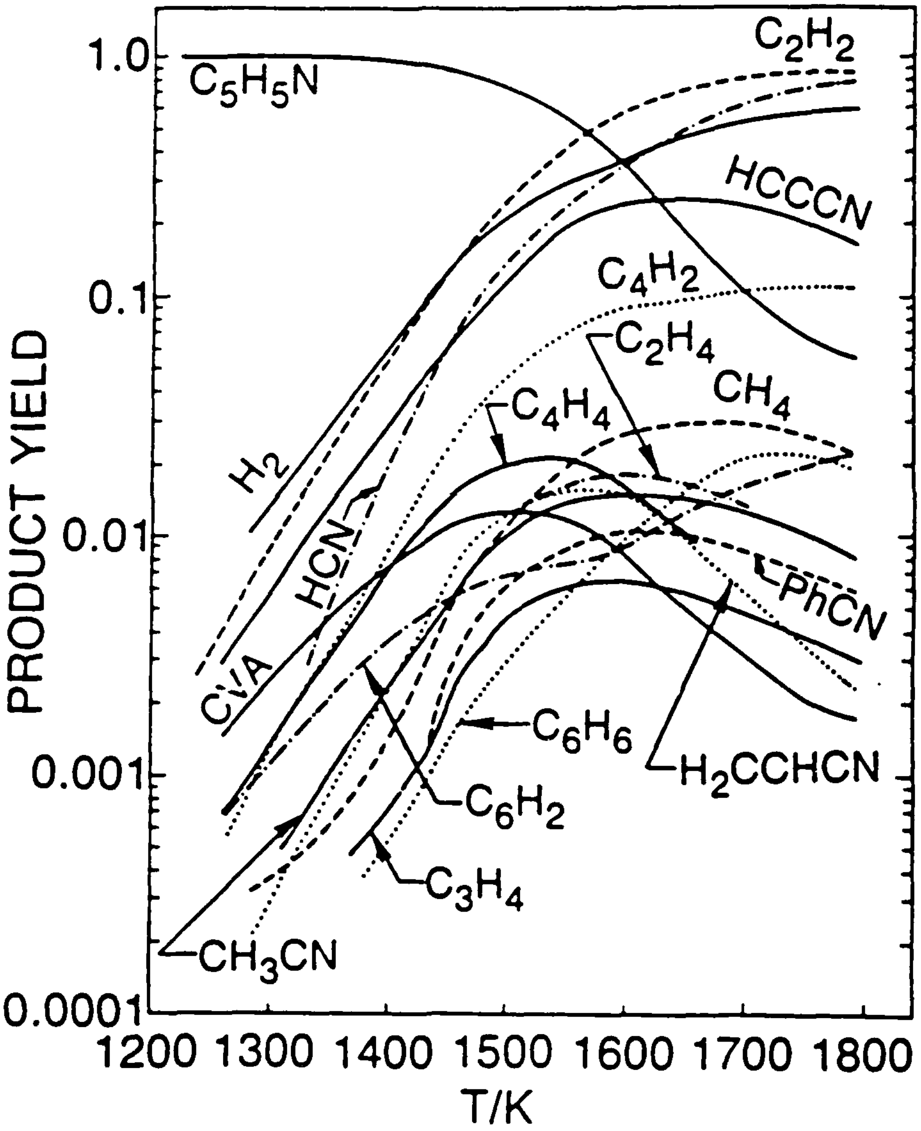
PRODUCT YIELD
1.0
0.1
0.01
0.001
0.0001
1200
1300
1400
1500
1600
1700
1800
T/K
C_5H_5N
C_2H_2
HCCCN
C_4H_2
C_2H_4
CH_4
C_4H_4
PhCN
H_2
CVA
HCN
C_6H_6
H_2CCHCN
C_6H_2
C_3H_4
CH_3CN

Fig. 2

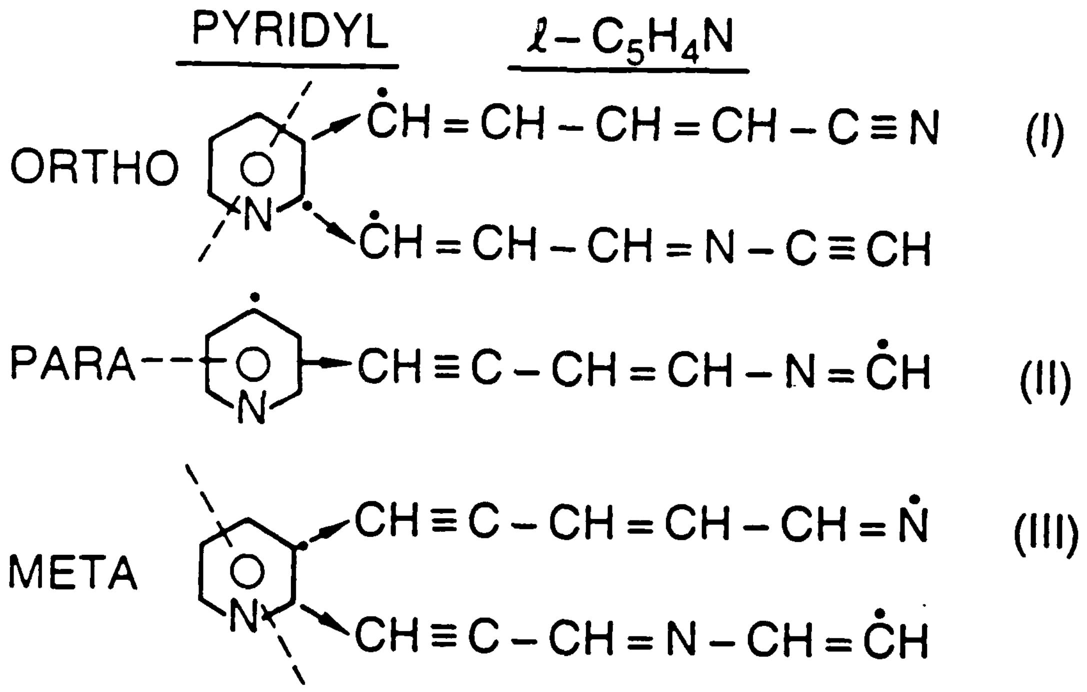
PYRIDYL
ℓ-C5H4N
ORTHO
N
ĊH = CH – CH = CH – C ≡ N
(I)
ĊH = CH – CH = N – C ≡ CH
PARA
N
CH ≡ C – CH = CH – N = ĊH
(II)
META
N
CH ≡ C – CH = CH – CH = Ṅ
(III)
CH ≡ C – CH = N – CH = ĊH

Fig. 5

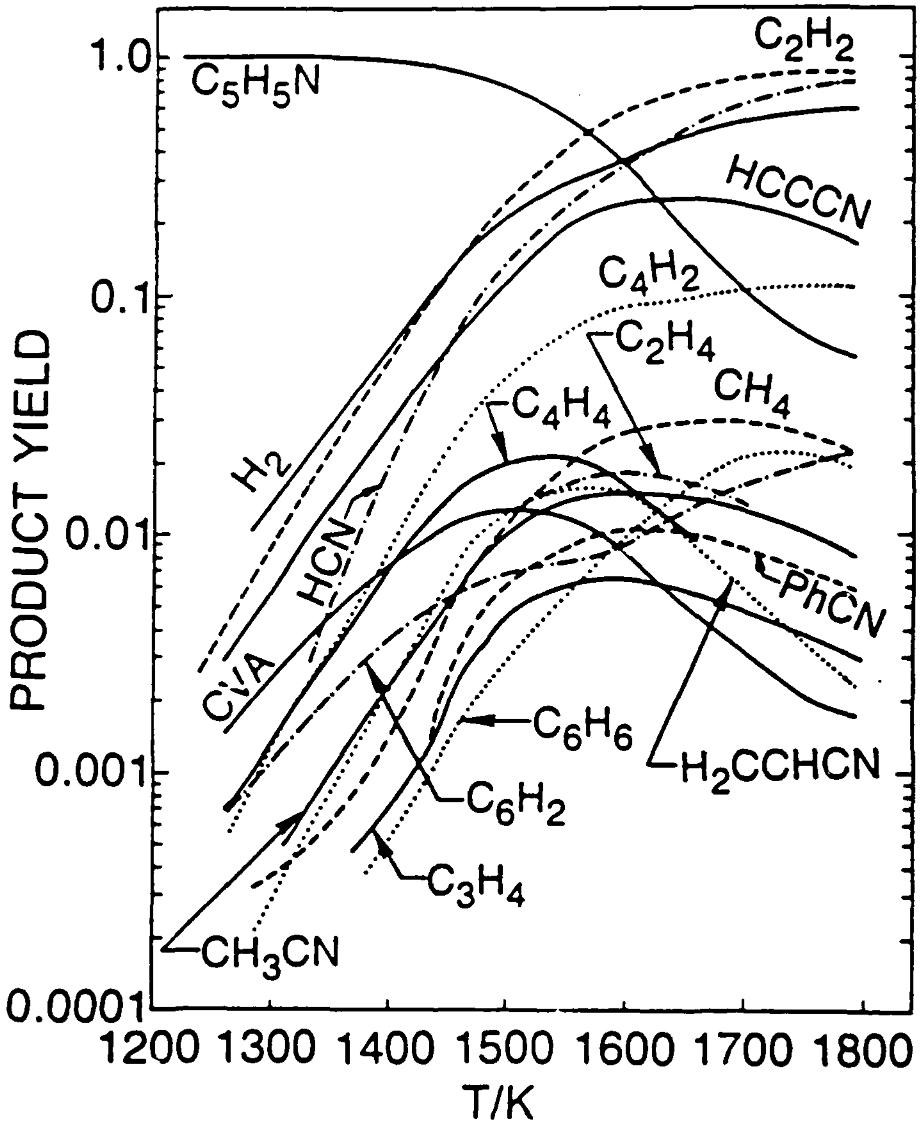
PRODUCT YIELD
T/K
1.0
0.1
0.01
0.001
0.0001
1200
1300
1400
1500
1600
1700
1800
C_5H_5N
C_2H_2
HCCCN
C_4H_2
C_2H_4
CH_4
C_4H_4
H_2
HCN
CVA
PhCN
C_6H_6
H_2CCHCN
C_6H_2
C_3H_4
CH_3CN

Fig. 2

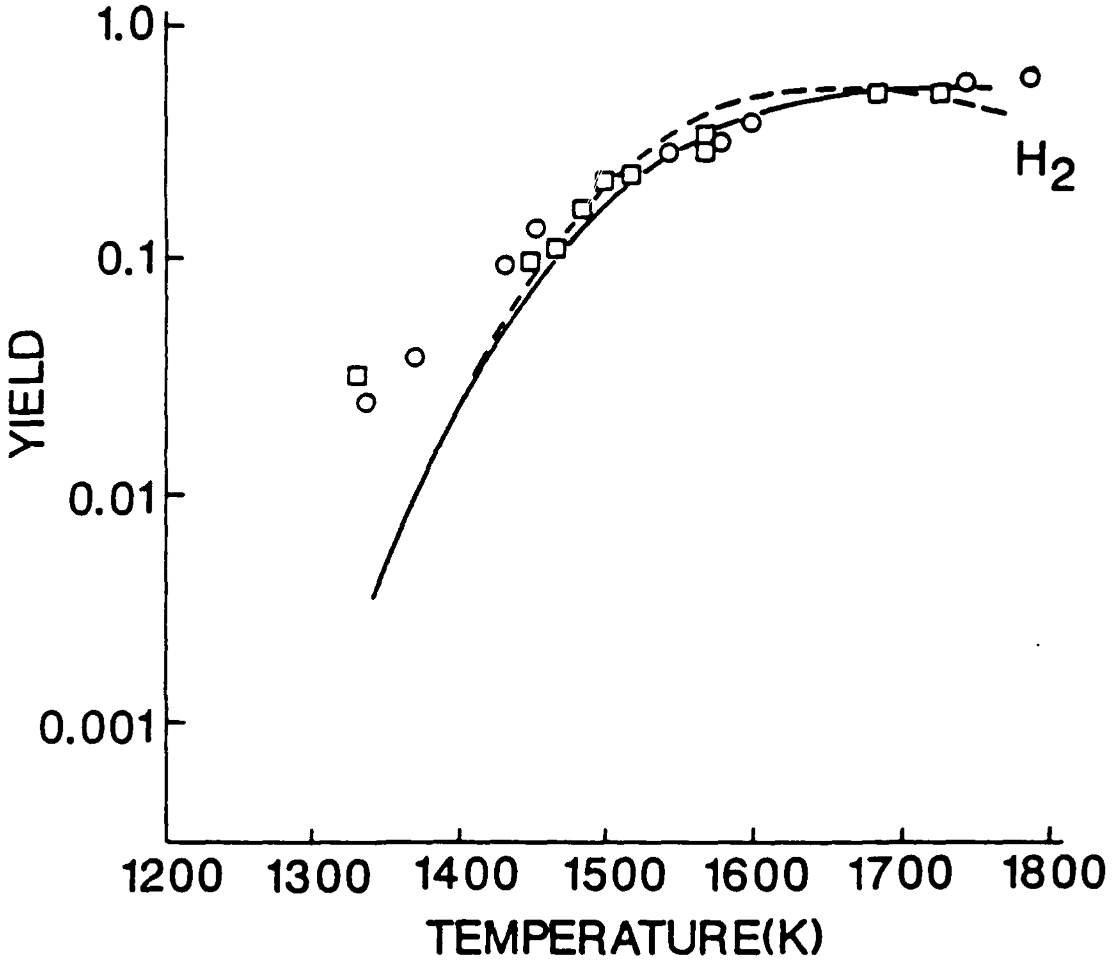
1.0
0.1
0.01
0.001
YIELD
H$_2$
1200
1300
1400
1500
1600
1700
1800
TEMPERATURE(K)

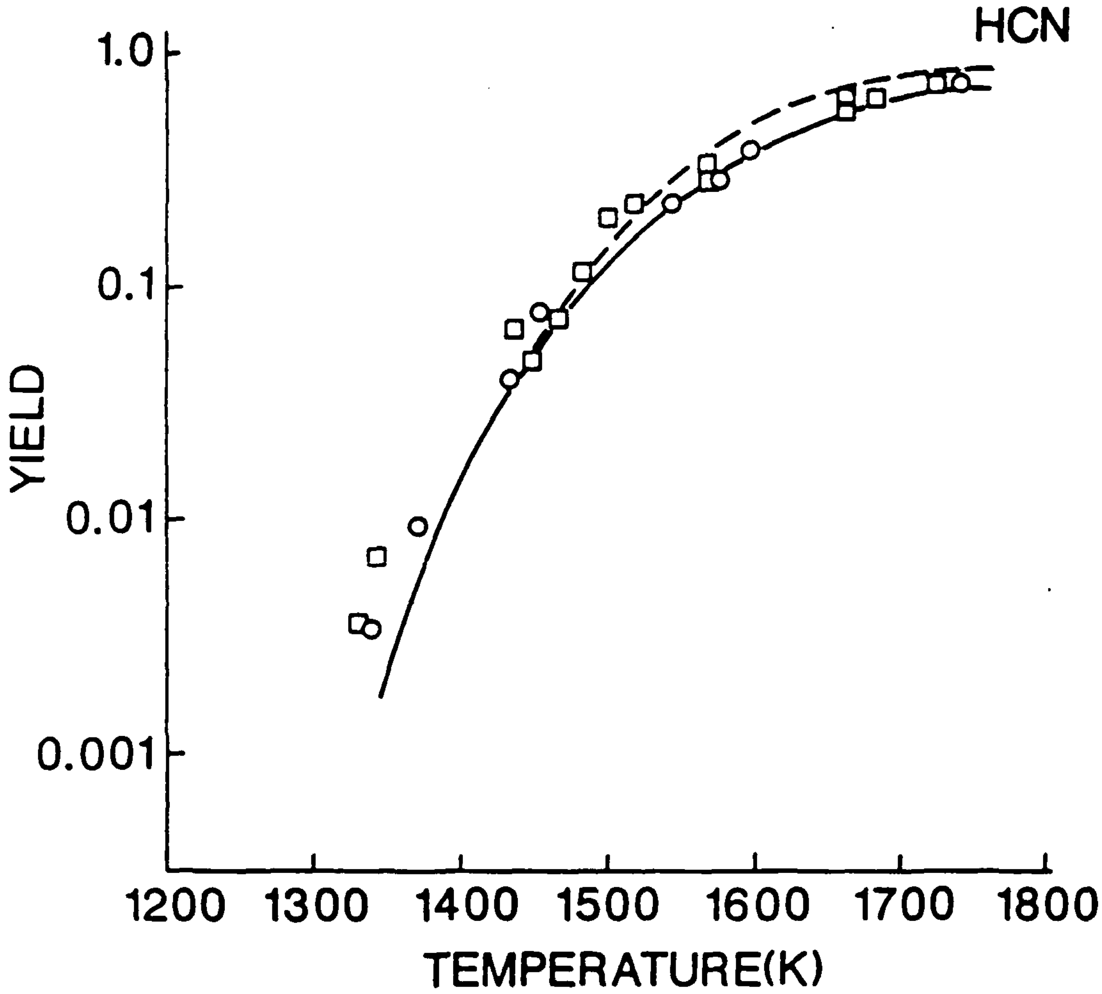
HCN
1.0
0.1
0.01
0.001
YIELD
1200
1300
1400
1500
1600
1700
1800
TEMPERATURE(K)

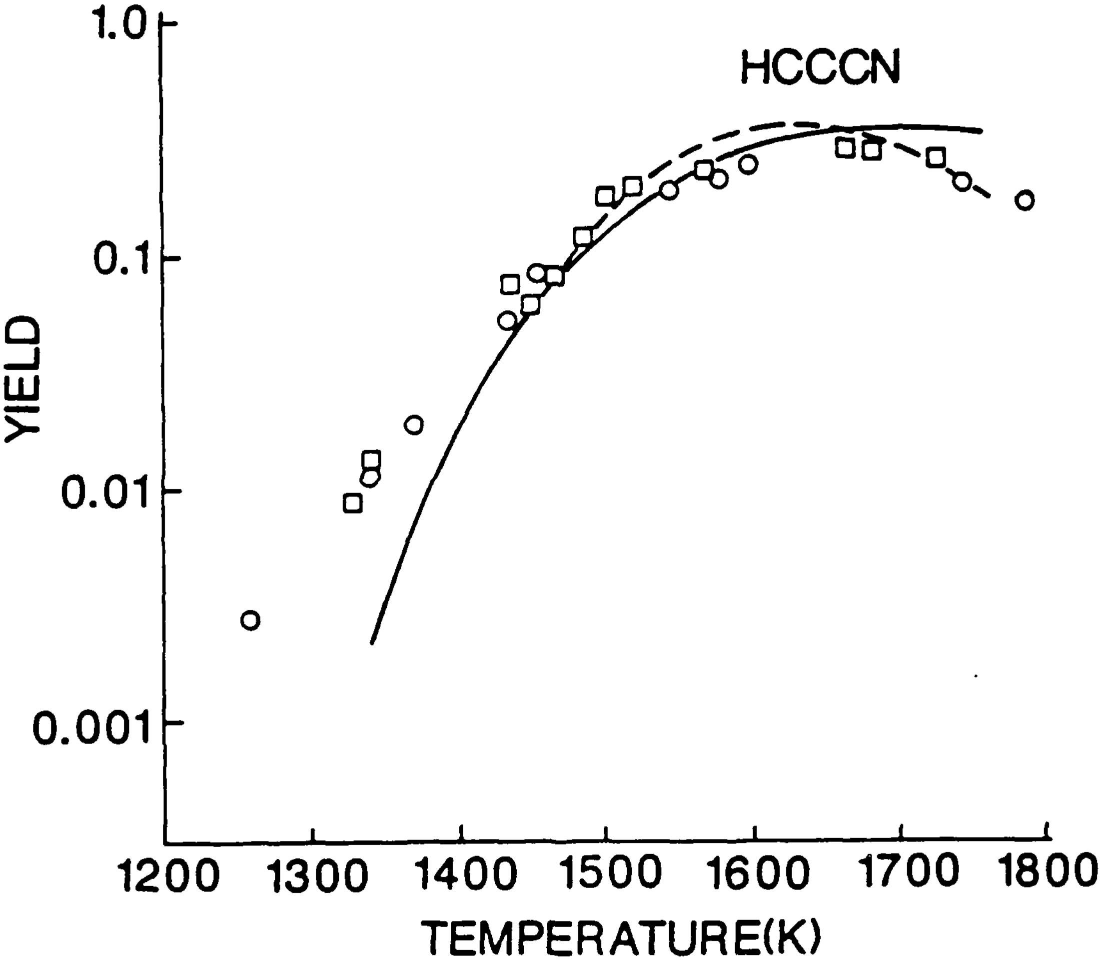
HCCCN
YIELD
1.0
0.1
0.01
0.001
1200
1300
1400
1500
1600
1700
1800
TEMPERATURE(K)

Fig. 6

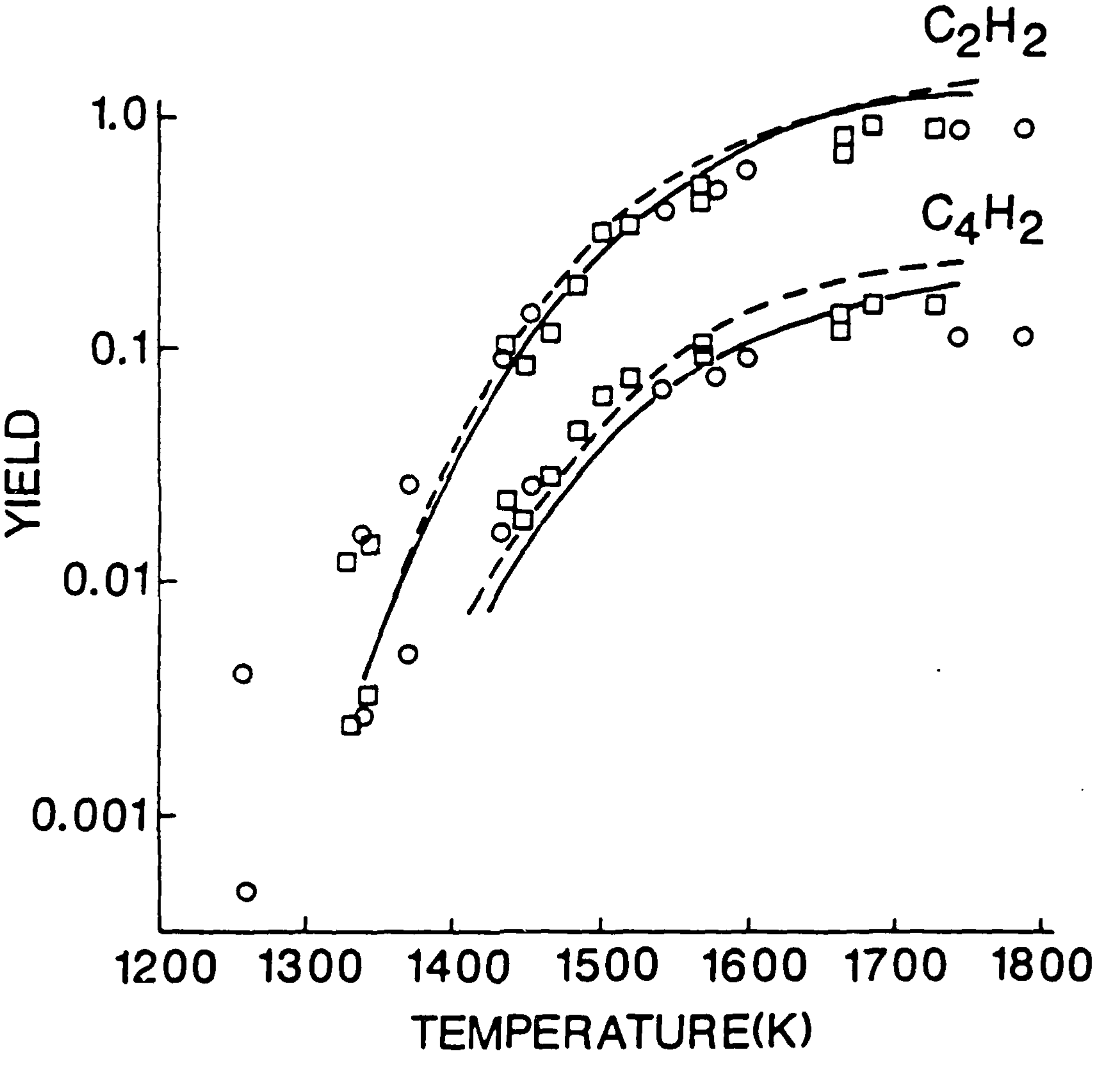

C_2H_2
C_4H_2
1.0
0.1
0.01
0.001
YIELD
1200
1300
1400
1500
1600
1700
1800
TEMPERATURE(K)

Appendix D

Shock Tube Pyrolysis of Pyrrole and Kinetic Modeling

SHOCK TUBE PYROLYSIS OF PYRROLE
AND KINETIC MODELING

John C. Mackie, Department of Physical Chemistry,
University of Sydney, NSW 2006, Australia

Meredith B. Colket III, United Technologies Research Center,
Silver Lane, East Hartford CT 06108

Peter F. Nelson, CSIRO Division of Coal Technology,
North Ryde, NSW 2113, Australia

Michael Esler, Department of Physical Chemistry,
University of Sydney, NSW 2006, Australia

Abstract

The kinetics of pyrolysis of pyrrole dilute in argon have been studied in a single pulse shock tube, using capillary column GC, together with GC/MS and FTIR for product identification, over the temperature range 1200-1700 K, total pressures of 7.5-13.5 atm and nominal mixture compositions of pyrrole of 5000 and 700 ppm . Time-resolved measurements of the rate of disappearance of pyrrole behind reflected shock waves have been made by absorption spectroscopy at 230 nm, at pressures of 20 atm and mixture compositions between 1000-2000 ppm pyrrole. At the lower end of the studied temperature range, the isomers of pyrrole - allyl cyanide and cis- and trans-crotononitrile - were the principal products, together with hydrogen cyanide and propyne/allene. At elevated temperatures, acetylene, acetonitrile, cyanoacetylene and hydrogen became important products.

The rate of overall disappearance of pyrrole, as measured by absorption spectrometry, was found to be first order in pyrrole concentration, with a rate constant $k_{dis}(\text{pyrrole})=10^{14.1\pm0.7} \exp(-74.1\pm3.0 \text{ kcal mol}^{-1}/RT)\ s^{-1}$ between 1350-1600 K and at a pressure of 20 atm. First order dependence of pyrrole decomposition and major product formation was also observed in the single pulse experiments over the range of mixture compositions studied.

A 74-step reaction model is presented and shown to substantially fit the observed temperature profiles of the major product species and the reactant profile. In the model the initiation reaction is postulated to be the reversible formation of pyrrolenine, (2H-pyrrole). Pyrrolenine can undergo ring scission at the C2-N bond forming a biradical which can rearrange to form allyl cyanide and crotononitrile or undergo decomposition to form HCN and C_3H_4 or acetylene and a precursor of acetonitrile. The model predicts an overall rate of disappearance of pyrrole in agreement with the experimental measurements.

Introduction

There is considerable recent interest in the reaction pathways whereby fuel-bound nitrogen evolves as NO_x in combustion of coals and other heavy fuels [1,2]. Coals and coal-derived liquids contain nitrogen in heterocyclic structures containing pyridine and pyrrole rings [3,4]. In furthering our understanding of NO_x-forming reactions in combustion of heavy fuels it is important to identify the volatile nitrogen-containing precursors which form upon initial thermal decomposition of the original naturally occurring fuel-nitrogen structures.

Recently, we investigated [5] the products of pyrolysis of pyridine and the kinetics of evolution of nitrogen products from this molecule which might be considered as representative of aromatic nitrogen functional groups in coals. In addition to hydrogen cyanide, organic nitriles, especially cyanoacetylene, were found to be important pyrolysis products of pyridine.

There have been few previous studies of the pyrolysis of pyrrole or its derivatives, however. Apart from some brief studies of thermal [6-8] and photochemical [9] decomposition of pyrrole, the only detailed kinetic study of the pyrolysis of pyrrole is the recent work of Lifshitz et al [10] published during the course of our present work. Lifshitz et al studied the thermal decomposition of 1% mixtures of pyrrole in argon in a single pulse shock tube (SPST) over the temperature range of 1050-1450 K and at pressures of about 3 atm. From product distributions measured by the SPST technique they found that cyanoalkene isomers of pyrrole (especially allyl cyanide and cis- and trans-crotononitrile) were important products of decomposition. Lifshitz et al also determined from product analyses apparent Arrhenius parameters for disappearance of pyrrole and for formation of major products. Although a mechanism was suggested for the pyrolysis of pyrrole, they did not carry out detailed kinetic modeling.

Our present work, also carried out by SPST, not only extends the results of Lifshitz et al to higher temperatures (1700 K), but also develops and evaluates a detailed chemical kinetic reaction model for pyrrole pyrolysis. In addition, we report a time-resolved ultraviolet absorption spectroscopic kinetic measurement of the direct decomposition of pyrrole in highly dilute mixtures in argon.

Experimental

Pyrolyses were carried out on two single pulse shock tubes, one of diameter 3.8 cm at United Technologies Research Center which was used primarily for SPST kinetic studies; the other at the University of Sydney (diam. 7.6 cm) was used for real-time ultraviolet absorption studies and for product identification in conjunction with a Finnegan GC/MS at CSIRO. The United Technologies Research Center shock tube and ancillary on-line GC analytical system have been described previously [11]. The Sydney tube was equipped with pairs of sapphire UV-transmitting windows. The absorption spectra at 230 nm of pyrrole vapour dilute in argon behind the reflected shock was measured at a distance of 35 mm from the endwall using a 0.3 m Spex Doublemate spectrometer with 2 nm slits and a 150 W extended UV high pressure xenon arc lamp as source. The time constant of the optical system, photomultiplier, oscilloscope and associated circuitry was ≤5 μs.

Pyrrole samples were purchased from Aldrich (stated purity 99%) and from Merck (purity 98%). Several bulb-to-bulb purifications were used to produce samples of purity exceeding 99.8% (by GC). The only detectable impurity peak was an unidentified species heavier than pyrrole and not present in the reaction products. No difference between the two sources of pyrrole was observed.

For the SPST kinetic measurements, mixtures of nominal compositions of 5000 and 700 ppm pyrrole in argon were prepared and stored in glass tanks. Pressures and temperatures behind the reflected shock were computed from the measured incident shock velocity. Residence times and quenching rates by the rarefaction wave were measured from pressure profiles recorded by Kistler gauges. Reflected shocked gas temperatures ranged from 1200-1700 K and total pressures from 7.5-13.5 atm. Residence times at uniform temperatures behind the reflected shock front ranged from 450-750 μs. Product analyses of the SPST runs on the United Technologies Research Center tube were made on a Chrompack CP Sil 5 capillary column.

The time-resolved UV absorption measurements of pyrrole decomposition were carried out on mixtures of 1000-2000 ppm pyrrole in argon at temperatures between 1300-1700 K, pressures of 20 atm and residence times up to 800 μs. In the absorption studies temperatures were calculated from measurements of both incident and reflected shock velocities.

Product identification and calibration were generally made by direct comparison with standards. The C_3H_5CN isomeric products were identified by GC/MS and retention times confirmed with commercial samples.

Cyanoacetylene was identified both by FTIR spectroscopy and GC/MS. Both hydrocarbons and nitrogen-containing compounds were analysed by FID. Hydrogen was detected by TCD. As reported previously [10] the capillary column and sampling system exhibited a 'memory effect' for the nitrogen-containing compounds, especially pyrrole and its cyanoalkene isomers, as well as acetonitrile and acrylonitrile. Repeatability of injections of these compounds was only ± 10%. Stock mixtures of pyrrole in argon slowly decreased in concentration with storage. It was found necessary to determine the concentration of pyrrole in the pre-shock mixture just prior to firing each shock. This was effected by injecting a very small volume of the pre-shock mixture via a sampling valve into the GC. Actual initial concentrations of pyrrole in argon ranged from 3700-5200 ppm for the nominally 5000 ppm mixture and from 550-870 ppm for the nominally 700 ppm mixture.

Results

Product distributions

Yields of all products of significance (scaled by the initial concentration of pyrrole) are shown in Figure 1 as a function of temperature for a mixture of 5000 ppm pyrrole in argon. The variation of pyrrole concentration with temperature is also given in this Figure. There is little difference in the normalized product distributions between the (nominally) 5000 and 700 ppm mixtures.

At the lowest temperatures at which decomposition can be detected, the cyanoalkene isomers of pyrrole - allyl cyanide and cis- and trans-crotononitrile - are the major products. HCN is also formed at low temperatures in approximately equal concentration with each C_3H_5CN isomer. Lesser amounts of propyne/allene (the capillary column did not fully resolve these two isomers) are observed. With increase in temperature, acetylene becomes an increasingly important product. Hydrogen, too, is a major product at higher temperatures. The apparent activation energies of formation of the last two products are higher than those of the cyanoalkenes and HCN and C_3H_4.

At elevated temperatures, yields of cyanoacetylene, acetonitrile and acrylonitrile rise steeply. Other products of significance which have large activation energies of formation are methane and ethylene. Much smaller amounts of ethyl cyanide and methylmethacrylate, the branched chain isomer of C_3H_5CN, were observed. Small amounts of benzene and benzonitrile are found at high temperatures. Traces of propene, 1,3-butadiene and ethane were also detected. A very small peak corresponding to the formula C_4H_3N was observed in the GC/MS. This was attributed either to CH_3CCCN or to $CH_2=C=CHCN$. Diacetylene and triacetylene only became important at temperatures above 1600 K. At high temperatures a loss of carbon was observed. This loss increased with increase in pyrolysis temperature and comprised about 7% of the carbon in the reactant at 1700 K. Some tarry material was observed in the high temperature pyrolysate.

The observed distribution of products is quite similar to those observed by Lifshitz et al [10] except that the temperatures of onset of products were lower in the earlier studies [10] because of the longer residence times (≈ 2 ms). Small differences in product distributions between the two studies involve the minor product, ethane (Lifshitz et al observe substantially more than we) and in the cis/trans ratio of crotononitrile. We found this ratio to vary little with temperature, ranging from approximately 1.5 at 1300 K to 1.2 at 1600 K at which temperature appreciable decomposition of crotononitrile took place. On the other hand, Lifshitz et al reported that the product was nearly all cis at the lowest temperatures of their study (≈ 1050 K) with the cis/trans ratio decreasing to about 1.4 around 1300 K. Presumably, the cis/trans ratio observed in the present work was a consequence of rapid cis-trans equilibration taking place at elevated temperatures.

The higher yields of ethane recorded by Lifshitz et al probably arose from enhanced secondary reactions taking place at their higher mixture concentrations (1% pyrrole in argon).

Time-resolved kinetic measurements

An oscilloscope trace of the 230 nm absorption by a shock heated pyrrole mixture (1000 ppm) is shown as a function of time in Figure 2. The wavelength studied corresponds to the lowest $^1\pi^* \leftarrow {}^1\pi$ transition of pyrrole [12,13]. In Figure 2, it may be seen that there is an increase in absorption due to the increase in density after passage of the incident shock front. A further large increase in absorption takes place initially upon passage of the reflected shock, followed by exponential decay of absorption resulting from decomposition of the pyrrole behind the reflected shock front. At the low densities of pyrrole employed in the absorption studies, the decrease in temperature due to reaction is less than 1 K.

A plot of $\ln\{-\ln(I/I_o)\}$ which is proportional to $\ln\{[\text{pyrrole}]_t\}$, is shown as a function of time for this run in Figure 3. (I_o and I are the unattenuated intensity and intensity at time t, respectively.)

These plots are linear except for a small curvature at late times. First order rate constants have been obtained from the initial linear portions of these plots. At high temperatures (>1650 K) the oscillograms of light transmission asymptote practically to I_o indicating there are only low concentrations of absorbers of 230 nm radiation in the high temperature products. At temperatures of 1700 K and above, the rate of decay of absorption at 230 nm becomes comparable with the time constant of the detection system.

An activation energy plot of the first order rate constants derived from the absorption of 230 nm radiation by pyrrole is shown in Figure 4. Regression analysis yields Arrhenius parameters for the rate constant, k_{dis}, for overall disappearance of pyrrole of $\log(A/s^{-1})=14.1\pm0.6$ and $E_a=74.1\pm3.0$ kcal mol^{-1} between 1480-1680 K.

Discussion

Thermochemical considerations

As shown earlier [10] the major pathways in the pyrolysis of pyrrole involve isomerization to the nitriles, C_3H_5CN, together with fragmentation principally into HCN, C_3H_4, C_2H_2 and CH_3CN. Based on measurements of apparent Arrhenius parameters for formation of the major products, Lifshitz et al [10] suggested that the nitrile isomers and the HCN and C_3H_4 arose from a single transition state which involved a simultaneous unimolecular C-N bond cleavage together with a simultaneous H-transfer of the N hydrogen to the C2 position. A further H-atom transfer in the biradical thus formed would be necessary for formation of C_3H_5CN.

In the case of furan, the O-analogue of pyrrole, pyrolysis is initiated by C-O fission followed by subsequent rearrangement and/or fragmentation of the biradical [14-16]. For furan, the rate constant for disappearance is [15,16] $k_{dis}(\text{furan}) = 10^{15.4}\exp(-78 \text{ kcal mol}^{-1}/RT)\ s^{-1}$, as expected for ring opening. In contrast, cur value for pyrrole, obtained from the time-resolved absorption measurements, of $k_{dis}(\text{pyrrole}) = 10^{14.1\pm0.6}\exp(-74.1\pm3.0 \text{ kcal mol}^{-1}/RT)\ s^{-1}$, does not appear to be representative of typical Arrhenius parameters for direct ring opening to a biradical.

A consideration of the thermochemistry of the pyrrole system can be of assistance in unravelling the pyrolysis mechanism. It is generally agreed that pyrrole is considerably more aromatic in character than furan [17]. Thus, the C-N bond in pyrrole should be significantly stronger than a typical C-N single bond. There are no experimental data available for the C-N bond dissociation energy in pyrrole. We are forced, therefore, to make approximate group additivity estimates of the thermochemistry of the pyrrole system. Biradical (I) formed on C-N scission would have resonance forms:

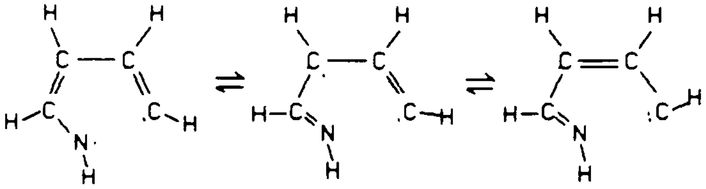

(I) (II) (III)

An approximate estimate of $\Delta H_{f,300}(II) = 123\pm5$ kcal mol^{-1} can be obtained from groups N_I-(H), C_d-(H)(C_d), $C\cdot_d$-(H)(C_d) and $C\cdot$-(H)$(C_d)_2$, available in the literature [18,19]. The biradical will be resonance stabilized. A stabilization energy of about 7 kcal mol^{-1}, similar to that in the biradical formed during furan decomposition [14,16], would lead to an enthalpy of formation of the stabilized biradical of about 116±6 kcal mol^{-1} and to a C-N bond dissociation energy in pyrrole of approximately 90 kcal mol^{-1}. If these estimates are correct, then our observed activation energy for disappearance of pyrrole of 74 kcal mol^{-1}, or, indeed, that reported by Lifshitz et al (75 kcal mol^{-1}) would not appear to correspond to direct ring scission.

Pyrroles are known to rearrange thermally at temperatures between 500-600°C [20]. Patterson et al [21-23] studied the thermal rearrangement of several N-substituted pyrroles to the corresponding 2-substituted pyrrole. Arrhenius parameters for several N-alkylpyrrole rearrangements have been measured by Jacobson and Jensen [24,25]. The rearrangements were found to be homogeneous intramolecular shifts. Pyrrolenine (2H-pyrrole) intermediates were postulated to be involved in the mechanism. Pyrrole itself undergoes this rearrangement. Patterson et al [23] pyrolysed N-deuterated pyrrole under similar conditions to the N-alkyl rearrangements and found 2-deuterated pyrrole. Although pyrrolenines have not been isolated from the pyrolysis products of simple N-substituted pyrroles, 2H-pyrroles have been observed in the photolysis of N-alkyl ring substituted pyrroles [20]. There is now considerable indirect evidence for the presence of pyrrolenine intermediates in both thermal and photochemical rearrangements of 1H-pyrroles.

Unlike its 1H-isomer, pyrrolenine would be expected to possess a relatively weak C-N bond with the C2 carbon. Again, there are no experimental thermochemical data available on pyrrolenine and we have been forced to resort to approximate group additivity methods to estimate the enthalpy of formation of this molecule. Under the assumption that the ring correction terms are the same as for cyclopentadiene, we estimate that $\Delta H_{f,300}$=45.5 kcal mol^{-1} for pyrrolenine. This is in satisfactory agreement with the value of 44.6 kcal mol^{-1} obtained by a MINDO/3 calculation of the pyrrole/pyrrolenine energy of tautomerization [26].

We suggest that the pyrolysis of pyrrole is initiated by the reversible hydrogen shift to pyrrolenine:

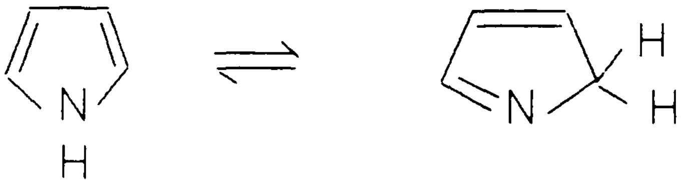

(1)

Pyrrolenine may then undergo thermolysis. It would be expected that the ring would open by scission of the C2-N bond.

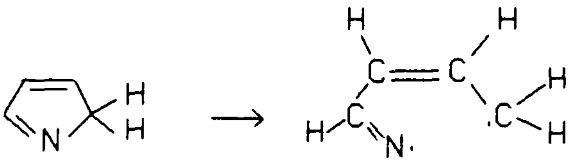

(IV)

Biradical (IV) could then undergo rapid H atom shifts to form cis-crotononitrile or allyl cyanide. The first isomer can be formed by a simple 1,4 H-shift although to form the second would appear to require a

1,2 H-shift, usually a process of relatively high activation energy. However, as pointed out by Benson [27], this shift can be facile and rapid in a biradical.

Hydrogen cyanide and propyne/allene could arise from a transition state resulting from contraction of the biradical to a cyclopropenyl ring with subsequent elimination of HCN. Propyne and allene would then be the products of isomerization of a 'hot' cyclopropene molecule [28].

In a process of higher activation energy, the biradical, having undergone 1,3-hydrogen shift, could then eliminate acetylene, forming a C_2H_3N precursor of CH_3CN such as 2H-aziridine (V) which would then rapidly rearrange to acetonitrile. This rearrangement has been studied theoretically by ab initio methods [29,30] and has been observed experimentally in the pyrolysis of vinyl azide [30,31].

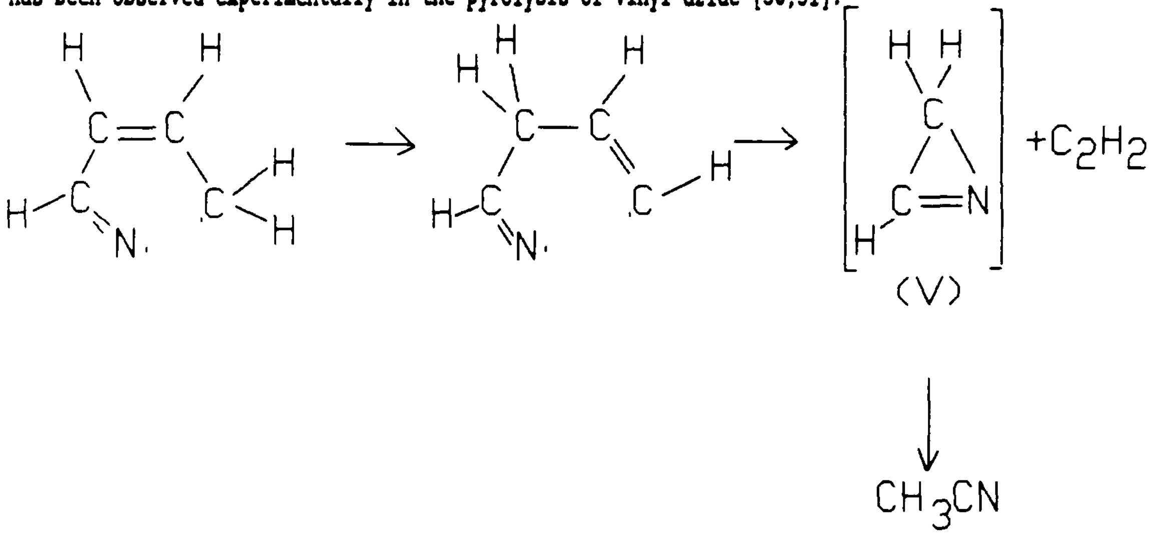

To consider the feasibility of this suggested mechanism it is necessary to have an estimate of the enthalpy of formation of biradical (IV). This biradical should possess allylic resonance stabilization. An approximate value of the enthalpy of formation can be obtained using groups from the allyl radical together with groups C_d-$(H)_2$, C_d-$(H)(C_d)$, C_d-$(H)(N_I)$ and $N^{\bullet}_I$. The last-mentioned group contribution is estimated [5] by comparing group differences between $H_2C{=}C^{\bullet}H$ and $H_2C{=}CH_2$ with $H_2C{=}N^{\bullet}$ and $H_2C{=}NH$. In this way we estimate $\Delta H_{f,300}$(IV) = 118±5 kcal mol^{-1}.

Thermochemical parameters used in the present study and not available in the thermochemical literature are presented in Table I.

Reaction model

The detailed reaction model to simulate the yields of the major products is given in Table II. As suggested above, initiation is via the reversible reaction (1) to form pyrrolenine. Although activation energies for N-alkyl rearrangements in pyrroles are between 57±3 kcal mol^{-1} and A-factors around $10^{13}s^{-1}$ [23,25], no kinetic data are available for N-H to C2 shifts. We have therefore chosen to optimize the rate parameters of reaction (1). As discussed below, the reaction model is very sensitive to the value of k_1. Optimization involved the systematic variation of A_1 and E_1 to best fit the experimental pyrrole profile and profiles of the major products. The optimized value of $k_1=3x10^{13}exp(-67\ kcal\ mol^{-1}/RT)\ s^{-1}$ was obtained. Reactions (2), (3), (4) and (5) of Table II are not elementary reactions but involve the intermediate biradical (IV) above, whose subsequent decomposition is considered to be rapid by parallel pathways, one, a rearrangement to the C_3H_5CN isomers, the second, a fission to HCN and propyne/allene (probably via a cyclopropene intermediate), whereas the third involves the elimination of C_2H_2.

The same optimized value for the activation energies of reactions (3) and (4) was obtained, 68 kcal mol^{-1}. This activation energy is, within the error of estimating the enthalpies of formation, equal to the enthalpy difference between biradical (IV) and pyrrolenine. For purposes of modeling, both cis- and trans-crotononitrile have been lumped together. A-factors for reactions (3) and (4) are $5x10^{15}\ s^{-1}$, normal values for ring scission to a biradical [15,16]. The optimized rate constant for reaction (2) is $k_2=3x10^{13}exp(-56\ kcal\ mol^{-1}/RT)\ s^{-1}$. This preexponential factor is suggestive of a cyclic transition state and the activation energy is sufficiently high to permit a cyclopropene intermediate. In the model, C_3H_4 has been considered to be propyne, the more thermodynamically stable form at high temperatures. The rate constant for reaction (5) derived from the modeling is $k_5=6x10^{15}exp(-76\ kcal\ mol^{-1}/RT)\ s^{-1}$. The derived activation energy is probably high enough to enable biradical (IV) to split into C_2H_2 and a C_2H_3N precursor of acetonitrile such as 2H-aziridine although other intermediates of lower energy such as ketenimine have been identified on the C_2H_3N surface [29,30].

The model contains secondary reactions of the major products. Radicals important in the mechanism can be identified by their products of termination. Presumably, ethane arises from methyl radical recombination. Ethyl cyanide results from combination of CH_3 and CH_2CN. A important reaction for production of the latter radical is the unimolecular fission reaction of allyl cyanide [reaction (-32)].

Homogeneous termination of vinyl radicals would be expected to produce 1,3-butadiene. The presence of a C_4H_3N product (either CH_3CCCN or $CH_2=C=CHCN$) suggests the intermediacy of a cyanoallyl radical. This radical can be produced by H-abstraction reactions of allyl cyanide.

The observed yields of hydrogen and methane could not be simulated merely from secondary reactions of product species. To model the experimental H_2 and CH_4 it was necessary to include abstraction reactions of pyrrole in the mechanism. The weakest bond involving hydrogen should be the N-H bond which might be expected to be somewhat weakened owing to the partial aromaticity of the CNC bonds. The pyrrolyl radical formed from H and CH_3 abstraction of the N-hydrogen is analogous to the cyclopentadienyl radical and should possess considerable resonance stabilization. An estimate of the enthalpy of formation of pyrrolyl can be made under the assumption that the ring stabilization energy is similar to that in cyclopentadienyl. The value thus obtained is $\Delta H_{f,300}$(pyrrolyl) = 54.4 kcal mol^{-1}. The H-bond fission reaction of pyrrole [reaction (56)] has been included in the model together with H and CH_3 abstraction reactions (59,60).

Ring opening reactions of the stabilized pyrrolyl radicals are likely to have high activation energies. These radicals, like cyclopentadienyl radicals [32], should be unreactive. In the model, termination reactions of these radicals to form a bipyrrolyl product have been included. Whilst this product has not been specifically identified, experimentally there was a loss of carbon and production of heavy product which might have contained some nitrogen.

Integration of the kinetic equations of Table II was made using the CHEMKIN package [33], LSODE [34] and the SANDIA shock tube code [35] modified to account for the effects of quenching by the reflected rarefaction wave. Rate of production and sensitivity analyses were carried out by the SENKIN code [36].

Comparison of the kinetic model with experiment is given in Figures 5-11 for the major products. The model adequately describes the temperature dependence of these products for both series of runs (5000 and 700 ppm). The model also reproduces the experimental pyrrole profiles up to about 80% decomposition (Figure 12). The residual pyrrole concentration at high temperatures results from boundary layer effects in the shock tube. The failure of the model to simulate the experimental tailing off in decomposition of the C_3H_5CN isomers and the C_3H_4 at high temperatures is also probably a consequence of boundary layer effects.

A brief selection of the results of sensitivity analyses of the reaction mechanism is given in Table III. This table contains normalized sensitivity coefficients evaluated at 1398 K and at 100 µs for the 5000 ppm mixture in argon. The sensitivity analysis shows that the reactions most important to the decomposition of pyrrole and formation of major products are reactions (1)-(5),(32),(56) and (59). The first five reactions all involve formation or decomposition of pyrrolenine. Reaction (32) which produces vinyl radicals from allyl cyanide is important in determining the production of H atoms and acetylene. Decomposition of pyrrole via H atom fission (56) and H-abstraction (59) is a relatively minor pathway. The Arrhenius parameters of k_{56} were obtained by optimization to low-temperature experimental H_2 profiles which show sensitivity to this rate constant. The value thus obtained of $A_{56}= 10^{13.7}$ s^{-1}. This value might appear to be somewhat low for a unimolecular H-fission reaction. Increase in A_{56} by a factor of two to $10^{14.0}$ would still predict the low-temperature H_2 profiles and the pyrrole decay profiles within experimental error, whereas an increase in A_{56} to $10^{14.3}$ would significantly overpredict the low temperature yields of hydrogen and rate of pyrrole decomposition. However, the A-factor for reaction (56) might well be abnormally low - the transition state probably resembles the tight resonance stabilized pyrrolyl radical.

It remains to interpret the experimental rate constant k_{dis} for overall disappearance of pyrrole. The reaction model was run for temperatures between 1300-1600 K. Over the entire uniform residence time the model predicted that the rate of disappearance of pyrrole obeyed kinetics which were first order in pyrrole concentration. Linear regression of an Arrhenius plot of the theoretically derived rate constants gave $k_{dis,model}$(pyrrole)=$10^{14.70}$exp(-77.2 kcal mol^{-1}/RT) s^{-1}. The model thus yields a rate constant for overall disappearance of reactant which lies within the error limits of the rate constant measured by time-resolved absorption spectrometry at 230 nm. These values may also be compared with an initiation rate constant obtained by Lifshitz et al [10] of k_{init}(pyrrole)=$10^{14.83}$exp(-75 kcal mol^{-1}/RT) s^{-1}. No error limits were stated by these authors. However, since their values were derived in the limit of low extents of decomposition where errors in rate parameters can result due to low product yields, it would appear that our Arrhenius parameters agree with their initiation rate constant within reasonable experimental errors. Lifshitz et al also present a rate constant for overall disappearance of pyrrole of $k_{overall}$=$10^{15.9}$exp(-80 kcal mol^{-1}/RT) obtained from measurements of [pyrrole]$_t$ ($t=t_{res}$) at different temperatures. At 1300 K their value of $k_{overall}$ is a factor of five larger than our value of k_{dis}. The reason for this disagreement is uncertain. Our value of k_{dis} has been obtained in two different laboratories and by two different techniques. Possibly the use by Lifshitz et al of more concentrated pyrrole mixtures leads to a greater importance of bimolecular decomposition of pyrrole. Another possibility is the neglect of reaction in the cooling transient in the analysis made by Lifshitz et al. (Reaction through the rarefaction cooling was taken into account in our modeling studies.)

We have also unsuccessfully tested other pyrolytic mechanisms. In particular, we have been unable to fit a H-chain model to the experimental data. In that model rate constants for N-H fission [Reaction (56)] and for abstraction from pyrrole by H atoms [Reaction (59)] were increased to simulate the experimental decay of pyrrole. It was possible to postulate a H-chain decomposition of pyrrole by invoking the intermediacy of a hydrogen adduct to pyrrole which could then rearrange and decompose to the pyrrole isomers, allyl cyanide and crotononitrile, regenerating H atoms. This model greatly over-predicted the experimental yields, however. Additionally, if k_{56} and k_{59} were adjusted to fit the experimental pyrrole profiles for the 5000 ppm mixture, the model greatly underestimated the experimental pyrrole decomposition rate in the 700 ppm mixtures. The experimental species yields at the two different mixture compositions cannot both be simulated by a bimolecular mechanism of pyrrole decomposition.

A model in which the pyrrole decomposed via hydrogen abstraction reactions with formation of pyrrolyl but without hydrogen addition to pyrrole, was also tested. It is necessary to postulate ring opening of pyrrolyl followed by addition of H atoms and abstraction of H from all donors to form the pyrrole isomeric products, crotononitrile and allyl cyanide. This model was also incapable of predicting the experimental species profiles at both mixture compositions studied.

On the other hand, our pyrolysis model involving pyrrolenine, although somewhat speculative, is in accord with the pyrrole thermochemistry and is capable of reproducing the experimental product distributions and rates. Our reaction model has similarities to the pyrolysis scheme suggested by Lifshitz et al [10]. Although they did not invoke the intermediate pyrrolenine, their mechanism did involve the same transition state for formation of the C_3H_5CN isomers as well as acetylene and C_3H_4.

Conclusions

The pyrolysis kinetics and distribution of major products can be satisfactorily modeled by a reaction mechanism in which pyrolysis is initiated by the reversible formation of pyrrolenine (2H-pyrrole). Pyrrolenine is postulated to undergo C2-N scission to form a biradical which can rearrange to allyl cyanide and crotononitrile. The same biradical can decompose into HCN and propyne/allene (probably via a cyclopropene intermediate) or into acetylene and a precursor of acetonitrile such as 2H-aziridine or ketenimine. Experimentally it was found that the overall rate of disappearance of pyrrole is first order in pyrrole concentration. The rate constant for overall disappearance of pyrrole derived from the model is in agreement within experimental error with an experimental determination by time-resolved absorption spectrometry and with a value obtained earlier by Lifshitz et al [10].

Acknowledgements

The authors wish to thank D. Seery and J.D. Freihaut for helpful discussions. Mr D. Kocum (UTRC) is thanked for technical assistance with experiments. J.C.M. gratefully acknowledges the assistance and encouragement of United Technologies Research Center through the agency of Drs J.D. Freihaut and D. Seery whilst on leave from the University of Sydney on a Special Studies program. Financial assistance of the Australian Research Council is acknowledged.

References

[1] P.R. Solomon and M.B. Colket, Fuel, 57, 749 (1978)

[2] L.A. Kennedy, "Nitric Oxide Production from Chemically Bound Nitrogen in Fuel-Rich Coal Flames", Proc. Int. Coal Sci. Conf. Dusseldeorf, p.284, 1981.

[3] L.R. Snyder, Anal. Chem. 41, 314 (1969)

[4] A. Attar and G.G. Hendrickson, in "Coal Structure", (Ed. R.A. Myers), Ch.5, Academic Press, New York, 1985.

[5] J.C. Mackie, M.B. Colket and P.F. Nelson, "Shock Tube Pyrolysis of Pyridine", J. Phys. Chem. (1990), in press.

[6] J.M. Patterson, A. Tsamasfyros and W.T. Smith, J. Heterocycl. Chem., 5, 727 (1968)

[7] W.R. Johnson and J.C. Kang, J. Org. Chem., 36, 189 (1971).

[8] A.E. Axworthy, V.H. Dayan and G.B. Martin, Fuel, 57, 29 (1978)

[9] E.C. Wu and J. Heicklen, J. Am. Chem. Soc. 93, 3432 (1971)

[10] A. Lifshitz, C. Tamburu and A. Suslensky, J. Phys. Chem., 93, 5802 (1989)

[11] M.B. Colket, in "Shock Tubes and Waves", Proceedings of the 15th International Symposium, Stanford Univ. Press, Stanford, p.311, 1986.

[12] P.A. Mullen and M.K. Orloff, J. Chem. Phys., 51, 2276 (1969)

[13] M. Bavia, F. Bertinelli, C. Taliani and C. Zauli, Mol. Phys., 31, 479 (1976)

[14] M.A. Grela, V.T. Amorebieto and A.J. Colussi, J. Phys. Chem., 89, 38 (1985)

[15] A. Lifshitz, M. Bidani and S. Bidani, J. Phys. Chem. 90, 5373 (1986)

[16] P.P. Organ, Ph D. Thesis, University of Sydney, 1989. P.P. Organ and J.C. Mackie, to be published.

[17] R.A. Jones and G.P. Bean, "The Chemistry of Pyrroles", Academic Press, London, 1977.

[18] S.W. Benson, F.R. Cruickshank, D.M. Golden, G.R. Haugen, H.E. O'Neal, A.S. Rodgers, R. Shaw and R. Walsh, Chem. Rev. 69, 279 (1969)

[19] H.E. O'Neal and S.W. Benson, Int. J. Chem. Kinet., 1, 221 (1969)

[20] W.A. Rendall, M. Torres, E.M. Lown and O.P. Strausz, Rev. Chem. Intermediates, 6, 335 (1986)

[21] J.M. Patterson and S. Soedigdo, J. Org. Chem., 33, 2057 (1968)

[22] J.M. Patterson, L.T. Burka and M.R. Boyd, J. Org. Chem., 33, 4033 (1968)

[23] J.M. Patterson, J.W. de Haan, M.R. Boyd and J.D. Ferry, J. Am. Chem. Soc., 94, 2487 (1972)

[24] I.A. Jacobson and H.B. Jensen, J. Phys. Chem., 66, 1245 (1962)

[25] I.A. Jacobson and H.B. Jensen, J. Phys. Chem., 68, 3068 (1964)

[26] A. Karpfen, P. Schuster and H. Berner, J. Org. Chem. 44, 374 (1979)

[27] S.W. Benson, Int. J. Chem. Kinet., 21, 233 (1989).

[28] T. Kakumoto, T. Ushirogouchi, K. Saito and A. Imamura, J. Phys. Chem., 91, 183 (1987)

[29] L.L. Lohr, M. Hanamura and K. Morokuma, J. Am. Chem. Soc., 105, 5541 (1983)

[30] H. Bock, R. Dammel and S. Aygen, J. Am. Chem. Soc., 105, 7681 (1983)

[31] H. Bock and B. Solouki, Angew. Chem. 93, 425 (1981)

[32] S. Furuyama, D.M. Golden and S.W. Benson, Int. J. Chem. Kinet., 3, 237 (1971)

[33] R.J. Kee, J.A. Miller and T.H. Jefferson, "CHEMKIN: A General-Purpose, Problem-Independent Chemical Kinetics Code Package", Sandia Report SAND80-8003, March, 1980.

[34] A.C. Hindmarsh, "LSODE and LSODI: Two New Initial Value Differential Equation Solvers:, ACM Signum Newsletter, 15 [4], 1980.

[35] R.E. Mitchell and R.J. Kee, "A General-Purpose Computer Code for Predicting Chemical Kinetic Behavior behind Incident and Reflected Shocks", Sandia Report SAND82-8205, March, 1982.

[36] A.E. Lutz, R.J. Kee and J.A. Miller, "SENKIN: A Fortran Program Predicting Homogeneous Gas Phase Chemical Kinetics with Sensitivity Analysis", Sandia Report SAND87-8248, February, 1988.

[37] W.A. Payne and L.J. Stief, J. Chem. Phys., 64, 1150 (1976).

[38] M.A. Weissman and S.W. Benson, J. Phys. Chem., 92, 4080 (1988).

[39] J. Warnatz in "Combustion Chemistry", (W.C. Gardiner, Ed.), Springer, New York, p.197, 1984.

[40] K.D. King and R.D. Goddard, J. Phys. Chem., 82, 1675 (1978).

[41] J.H. Kiefer, K.I. Mitchell and H.C. Wei, Int. J. Chem. Kinet., 20, 787 (1988).

[42] W. Tsang and R.F. Hampson, J. Phys. Chem. Ref. Data, 15, 1087 (1986).

[43] J. Warnatz, H. Bockhorn, A. Moser and H.W. Wenz, 19th Symp. (Int.) on Combustion, p.197, 1982.

[44] J.H. Kiefer, M.Z. Al-Alami and K.A. Budach, J. Phys. Chem., 86, 808 (1982).

[45] J.H. Kiefer, K.I. Mitchell, R.D. Kern and J.N. Yong, J. Phys. Chem., 92, 677 (1988).

[46] M.B. Colket, 21st Symp. (Int.) on Combustion, p.851, 1986.

[47] M. Weissman and S.W. Benson, Int. J. Chem. Kinet., 16, 307 (1984).

[48] P.R. Westmoreland, Preprints A.C.S. Division of Fuel Chem. 32 [3], 480 (1987).

Captions to Figures

Figure 1: Temperature distribution of all products of significance in the pyrolysis of a 5000 ppm mixture of pyrrole in argon. Total pressure 13 atm, residence time 400 µs.

Figure 2: Oscillogram of the transmission of light of wavelength 230 nm in a shock wave heated mixture of 1000 ppm pyrrole in argon. Reflected shocked gas temperature = 1513 K, pressure = 20 atm. ISF: incident shock front, RSF: reflected shock front. Positions of zero and unattenuated light intensity are indicated.

Figure 3: Plot of $\ln(I/I_o)$ versus time for the run shown in Figure 2. The rate constant derived from this run was $k_{dis}(1513\ K) = 2.35x10^{3}s^{-1}$.

Figure 4: Arrhenius plot of the first order rate constant, k_{dis}, for overall disappearance of pyrrole as measured by time resolved absorption spectrometry at 230 nm.

Figures 5-11: Comparison of the experimental product yields, Y, of esignated species with the predictions of the reaction model of Table II. o and □: data points for mixtures of 5000 ppm pyrrole in Ar, x and ●: data points for mixtures of 700 ppm pyrrole in Ar. —— model predictions for 5000 ppm. - - - model predictions for 700 ppm.

Figure 12: Comparison between the experimental pyrrole profiles and the predictions of the reaction model of Table II. O and ——: experimental points and model predictions for 5000 ppm mixture of pyrrole in Ar; x and - - - experimental points and model predictions for 700 ppm mixture of pyrrole in Ar.

Table I: Thermochemical Parameters for the Pyrrole System

Species	$\Delta H^\circ_{f,300}$ (kcal mol^{-1})	S_{300} (cal mol^{-1} K^{-1})	C_p 300	500	1000	1500	2000 K
C_4H_5N[a]	25.9	64.77	17.15	28.00	41.56	47.46	50.43
PYRLNE[b]	45.5	67.8	16.58	26.67	41.37	45.70	47.53
PYRLYL[c]	54.4	64.9	15.11	25.03	36.85	43.46	47.39
CH_2CN	59.0	59.8	12.34	15.49	20.21	22.59	23.78
AC_3H_4CN[d]	70.4	73.0	19.13	28.03	39.20	43.55	46.10

[a] pyrrole
[b] pyrrolenine (2H-pyrrole)
[c] pyrrolyl radical:

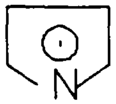

[d] cyanoallyl radical

TABLE II: Reaction Model

	REACTIONS	FORWARD RATE CONSTANT			REVERSE RATE CONSTANT			
		Log A	n	E	Log A	n	E	Ref.
1	C4H5N=PYRLNE	13.48	0.0	67.0	13.15	0.0	48.4	PW
2	PYRLNE=C3H4P+HCN	13.48	0.0	56.0	10.82	0.0	27.7	PW
3	PYRLNE=C3H5CN	15.70	0.0	68.0	14.51	0.0	76.9	PW
4	PYRLNE=ALLYLCN	15.70	0.0	68.0	13.47	0.0	74.6	PW
5	PYRLNE=C2H2+CH3CN	15.78	0.0	76.0	12.36	0.0	48.7	PW
6	H+C3H5CN=AC3H4CN+H2	13.70	0.0	5.0	12.19	0.0	21.6	est
7	H+C3H5CN=CH3+H2CCHCN	13.70	0.0	5.0	11.60	0.0	16.9	est
8	H+C3H5CN=C3H5+HCN	13.70	0.0	5.0	11.79	0.0	22.9	est
9	H+ALLYLCN=AC3H4CN+H2	13.60	0.0	5.0	13.13	0.0	23.9	est
10	H+ALLYLCN=C2H4+CH2CN	13.60	0.0	5.0	12.77	0.0	27.2	PW
11	H+ALLYLCN=C3H5+HCN	13.60	0.0	5.0	12.74	0.0	25.3	est
12	CH3+C3H5CN=AC3H4CN+CH4	11.70	0.0	9.0	11.66	0.0	26.2	est
13	CH3+ALLYLCN=AC3H4CN+CH4	11.60	0.0	9.0	12.61	0.0	28.6	est
14	H+HCCHCN=H2CCHCN	13.30	0.0	0.0	14.61	0.0	104.8	[5]
15	AC3H4CN=CH3CCCN+H	12.48	0.0	61.0	12.53	0.0	6.2	est
16	C3H5=C3H4P+H	13.00	0.0	58.0	13.43	0.0	2.8	[16]
17	CH3+H2CCHCN=HCCHCN+CH4	11.70	0.0	10.0	12.48	0.0	10.4	est
18	H+H2CCHCN=HCCHCN+H2	13.70	0.0	8.0	13.00	0.0	7.7	[5]
19	HCCHCN+M=HCCCN+H+M	15.90	0.0	40.0	16.14	0.0	0.2	[5]
20	H+H2CCHCN=HCN+C2H3	13.00	0.0	4.0	11.10	0.0	4.2	[5]
21	H+CH3CN=CH3+HCN	13.00	0.0	2.0	11.50	0.0	10.0	est
22	H+C2H2=C2H3	12.64	0.0	2.4	12.37	0.0	42.8	[37][a]
23	H+C2H4=C2H3+H2	13.70	0.0	8.0	11.86	0.0	6.8	[38]
24	CH3+H2=CH4+H	2.81	3.0	7.7	15.10	0.0	17.1	[39]
25	2CH3=C2H6	12.85	0.0	0.0	16.14	0.0	87.2	[39][a]

TABLE II(cont.): Reaction Model

	REACTIONS	FORWARD RATE CONSTANT			REVERSE RATE CONSTANT			
		Lcg A	n	E	Log A	n	E	REF.
26	C2H5CN=CH3+CH2CN	15.25	0.0	81.0	12.53	0.0	3.3	[40]
27	C2H5CN=HCN+C2H4	14.30	0.0	67.8	13.08	0.0	39.5	[40]
28	C2H5CN=H2CCHCN+H2	12.10	0.0	59.1	10.94	0.0	29.3	[40]
29	H+C3H5=C3H6	13.48	0.0	0.0	14.78	0.0	87.6	est
30	H+C3H5=C3H4P+H2	13.70	0.0	3.0	14.75	0.0	52.3	est
31	CH3+HCCHCN=C3H5CN	13.00	0.0	0.0	16.41	0.0	92.9	PW
32	C2H3+CH2CN=ALLYLCN	13.00	0.0	0.0	16.29	0.0	83.5	PW
33	2C2H3=C4H6	12.70	0.0	0.0	17.04	0.0	101.7	[41]
34	2C2H3=C2H4+C2H2	12.00	0.0	0.0	14.73	0.0	65.3	[42]
35	C3H5+CH2CN=C3H4P+CH3CN	13.30	0.0	2.0	15.57	0.0	36.8	est
36	C3H5+CH2CN=C4H6+HCN	13.30	0.0	3.0	14.59	0.0	42.6	est
37	AC3H4CN+CH3=C4H6+HCN	13.30	0.0	3.0	14.48	0.0	50.5	est
38	H+AC3H4CN=ALLYLCN	13.48	0.0	0.0	14.57	0.0	85.5	est
39	H+AC3H4CN=C3H5CN	13.48	0.0	0.0	15.61	0.0	87.9	est
40	C2H3+CH2CN=C2H2+CH3CN	13.30	0.0	3.0	15.41	0.0	52.6	est
41	H+CH2CN=CH3CN	12.70	0.0	0.0	14.54	0.0	89.9	est
42	CH3+C3H5CN→C3H4CN+CH4	11.70	0.0	8.0	0.00	0.0	0.0	est
43	C3H4CN→HCCCN+CH3	14.00	0.0	35.0	0.00	0.0	0.0	est
44	CH3+C2H3=CH4+C2H2	12.00	0.0	8.0	14.37	0.0	72.7	est
45	C3H5CN=C3H4P+HCN	14.70	0.0	82.0	13.23	0.0	44.8	est
46	ALLYLCN=C3H4P+HCN	13.70	0.0	75.0	13.27	0.0	40.1	est
47	CH2CN+ALLYLCN→C3H4CN+CH3CN	12.00	0.0	8.0	0.00	0.0	0.0	est
48	C3H4CN→C2H2+CH2CN	14.00	0.0	30.0	0.00	0.0	0.0	est
49	AC3H4CN=HCCCN+CH3	14.00	0.0	70.0	12.96	0.0	25.2	est
50	C2H4+M=C2H2+H2+M	17.41	0.0	79.3	15.85	0.0	37.7	[39]

TABLE II(cont.): Reaction Model

	REACTIONS	FORWARD RATE CONSTANT			REVERSE RATE CONSTANT			
		Log A	n	E	Log A	n	E	REF.
51	C4H6=C2H2+C2H4	15.30	0.0	82.5	13.69	0.0	46.1	[41]
52	CH3CN+C2H3=H2CCHCN+CH3	13.00	0.0	2.0	13.40	0.0	9.8	est
53	H+C3H4P=CH3+C2H2	13.30	0.0	2.4	11.04	0.0	11.4	[43]
54	CH3+CH3CN=CH2CN+CH4	11.70	0.0	7.0	11.96	0.0	22.2	est
55	2CH2CN=H2CCHCN+HCN	13.00	0.0	4.0	14.28	0.0	45.5	est
56	C4H5N=PYRLYL+H	13.70	0.0	81.0	12.70	0.0	2.0	PW
57	2PYRLYL→BIPRL	13.30	0.0	0.0	0.00	0.0	0.0	est
58	C2H3+C2H4=C4H6+H	11.70	0.0	4.0	13.59	0.0	0.0	[42][b]
59	H+C4H5N=PYRLYL+H2	13.30	0.0	5.0	12.92	0.0	30.4	PW
60	CH3+C4H5N=PYRLYL+CH4	11.70	0.0	7.0	12.80	0.0	33.1	PW
61	C3H4P=C3H3+H	15.25	0.0	89.1	12.70	0.0	0.0	[16]
62	CH3+C3H4P-C3H3+CH4	12.30	0.0	7.7	11.84	0.0	23.7	[44]
63	H+C3H4P=C3H3+H2	12.00	0.0	1.5	10.06	0.0	16.8	[44]
64	2C3H3=L-C6H6	12.70	0.0	0.0	15.00	0.0	58.1	[16]
65	L-C6H6=C6H6	12.00	0.0	33.0	16.86	0.0	115.9	[16]
66	H+C2H6=C2H5+H2	2.74	3.5	5.2	14.62	0.0	21.7	[39]
67	C2H5=C2H4+H	13.00	0.0	39.7	12.22	0.0	2.1	[39]
68	2C2H2=C4H4	13.77	0.0	44.6	15.19	0.0	81.2	[45]
69	C4H4=H2+C4H2	14.32	0.0	87.0	13.32	0.0	45.3	[45]
70	C2H3+C2H2=N-C4H5	12.04	0.0	4.0	14.31	0.0	38.4	[46]
71	N-C4H5=C4H4+H	14.00	0.0	41.4	13.42	0.0	3.3	[47]
72	C2H+H2=H+C2H2	12.85	0.0	0.0	13.59	0.0	20.4	[42][b]
73	C2H+C2H2=C4H2+H	12.00	0.0	0.0	13.16	0.0	15.2	[48][c]
74	C2H+C2H3=C4H4	13.00	0.0	0.0	16.05	0.0	121.1	[43][b]

TABLE II (cont.)

Notes: Units for A: cm^3, mol, s
Units for E: kcal mol^{-1}
PW indicates rate constant evaluated in present work
est indicates rate constant was estimated in present work
[a] Fall-off value. Pressure dependence as given in Reference
[b] Value is within limits of uncertainty stated in Reference
[c] Reverse rate constant agrees with value given in Reference at 1400 K.

Species Indentification

C4H5N: pyrrole, PYRLNE: pyrrolenine (2H-pyrrole), C3H4P: propyne, C3H5CN: cis- and trans-crotononitrile, ALLYLCN: allyl cyanide, AC3H4CN: cyanoallyl radical, C3H4CN: non-allylic cyano- radical - $\bullet CH{=}CHCH_2CN$ or $CH_3CH{=}C\bullet CN$, C3H5: allyl radical, C4H6: 1,3-butadiene, L-C6H6: alkene-yene isomer of benzene, C3H3: propargyl radical, N-C4H5: 1-C_4H_5 radical,

BIPRL:

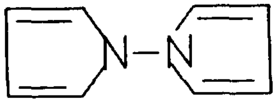

or

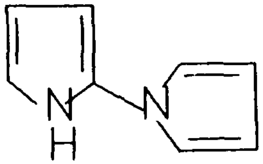

etc.

PYRLYL:

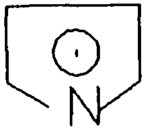

Table III: Sensitivity Analysis for the Reaction Model of Table II.
Entries are the normalised mass fraction sensitivities for the given species evaluated at 100 μs and temperature 1398 K.

Rxn. No.	C_4H_5N	HCN	C_3H_5CN	ALLYL-CN	CH_3CN	HCCCN	C_2H_2	C_3H_4	H_2	CH_4
1	-0.020	0.440	0.432	0.432	0.444	0.463	0.441	0.434	0.206	0.567
2	-0.004	0.882	-0.082	-0.082	-0.083	-0.086	-0.074	0.897	-0.058	
3	-0.009	-0.160	0.814	-0.172	-0.173	0.762	-0.074	-0.163	-0.071	0.562
4	-0.010	-0.148	-0.182	0.815	-0.139	-0.086	0.362	-0.168	0.399	0.072
5	-0.001	-0.012	-0.012	-0.012	0.962		0.442	-0.012		
7										0.317
8		0.007								
11				-0.002						
19						0.040				
22							0.026		0.028	
31			-0.004			0.890			0.024	0.447
32	-0.001	0.015	-0.006	-0.089	0.026	0.039	0.502	-0.002	0.479	0.279

Table III (cont.)

Rxn. No.	C_4H_5N	HCN	C_3H_5CN	ALLYL-CN	CH_3CN	HCCCN	C_2H_2	C_3H_4	H_2	CH_4
35					0.007					
39			-0.004			0.029			0.023	
40					0.005					
45		0.008						0.008		
46		0.009		-0.004				0.009		
47					0.011		0.004			
49						0.078				
53							0.010	-0.003		0.150
56	-0.002		-0.004	-0.003					0.425	0.204
59		-0.011	0.008	0.006	-0.007	-0.033	-0.007	0.003	0.095	-0.437
60										0.656

Figure 1

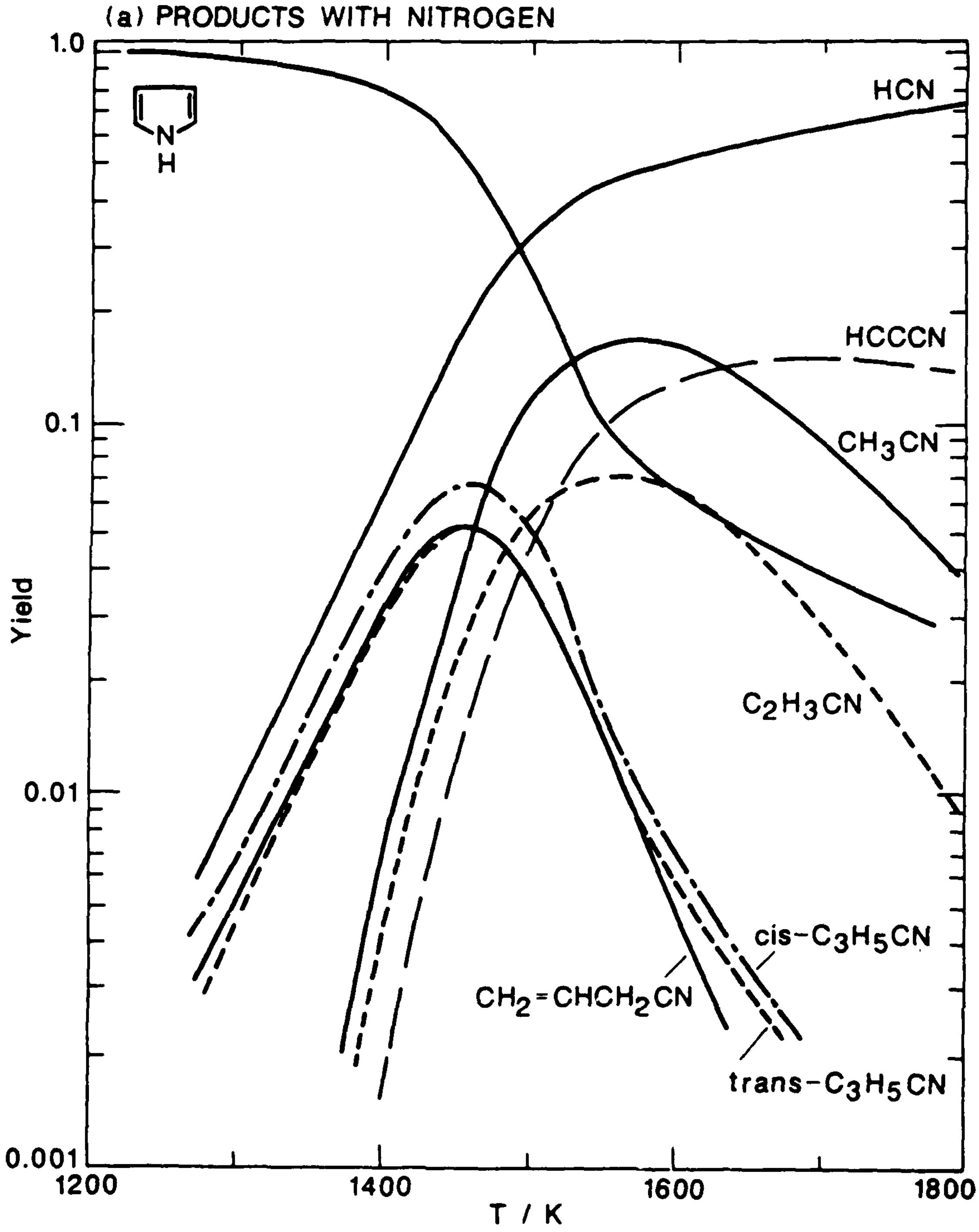

(a) PRODUCTS WITH NITROGEN
N
H
1.0
0.1
0.01
0.001
Yield
1200
1400
1600
1800
T / K
HCN
HCCCN
CH_3CN
C_2H_3CN
cis-C_3H_5CN
$CH_2=CHCH_2CN$
trans-C_3H_5CN

Figure 1

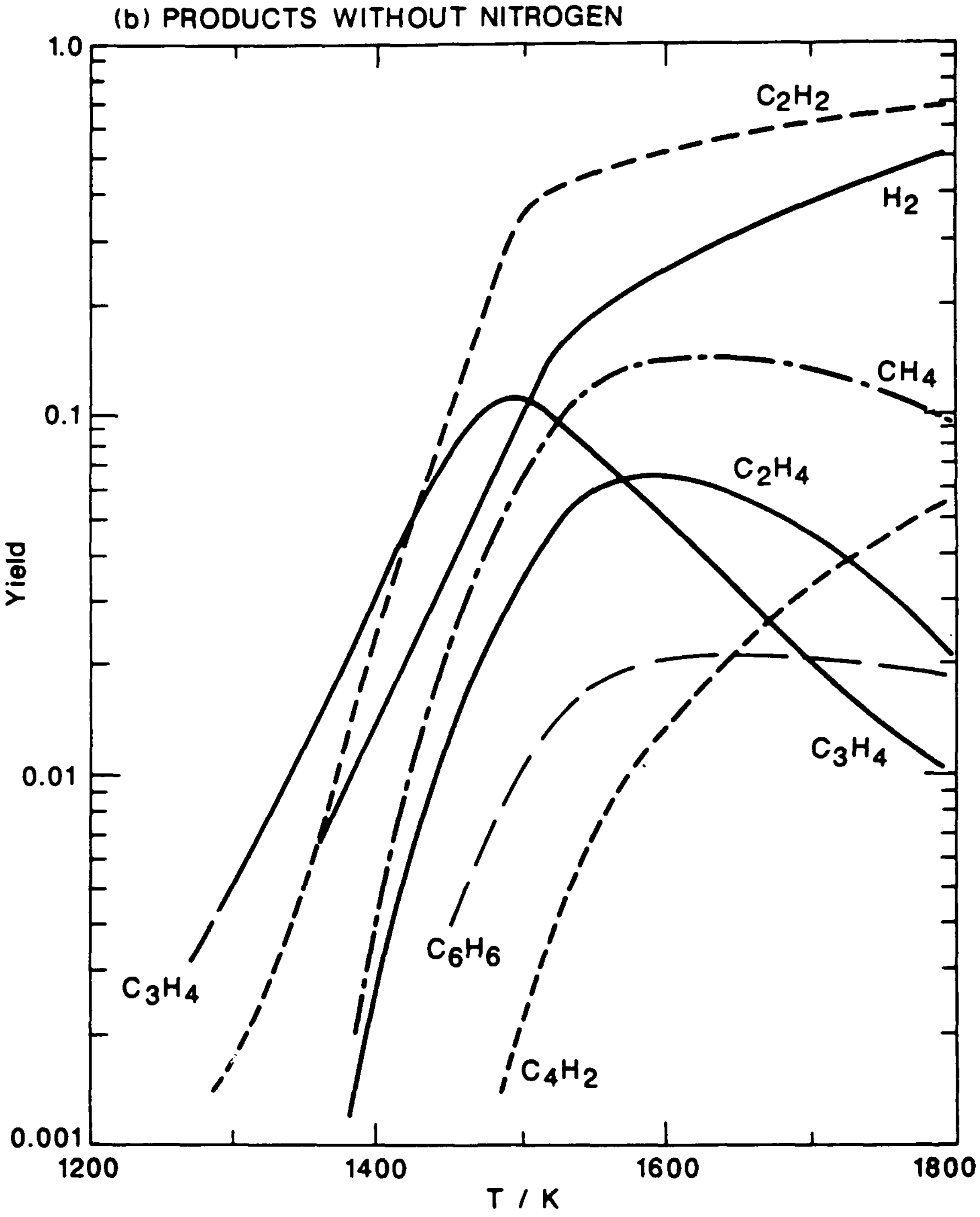
(b) PRODUCTS WITHOUT NITROGEN
1.0
0.1
0.01
0.001
Yield
1200
1400
1600
1800
T / K
C_2H_2
H_2
CH_4
C_2H_4
C_3H_4
C_3H_4
C_6H_6
C_4H_2

Figure 2

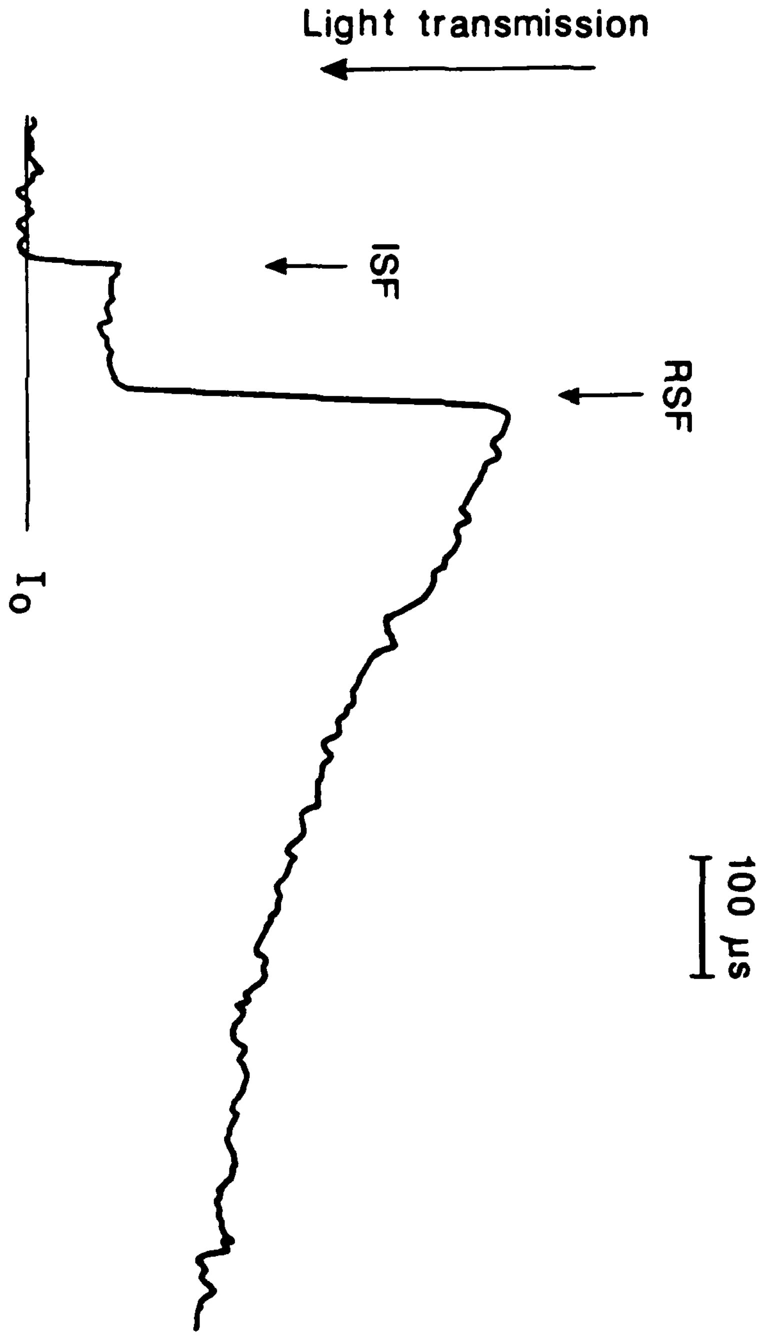

Figure 3

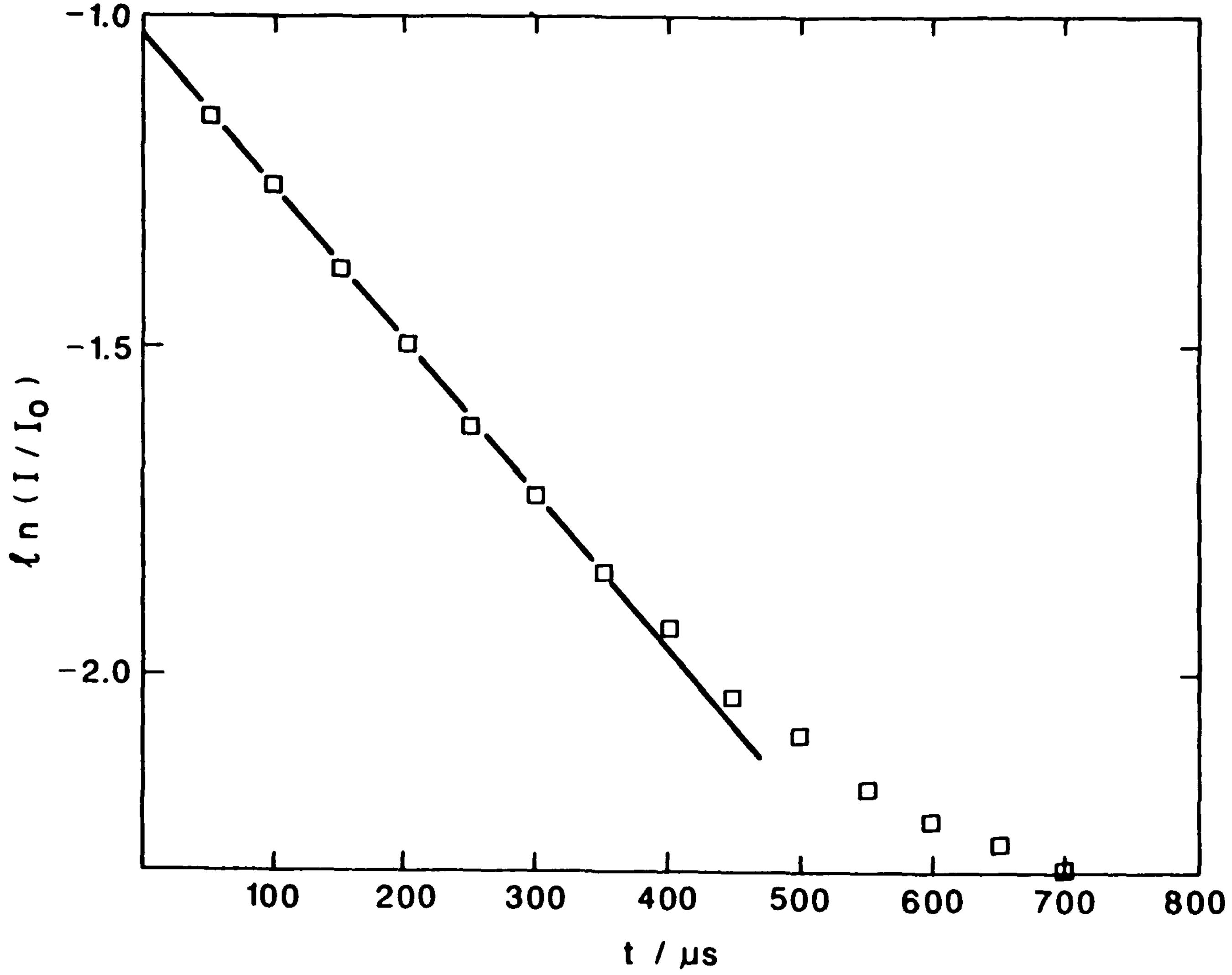

Figure 4

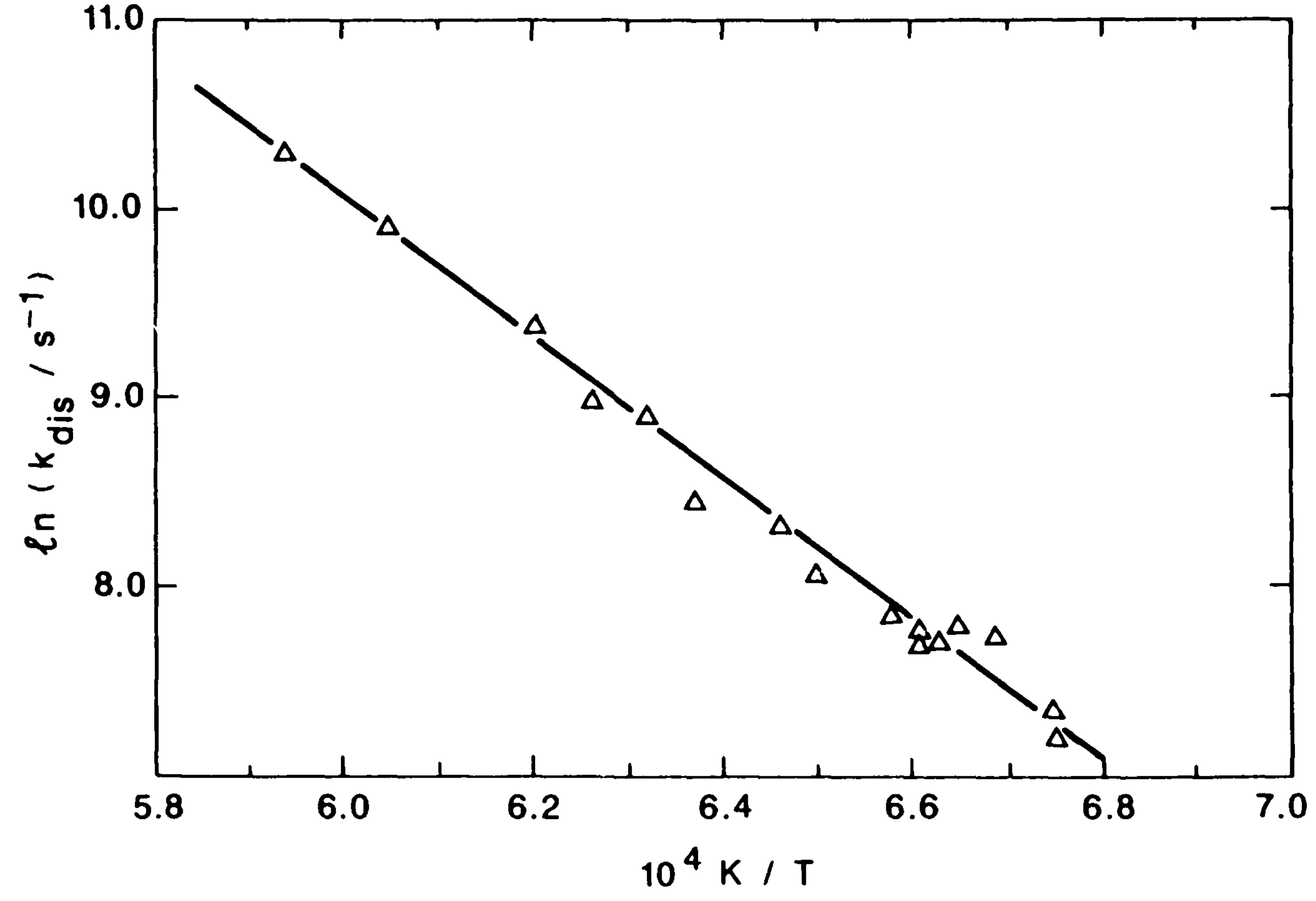

Figure 5

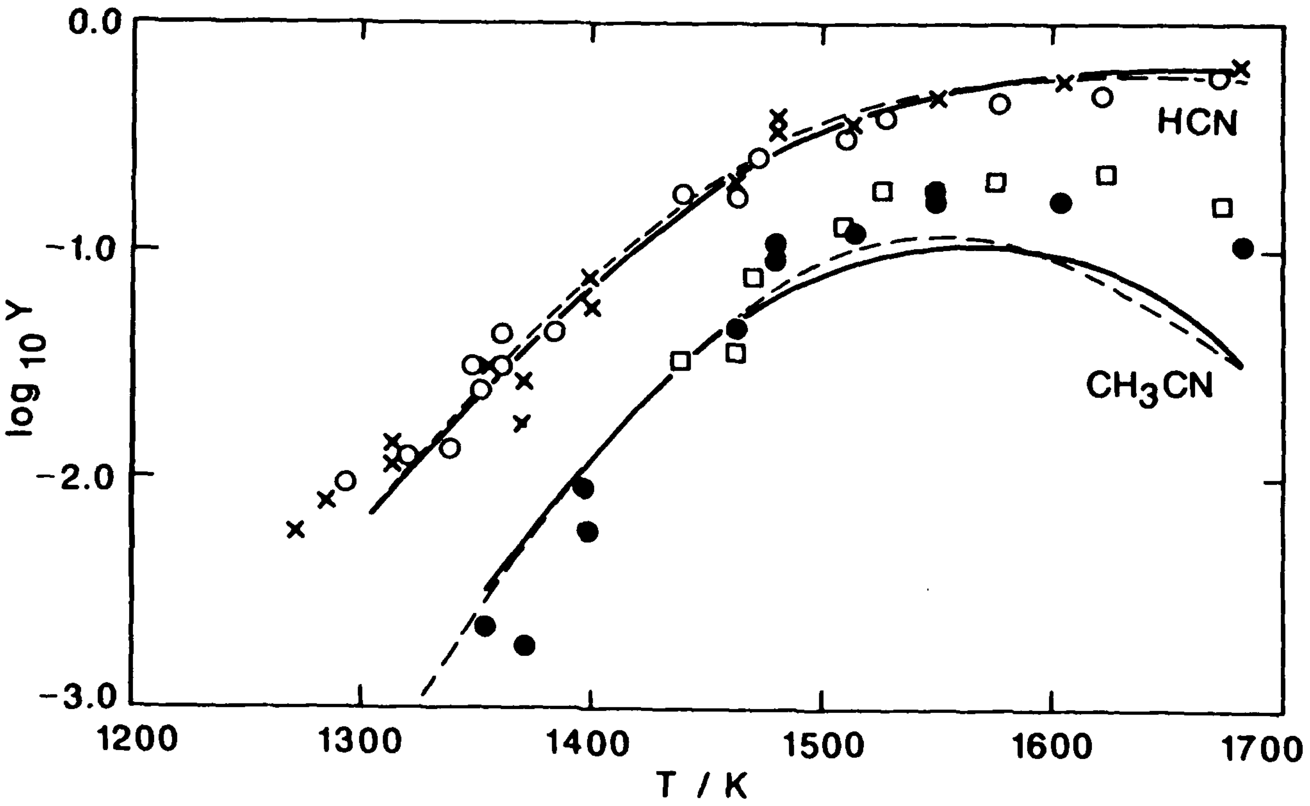

Figure 6

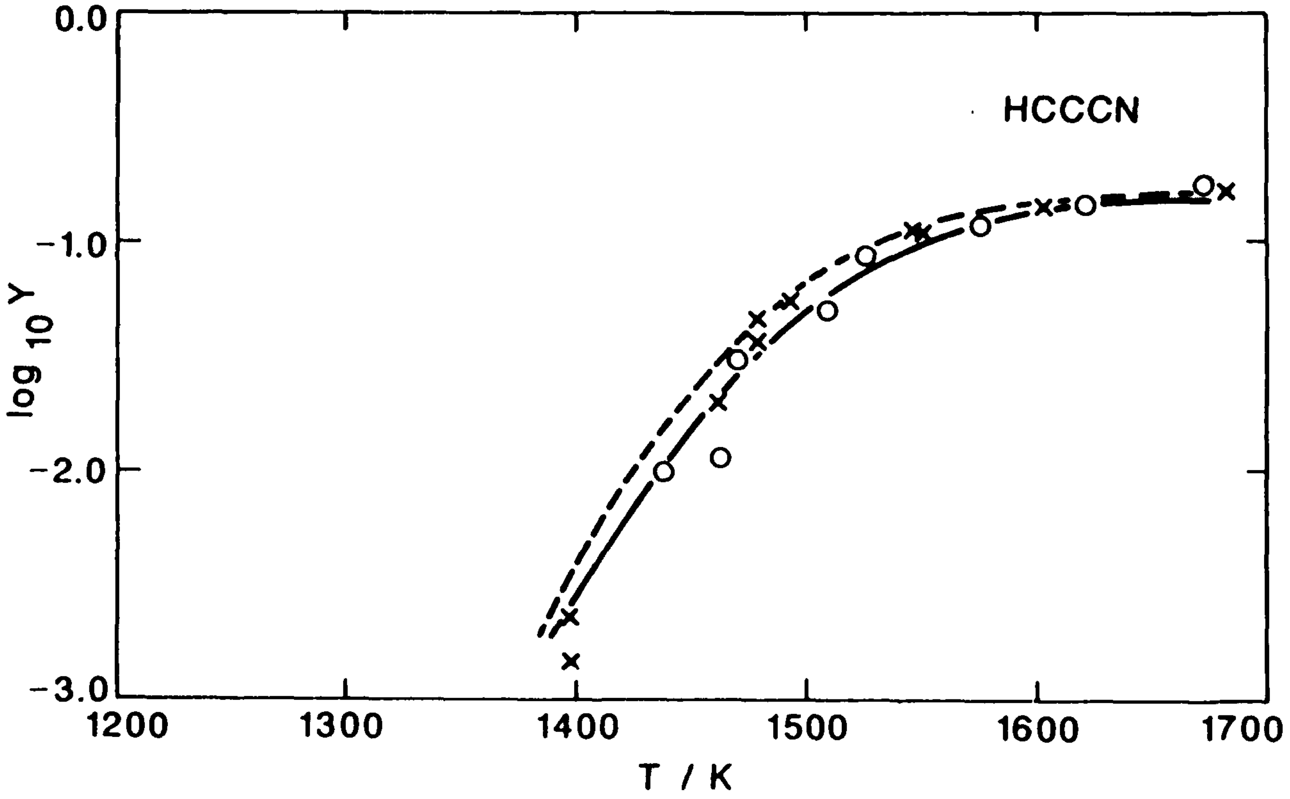

Figure 7

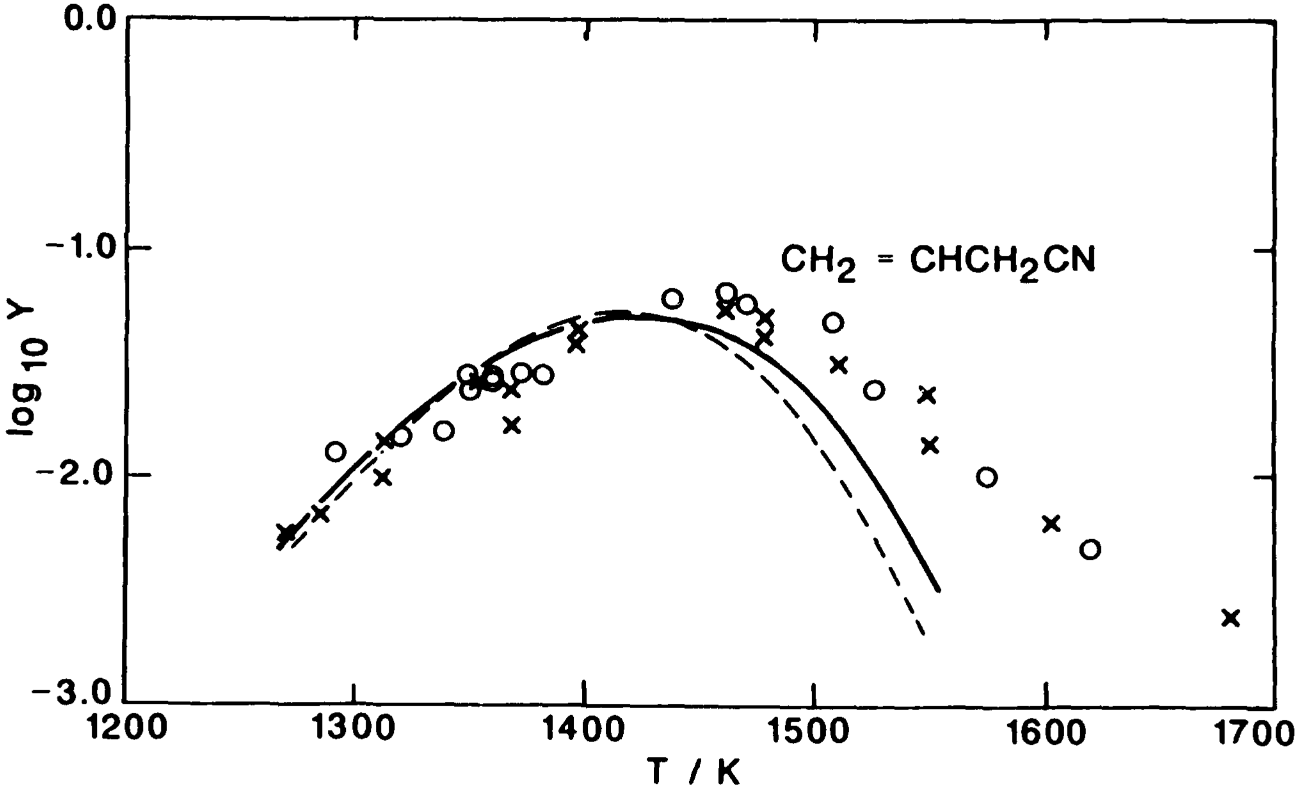

$CH_2 = CHCH_2CN$
0.0
−1.0
−2.0
−3.0
$\log_{10} Y$
1200
1300
1400
1500
1600
1700
T / K

Figure 8

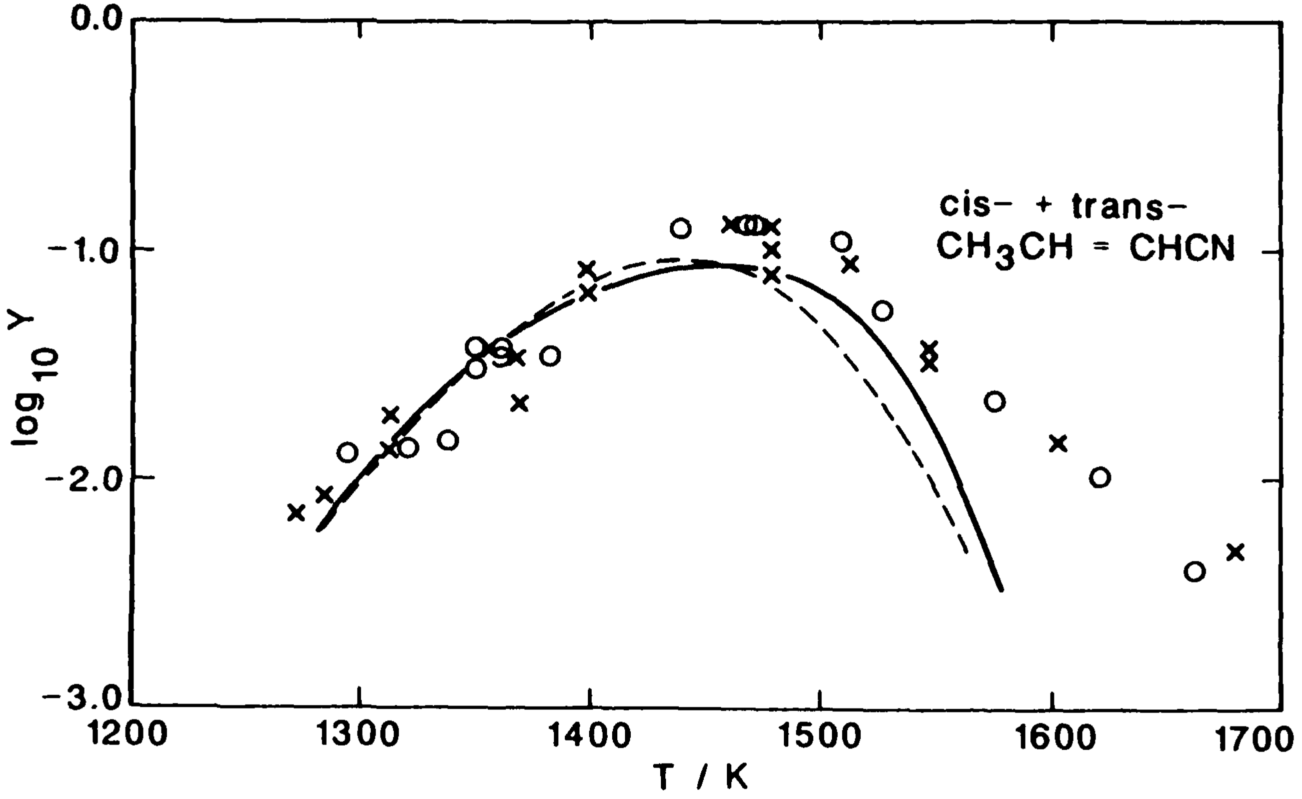
cis- + trans-
$CH_3CH = CHCN$
0.0
−1.0
−2.0
−3.0
$\log_{10} Y$
1200
1300
1400
1500
1600
1700
T / K

Figure 9

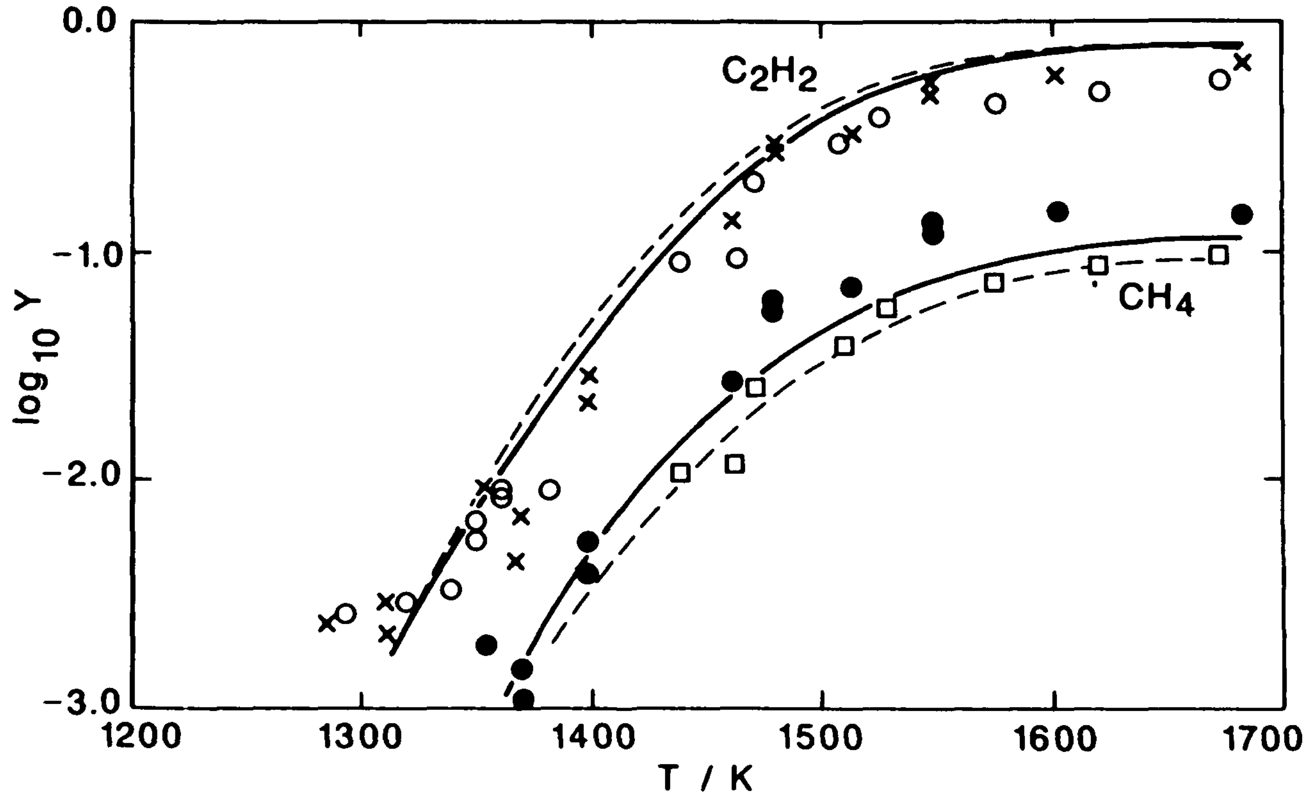

Figure 10

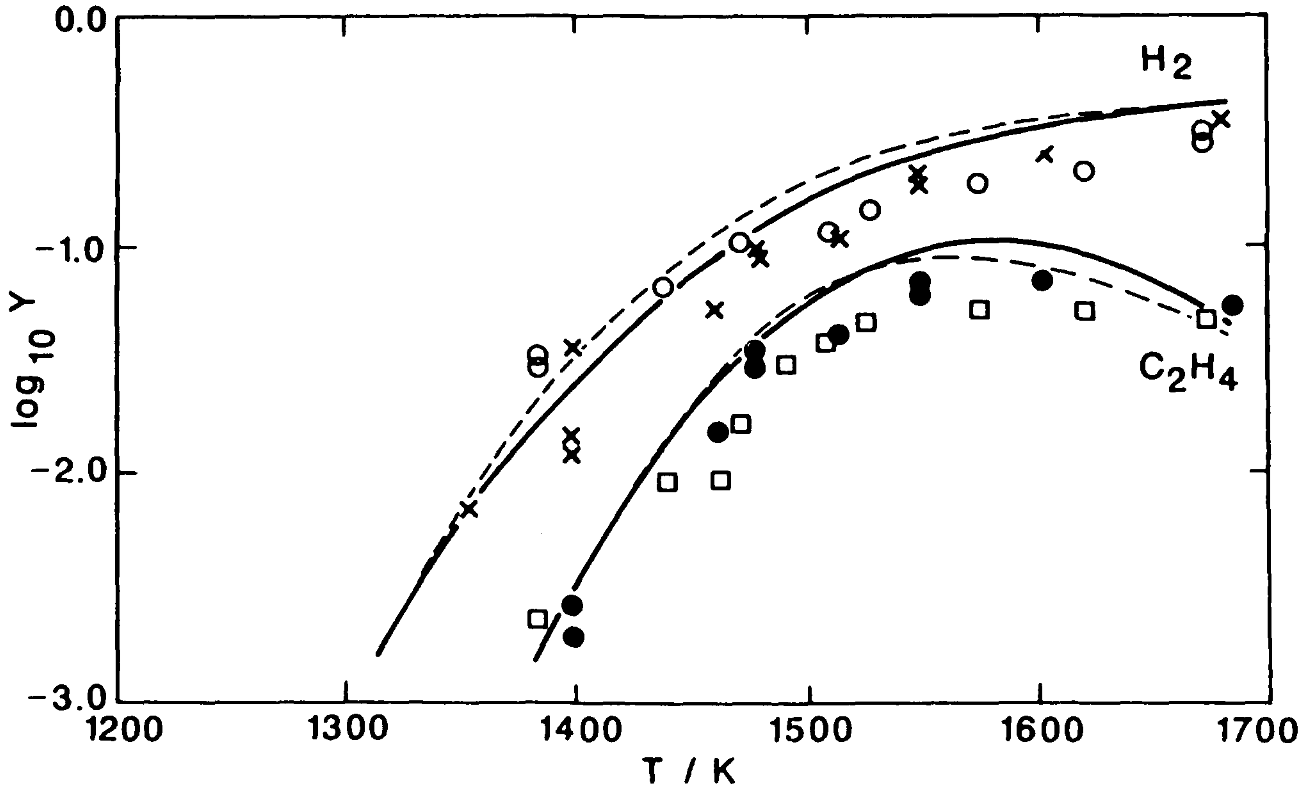

.Figure 11

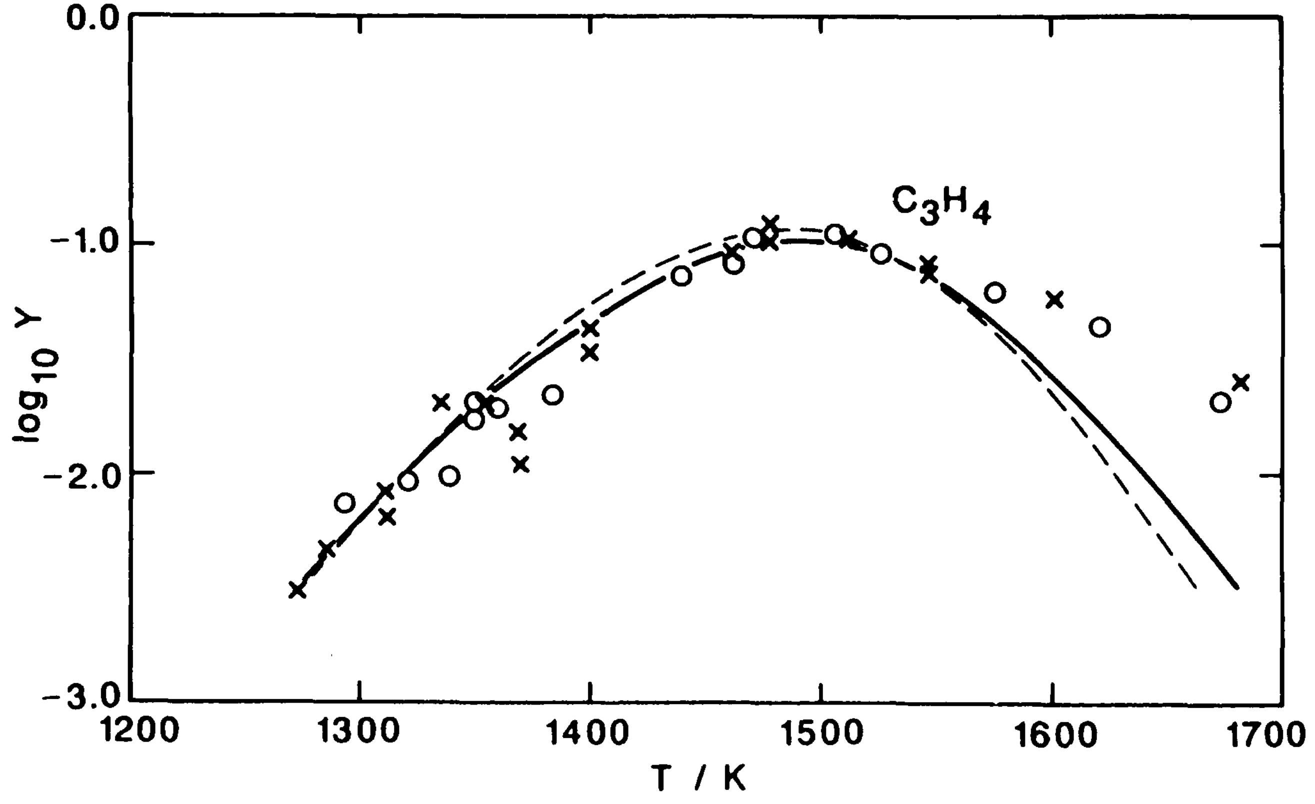

Figure 12

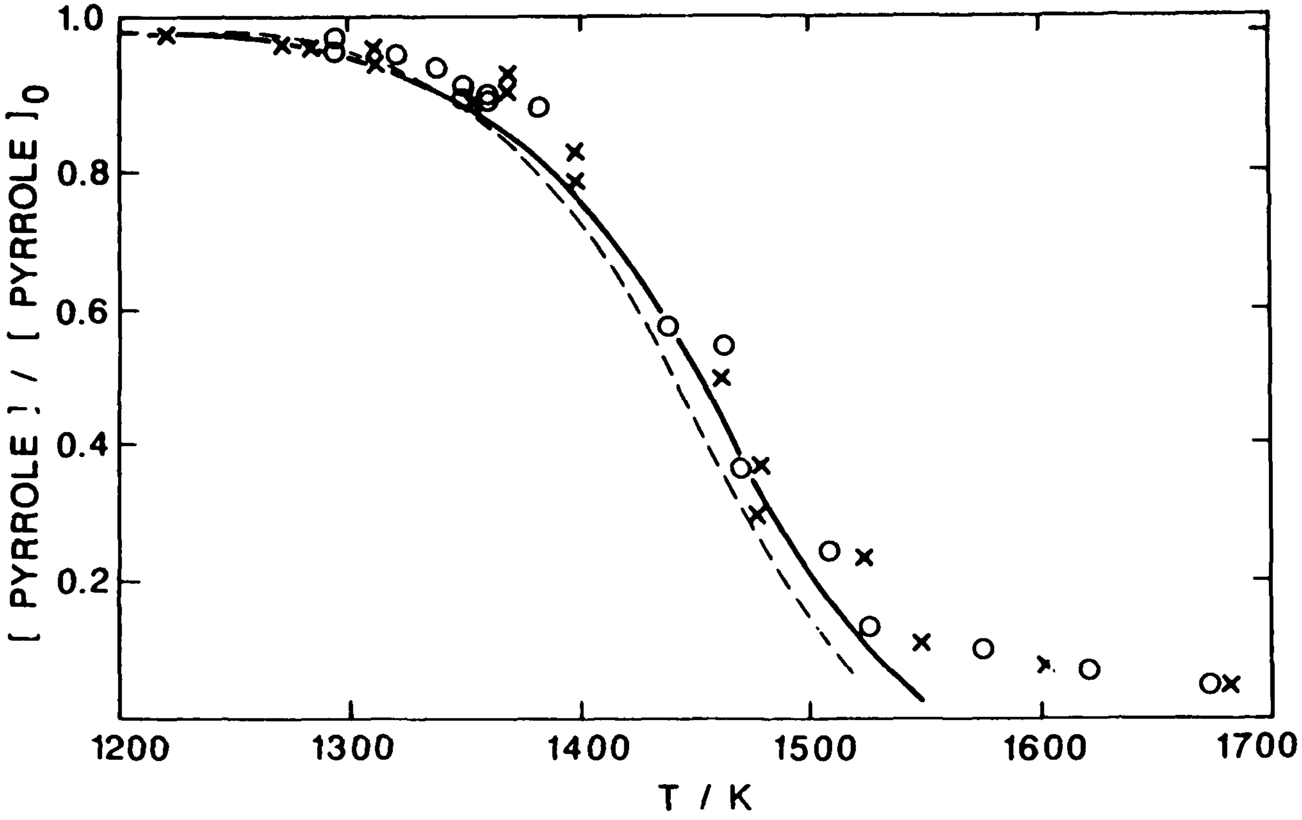
1.0
0.8
0.6
0.4
0.2
[PYRROLE] / [PYRROLE]$_0$
1200
1300
1400
1500
1600
1700
T / K